

Collision Processes of Hydrocarbon Species in Hydrogen Plasmas: II. The Ethane and Propane Families

R.K. Janev^{1,2} and D. Reiter^{1,3}

Abstract

Cross sections and rate coefficients are provided for collision processes of electrons and protons with C_xH_y and $C_xH_y^+$ ($x = 2, 3; 1 \leq y \leq 2x + 2$) hydrocarbon species in a wide range of collision energies and plasma (gas) temperatures. The considered processes include: electron-impact ionization and dissociation of C_xH_y , dissociative excitation, ionization and recombination of $C_xH_y^+$ with electrons, and both charge transfer and atom exchange in proton channels are considered separately. Information is also provided for the energies of each individual reaction channel. The cross sections and rate coefficients are presented in compact analytic forms.

¹Institut für Plasmaphysik, Forschungszentrum Jülich GmbH, EURATOM Association, Trilateral Euregio Cluster, D-52425 Jülich, Germany

²Macedonian Academy of Sciences and Arts, 1000 Skopje, Macedonia

³Institut für Laser- und Plasmaphysik, Heinrich-Heine-Universität, D-40225 Düsseldorf, Germany

Contents

1	Introduction	5
2	Basic Properties of Hydrocarbons and their Collisions with Electrons and Protons	7
2.1	Thermo-chemical and energy structure properties of C_xH_y	8
2.2	Basic relations for reaction energetics	10
2.3	General properties of collision cross sections	15
2.3.1	Energy behaviour of cross sections	15
2.3.2	Cross section scaling relationships	16
2.3.3	Cross section branching ratios for multichannel processes	17
3	Collision Processes of C_2H_y and $C_2H_y^+$ with Electrons and Protons	22
3.1	Electron-impact ionization of C_2H_y (I,DI)	22
3.1.1	Cross section availability, reaction channels and energetics	22
3.1.2	Cross section determination	23
3.1.3	Analytic representation of cross sections	25
3.2	Electron-impact dissociative excitation of C_2H_y to neutrals (DE)	26
3.2.1	General remarks, reaction channels and energetics	26
3.2.2	Determination of cross sections	28
3.3	Electron-impact dissociative excitation of $C_2H_y^+$ ions (DE ⁺)	30
3.3.1	General remarks, reaction channels and energetics	30
3.3.2	Determination of total and partial cross sections	32
3.4	Electron-impact dissociative ionization of $C_2H_y^+$ ions (DI ⁺)	34
3.4.1	General remarks, reaction channels and energetics	34
3.4.2	Determination of total and partial cross sections	34
3.5	Dissociative electron recombination with $C_2H_y^+$ (DR)	35
3.5.1	Data availability, reaction channels and energetics	35
3.5.2	Total and partial rate coefficients for DR	38
3.6	Charge exchange and particle rearrangement reactions of protons with C_2H_y , (CX)	39
3.6.1	Data availability, reaction channels and energetics	39
3.6.2	Charge exchange cross sections	41
4	Collision Processes of C_3H_y and $C_3H_y^+$ with Electrons and Protons	44
4.1	Electron-impact ionization of C_3H_y (I, DI)	44
4.1.1	Data availability, reaction channels and energetics	44
4.1.2	Total and partial cross sections	46

CONTENTS

4.2	Electron-impact dissociative excitation of C_3H_y to neutrals (DE)	47
4.2.1	General remarks, reaction channels and energetics	47
4.2.2	Total and partial cross sections	48
4.3	Electron-impact dissociative excitation of $C_3H_y^+$ ions (DE ⁺)	49
4.3.1	General remarks, reaction channels and energetics	49
4.3.2	Total and partial cross sections	51
4.4	Electron-impact dissociative ionization of $C_3H_y^+$ ions (DI ⁺)	51
4.4.1	General remarks, reaction channels and energetics	51
4.4.2	Total and partial cross sections	52
4.5	Dissociative electron recombination with $C_3H_y^+$ (DR)	52
4.5.1	Data availability, reaction channels and energetics	52
4.5.2	Total and partial DR rate coefficients	54
4.6	Charge exchange and particle rearrangement reactions of protons with C_3H_y , (CX)	55
4.6.1	Data availability, reaction channels and energetics	55
4.6.2	Charge exchange cross sections	56
5	Unified Analytic Representation of Total Cross Sections	57
5.1	General considerations	57
5.2	Unified total cross sections for electron-impact processes	58
5.3	Unified cross section for resonant charge exchange reactions	60
6	Reaction Rate Coefficients	61
6.1	Electron-impact collision processes	61
6.2	Charge exchange processes	64
7	Concluding Remarks	65
8	References	68
9	Tables	73
A	Appendix	110
A.1	Values of fitting parameters I_c and A_i in Eq.(47) for total and partial ionization cross sections of C_2H_y ($y = 1 - 6$).	110
A.2	Values of fitting parameters I_c and A_i in Eq.(81) for total ionization cross sections of C_3H_y ($y = 1 - 8$) and partial ionization cross sections of C_3H_8	117

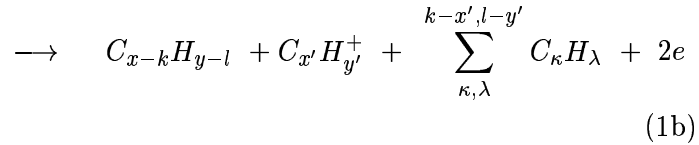
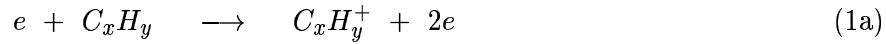
1 Introduction

The interaction of a hydrogen plasma with the carbon-containing wall or with divertor plate materials of a fusion device leads to generation of hydrocarbon molecules C_xH_y that are released into the plasma. In subsequent collisions with plasma electrons and protons, C_xH_y molecules are ionized and dissociated, producing a broad spectrum of $C_{x'}H_{y'}$ and $C_{x'}H_{y'}^+$ hydrocarbon species with $1 \leq x' \leq x$, $1 \leq y' \leq y$, as well as H, H_2 , $C_{x'}$ ($1 \leq x' \leq x$), and their ions. These processes obviously play an important role in the transport and radiation of hydrocarbon species in the plasma (as well as carbon atoms and molecules). The information on their cross sections (or rate coefficients) and reaction energetics is, therefore, a crucial element in any transport analysis or diagnostic study involving, amongst others, these species.

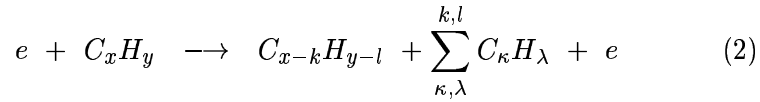
Laboratory experiments show that under hydrogen ion or atom bombardment of carbon materials with impact energies in the range $\sim 1 - 100$ eV, the most abundant constituents of released hydrocarbon fluxes are CH_3 , CH_4 , C_2H_2 , C_2H_4 , C_2H_6 and C_3H_8 [1]. The contribution of heavier hydrocarbons, C_2H_y and C_3H_y , to these fluxes becomes increasingly larger with decreasing the ion impact energy, and are even dominant in the sub-eV region.

The most important electron-impact processes of C_xH_y molecules and their ions $C_xH_y^+$ are:

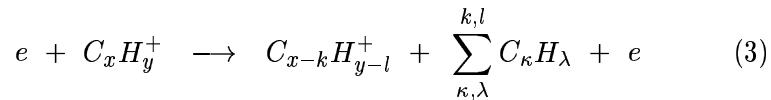
1) Direct (I) and dissociative (DI) ionization of C_xH_y :



2) Dissociative excitation (DE) of C_xH_y neutrals:

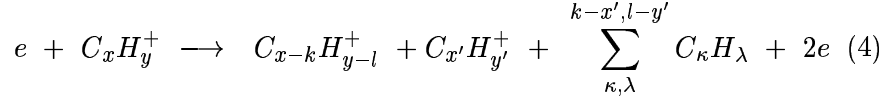


3) Dissociative excitation (DE⁺) of $C_xH_y^+$ ions:

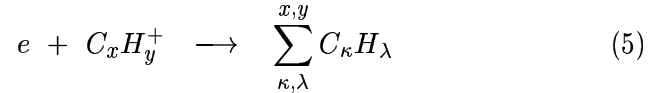


1 Introduction

4) Dissociative ionization (DI⁺) of C_xH_y⁺ ions:



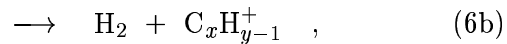
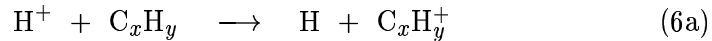
5) Dissociative recombination (DR):



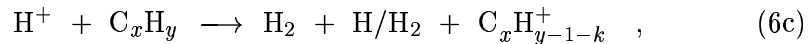
where the summations in (1b)–(5) go over all dissociative channels. The typical thresholds of reactions (1)–(3) are in the range $\sim 5 - 20$ eV, those of reactions (4) are above ~ 25 eV, whereas the DR process is always exothermic (with no threshold).

The most important processes of plasma protons with C_xH_y molecules are:

6) Charge exchange and particle rearrangement (CX):



of which the rearrangement channel (6b) is important only at collision energies below ~ 1 eV. In the thermal energy region also the process of dissociative particle rearrangement may take place,



particularly when the reaction is highly exothermic and the number of H atoms in the molecule is large. The number of hydrocarbon species C_xH_y and C_xH_y⁺ with $x = 1 - 3$ and $1 \leq y \leq 2x + 2$ is 36, and the number of important reactions comprised by processes (1)–(6) is very large. On the other hand, the experimental and theoretical cross section information on these reactions is very limited. It covers mainly the "stable" species (non-radicals) and, in most cases, only the total cross sections (without identification of individual reaction channels). In plasma modeling or diagnostic applications, however, a complete set of channel resolved cross section data is required for a given family (or families) of hydrocarbons (C_xH_y and C_xH_y⁺, with fixed x). In this situation, the unavailable cross section information has to be generated ("derived") on the basis of the available one, and by using certain well established cross section scaling rules and other well grounded physical arguments. Using such an approach, a complete cross section database for the methane family (CH_y, CH_y⁺, $1 \leq y \leq 4$) of hydrocarbons has been established recently [2], including also the information on

2 Basic Properties of Hydrocarbons and their Collisions with Electrons and Protons

reaction energetics (energy loss by reactants and gain by reaction products) required as input in kinetic (e.g. Monte-Carlo) transport codes [3]. That approach will be used also in the present work. We mention that the earlier database on collision processes of the methane family of hydrocarbons [4] is greatly superseded by the recent one [2], both in terms of accuracy and the number of reaction channels included. The process (4) was omitted in Ref. [4] altogether.

In the present work we consider the collision processes (1)–(6) for the ethane (C_2H_y , $C_2H_y^+$; $1 \leq y \leq 6$) and propane (C_3H_y , $C_3H_y^+$; $1 \leq y \leq 8$) families of hydrocarbons. An attempt was made recently [5] to construct a collision cross section database for these hydrocarbon species (excluding C_3H_7 , C_3H_8 , and their ions). This database, however, does not include processes (3) and (4), does not take into account the most recent experimental and theoretical information on I/DI, DR and CX processes for these systems, and the physical basis of "derived" cross sections in most cases is difficult to justify. An adequate account of recent experimental and theoretical data for I/DI and CX processes of C_xH_y systems, as well as of the understanding of physical mechanisms governing these processes, was recently made, respectively, in Ref. [6] and Ref. [7]. The parts of the present work related to I/DI and CX processes of $C_{2,3}H_y$ will be based on the cross section information contained in these references.

The organization of this report is as follows. In the next section we give some general information on the basic properties of C_xH_y hydrocarbons and their collision processes with electrons and protons (including the cross section scaling properties and reaction energetics). In Section 3 we consider processes (1)–(6) for the $C_2H_y / C_2H_y^+$ "ethane family" of hydrocarbons, while in Section 4 we consider the collision processes of C_3H_y and $C_3H_y^+$ ("propane family"). The basic cross section and reaction energetics information for all studied collision systems and reactions is given in these two sections. In Section 5, we give unified analytic expressions for the total cross sections of processes (1)–(6) for all hydrocarbon species $C_xH_y / C_xH_y^+$ with $x = 1 - 3$ and $1 \leq y \leq 2x + 2$. In section 6, approximate analytic expressions are presented for the rate coefficients of all considered reactions. Finally, in section 7 we give some concluding remarks.

2 Basic Properties of Hydrocarbons and their Collisions with Electrons and Protons

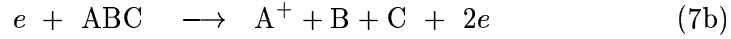
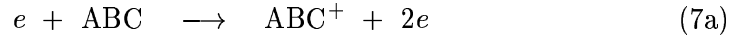
In this section we provide certain basic information on the properties of hydrocarbon molecules and their collision processes with electrons and protons that will be frequently used in Sections 3 and 4 for determination the total and partial cross sections for processes (1)–(6), their threshold energies and the energetics of individual reaction channels. The provided

2.1 Thermo-chemical and energy structure properties of C_xH_y

information and the discussions in this section hold for all hydrocarbons C_xH_y ($x = 1 - 3$; $1 \leq y \leq 2x + 2$) and their ions.

2.1 Thermo-chemical and energy structure properties of C_xH_y

The energy threshold (E_{th}) of all endothermic reactions, like those represented by Eqs. (1)–(4), is a parameter that critically affects the magnitude of inelastic cross section in general, and particularly in the near-threshold region ($E_{th} \leq E \lesssim 2E_{th}$). In the case of direct ionization (I), the threshold is defined by the ionization potential (I_p) of the target (C_xH_y or $C_xH_y^+$), while in case of dissociative processes (DI, DE, DE^+ and DI^+) the reaction threshold is defined by the "appearance potential" (A_p) of reaction products. Both I_p and A_p can be measured (A_p for a given process only) experimentally. They also satisfy certain thermo-chemical relations. For instance, for the direct and dissociative ionization channels of a molecule A B C, namely, for the processes



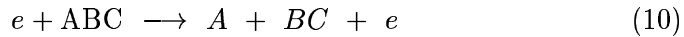
I_p (for (7a)) and A_p (for (7b)) can be expressed as

$$I_p(ABC^+) = \Delta H_f^0(ABC^+) - \Delta H_f^0(ABC) + \Delta E \quad (8)$$

$$A_p(A^+) = \Delta H_f^0(A^+) + \Delta H_f^0(B) + \Delta H_f^0(C) - \Delta H_f^0(ABC) + \Delta E \quad (9)$$

where $\Delta H_f^0(X)$ is the heat of formation (enthalpy) of particle X at $T=273K$, and ΔE is the (possible) internal excitation energy of the fragments. (It is well assumed that the fragments are in their ground state, i.e. $\Delta E = 0$. If it is not the case, then that fact can be explicitly accounted for by writing Eqs. (8), (9) for that specific channel, i.e. by associating ΔE with ΔH_f^0 for the excited product(s). Therefore, we may always set $\Delta E = 0$ in Eqs. (8) and (9).)

For the dissociative excitation (to neutrals) process



the appearance potential (for this specific fragmentation) is

$$A_p(A) = A_p(BC) = \Delta H_f^0(A) + \Delta H_f^0(BC) - \Delta H_f^0(ABC) \quad (11)$$

It is obvious that Eq. (11) also defines the dissociation energy D_0 of the molecule ABC with respect to its A+BC dissociation channel. If ABC represents a positive molecular ion, ABC^+ , then its dissociation energy for the specific fragmentation (e.g by electron impact)



2.1 Thermo-chemical and energy structure properties of C_xH_y

is

$$\begin{aligned} D_0(ABC^+ \rightarrow B^+ + AC) &= A_p(B^+) = A_p(AC) \\ &= \Delta H_f^0(B^+) + \Delta H_f^0(AC) - \Delta H_f^0(ABC^+) \end{aligned} \quad (13)$$

We note that Eq. (8) connects $\Delta H_f^0(X^+)$ with $I_p(X)$ and $\Delta H_f^0(X)$,

$$\Delta H_f^0(X^+) = \Delta H_f^0(X) + I_p(X), \quad (14)$$

so that the appearance potentials (and dissociation energies) for dissociative excitation and ionization processes involving positive molecular ions (e.g. DE^+ and DI^+ processes) require knowledge of ΔH_f^0 and I_p for the corresponding neutral species only. In Table 1 we give the values of ΔH_f^0 and I_p for all C_xH_y molecules with $x = 1 - 3$ and $1 \leq y \leq 2x + 2$ taken from Ref. [8]. Included in Table 1 are also the ΔH_f^0 and I_p values for H, H_2 , C, C_2 and C_3 (from the same reference) which are also needed in determination of energetics of some dissociative processes. We note that for some of the considered C_xH_y species, this more recent source gives somewhat different values for ΔH_f^0 and I_p than the earlier recommended values [9], which were used in Refs. [3, 6, 7]. We also note that several of C_2H_y (e.g., C_2H_2 , C_2H_5), and almost all C_3H_y molecules, appear in two or more isomeric forms (see Table 2. In Table 1 are included the isomers with the lowest heat of formation, assuming that their abundance in hydrocarbon fluxes released from carbon plasma facing materials in fusion devices is significantly larger than that of other isomers (i.e. less energy is required for their formation on carbon surfaces). The values of ΔH_f^0 and I_p given in Table 1 will be used throughout in this work.

For most of the considered hydrocarbon molecules bound excited states have been experimentally observed. The lowest of them are listed in Table 3, compiled from Ref. [8]. These excited states play an important role in considered electron-impact processes, affecting particularly their energetics. For instance, the dominant mechanism of dissociative recombination of an ion AB^+ requires existence of doubly excited state AB^{**} of its parent molecule, which in the dissociation limit correlates with an excited state of one of reaction products. For the DE process (2), more important role play the non-observable dissociative (anti-bonding) excited states of C_xH_y and the bound states that quickly pre-dissociate. Information about these states can be provided only through elaborate quantum-chemistry molecular structure calculations that presently exist only for CH and C_2 [10, 11]. Stable bound states of the $C_xH_y^+$ ions have so far been observed only for CH_4^+ (three states) and $C_2H_2^+$ (two states) [8]. Quantum-chemistry calculations for CH^+ [12, 13] have shown that many bound states can be formed in this system, the vast majority of which pre-dissociates along the numerous dissociative states of the ion. For other $C_xH_y^+$ ions such calculations do not exist, but the physical picture has to be similar.

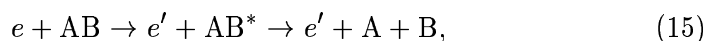
2.2 Basic relations for reaction energetics

2.2 Basic relations for reaction energetics

Kinetic Monte-Carlo particle transport modeling codes require information not only about the reaction rate coefficient but also information about the energy and momentum of reactants and reaction products [3]. Total energy and momentum of the collision system should, of course, be conserved in the collision event. We shall discuss here only the energy conservation aspect; more specifically, the energy lost by the reactants, or gained by reaction products (including any involved electrons). Since all the processes considered in the present work (except the direct electron-impact ionization and CX) involve excited states of C_xH_y and $C_xH_y^+$ (pre-dissociating bound and anti-bounding states), it is obvious that for determining the energy loss of reactants and energy gain by the products, knowledge of the energies of these excited states is required. As we mentioned in the preceding sub-section, such knowledge is presently available only for the CH/CH⁺ system. In this situation, the determination of reaction energetics for other collision systems has to rely on certain plausible assumptions about the energies of excited electronic dissociating states. Such a highly approximative approach, however, cannot offer more than rough estimates for the average values of the energy lost/gained in a reaction. Below we briefly describe the methodology and the assumptions (as well as the physical arguments behind them) used in determination of energetics of dissociative processes studied in this work. (For the direct ionization process, $C_xH_y \rightarrow C_xH_y^+ + e$, the energy lost by the incident electron coincides with the ionization potential of C_xH_y .)

In an electron-impact dissociative process, such as represented by Eq. (10), or Eq. (12), the minimum energy lost by the electron equals to the dissociation energy, D_0 (for a given dissociation mode). This energy is sufficient to bring the system from its initial (e.g ground) vibrational state to its dissociative continuum, with zero kinetic energy of the products, and it corresponds to the appearance potential A_p for that particular dissociation channel. However, this dissociation mechanism, involving overlap of the initial (discrete) and final (continuum) state wave-function of the system is rather weak, particularly when the initial state is the ground vibrational state. Much stronger is the dissociative excitation mechanism which involves a strong coupling (e.g. via a dipole, or higher multi-pole interaction) of the initial (ground) electronic state of the molecule with its lower excited dissociative electronic states. With respect to the dissociative excitation mechanism, the contribution of direct vibrational dissociation to the total dissociation cross section can (usually) be neglected.

The energy threshold for the electron -impact dissociative excitation of a molecule AB, i.e. for the process

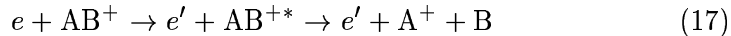


2.2 Basic relations for reaction energetics

is obviously

$$E_{th}^{DE} = E_{exc}(AB^*) \equiv D_0(AB) + \Delta E_{exc}(AB^*) \quad (16)$$

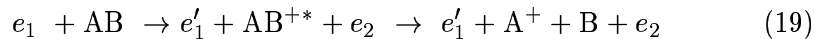
where $E_{exc}(AB^*)$ is the excitation energy of AB^* dissociative state at the inter-nuclear distance which corresponds to the equilibrium nuclear distance in AB ("vertical" Frank-Condon transition), $D_0(AB)$ is the dissociation energy of AB to produce the fragments A+B, and $\Delta E_{exc}(AB^*)$ is the part of excitation energy of AB^* above the dissociation limit, A+B. The energy lost by the incident electron in order to induce this process is, thus, $E_{el}^{(-)} = E_{th}^{DE}$. (The "prime" on the electron symbol "e" on the right-hand-side of Eq. (15) indicates that, after the collision, the electron has an energy reduced by $E_{el}^{(-)}$.) The amount of energy $\Delta E_{exc}(AB^*)$ is released in the dissociation process and constitutes the total kinetic energy E_K of products A and B. (In Eq. (15) A and B may obviously represent complexes of more than one atom. Consequently, the number of dissociation products on the right side of Eq. (15) may be larger. This, however, does not change the form of Eq. (16). $D_0(AB)$ is always relates to the specific mode of dissociation.) For the dissociative excitation of AB^+ ions (DE^+),



$E_{th}^{DE^+}$ is defined by a relation analogous to (16),

$$E_{th}^{DE^+} = E_{exc}(AB^{+*}) = D_0(AB^+) + \Delta E_{exc}(AB^{+*}) \quad (18)$$

For the dissociative ionization process (DI)



where e_1 (e_1') is the incident electron before (after) the collision and e_2 is a target electron ejected in the continuum, the situation is slightly different. (We note that electron exchange effects, pronounced at low collision energies, make the distinction between e_1' and e_2 ambiguous. This ambiguity is resolved in the theory by explicitly taking into account these effects through proper symmetrization of the two-electron wave function.) In order to bring the system AB from its ground (electronic and vibrational) state to the dissociative excited state AB^{+*} by a vertical Franck-Condon transition, the incident electron has to loose an amount of energy $E_{el}^{(-)}$

$$E_{el}^{(-)DI} = I_p(AB) + E_{exc}(AB^{+*}) = I_p(AB) + D_0(AB^+) + \Delta E_{exc}(AB^{+*}) \quad (20)$$

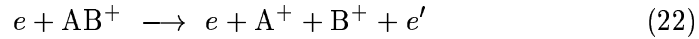
where I_p is the ionization potential of AB and $E_{exc}(AB^{+*})$ is the energy of excited dissociative state AB^{+*} at the equilibrium inter-nuclear distance of AB molecule. The measured energy spectra of products from electron-impact dissociative ionization of some hydrocarbon molecules (see, e.g. [14])

2.2 Basic relations for reaction energetics

show that the dissociation products may also have energies close to zero. This can be an indication that some of the AB^{+*} excited states energetically lie (in the Franck-Condon region) not far from their dissociation continuum or, else, that because of the large value of transition energy ($I_p \sim 10$ eV, $D_0(AB^+) \sim 4$ eV), the transition of the system to the dissociative AB^{+*} state is not anymore vertical. Thus, in the case of dissociative ionization of C_xH_y , it is appropriate to define the reaction threshold as

$$E_{th}^{DI} \simeq I_p(AB) + D_0(AB^+). \quad (21)$$

The energetics of the electron-impact dissociative ionization process of positive molecular ions (DI^+)



has some specific aspects. The process takes place when AB^+ ion from its initial (e.g. ground) state is brought to the repulsive potential curve of $(A^+ + B^+)$ system by a vertical Franck-Condon transition. The threshold energy for this process is, thus,

$$\begin{aligned} E_{th}^{DI+} &= I_p(AB^+) + \Delta E_{exc}(A^+, B^+), \\ I_p(AB^+) &= D_0(AB^+ \rightarrow A + B^+) + I_p(A) \end{aligned} \quad (23)$$

where $\Delta E_{exc}(A^+, B^+)$ is the Coulomb interaction energy of ions A^+ and B^+ at the inter-nuclear distance equal to the equilibrium nuclear distance of the AB^+ ion, i.e. $\Delta_{exc}(A^+, B^+) = 1/r_e(AB^+)$, (in the atomic units for the energy and distance). With respect to other dissociative processes, where the process can take place through many dissociative excited states (AB^* for DE, and AB^{+*} for DE^+ and DI), the dissociative ionization of ions can proceed only via a single "excited" state, $(A^+ + B^+)$. The total kinetic energy of reaction products A^+ and B^+ is, thus, defined uniquely,

$$E_K^{DI+} = \Delta E_{exc}(A^+, B^+) = \frac{27.2/[eV]}{r_e(AB^+)/[a_0]} \quad (24)$$

where a_0 is the Bohr radius. In the case of other dissociative processes (DE , DE^+ and DI), one can plausibly assume that dominant contribution to the cross section of the process comes from the low-lying dissociative excited states of the target (the excitation cross sections are inversely proportional to the transition energy), and, in absence of any quantitative information about the excitation energy of these states in the Franck-Condon region, introduce the concept of an "average" excited dissociative state (\overline{AB}^* or \overline{AB}^{+*}) as a representation of the group of low-lying dissociative states. Consequently, the threshold energies for these processes (except E_{th}^{DI}), the associated electron energy losses and the total kinetic energies of reaction products ($= \Delta E_{exc}(\overline{AB}^*)$, or $\Delta E_{exc}(\overline{AB}^{+*})$) can be characterized only by

2.2 Basic relations for reaction energetics

certain mean values. Inherent to the mean values for E_{th} , $E_{el}^{(-)}$ and E_K is uncertainty of about 0.5 to 1 eV, and in certain cases even larger. For $E_{el}^{(-)}$ and E_K , this uncertainty is not much relevant because these quantities have a "natural" distribution of a few eV, caused by the finiteness of Franck-Condon region of the (target) initial vibrational state and the repulsive character of the potential energy of dissociative state.

Since the dissociation energies $D_0(AB)$ and $D_0(AB^+)$ can be calculated from the known values of the heat of formation of AB and AB^+ , and their fragments (see Table 1 and Eq. (14)), the determination of E_{th} (or $E_{el}^{(-)}$) and E_K requires knowledge only on $\Delta E_{exc}(\overline{AB}^*)$ (for the DE process) and $\Delta E_{exc}(\overline{AB}^{+*})$ (for DE^+ and DI) (see Eqs. (16), (18) and (20)). Since $\Delta E_{exc}(\overline{AB}^+)$ and $\Delta E_{exc}(\overline{AB}^{+*})$ are directly related to the energies of the dissociation products (see later, Eq. (26)), they can be determined from the energy spectra of products, if there are experimentally known. Alternatively, they can be also determined from the experimental thresholds for the corresponding reaction channels by using the relations (16) and (18), respectively. Thus, the experimental thresholds for the H- and H_2 -production channels of dissociative excitation of CH_y^+ ions [15, 16] consistently show that $\Delta E_{exc}(AB^{+*})$ for the methane family of ions is related to $D_0(AB^+)$ by

$$\Delta E_{exc}(\overline{AB}^{+*}) = \chi D_0(AB^+), \quad \chi \simeq 0.3 - 0.35 \quad (25)$$

This relation is consistent also with the mean value of measured energies of H products from the DI process $e+CH_4 \rightarrow CH_3^+ + H + 2e$ [17]. In the present work we shall assume that relation (25) holds also for the higher hydrocarbon ions, $C_{2,3}H_y^+$, and the value $\chi = 0.35$ will generally be used. The only hydrocarbon molecule for which $\Delta E_{exc}(\overline{AB}^*)$ can be estimated is CH, for which the energies of lowest excited states are available [10]. The span of these energies suggests that the relation $\Delta E_{exc}(\overline{AB}^*) \simeq 0.35 D_0(AB)$ can also be used for this molecule. In absence of any similar information for $C_{2,3}H_y$ molecules, we shall use, as a rule, this relation for them as well.

It is noteworthy to emphasize that the above estimates of $\Delta E_{exc}(\overline{AB}^*)$ and $\Delta E_{exc}(\overline{AB}^{+*})$ relate to the lowest dissociative excited states of AB and AB^+ , respectively, which give the main contribution to the dissociative (excitation or ionization) cross sections. The higher dissociative states, while not so much important for the absolute value of the cross section, can nevertheless affect the mean electron energy loss and the mean total kinetic energy of dissociation products. An additional amount of energy, $\delta E_{exc}(\overline{AB}^*)$ should be added to $\Delta E_{exc}(\overline{AB}^*)$ (and similarly for $\Delta E_{exc}(AB^{+*})$) in order to account for this effect. Since, generally, the higher dissociative excited states are (co-) related to the bound excited states (when these exist), a rough estimate of $\delta E_{exc}(\overline{AB}^*)$ can be made from the known energies of the latter (see Table 3). This approach was used when determining $\Delta E_{exc}(\overline{AB}^*)$ and

2.2 Basic relations for reaction energetics

$\Delta E_{exc}(\overline{AB}^{+*})$ in Ref. [2]. However, in view of involved uncertainties, we shall refrain from it in the present work.

We also note that the relation $\Delta E_{exc} = \chi D_0$, with $\chi \simeq 0.35$ is not expected to be applicable when D_0 is very small ($\lesssim 1$ eV, as in the case of C_xH_y and $C_xH_y^+$ with $x = 2, 3$ and $y \approx 2x$). A more appropriate value for χ in such cases would be $\chi \sim 1$. It is also obvious that the upper limit for $\Delta E_{exc}(\overline{AB}^*)$ (or $\Delta E(\overline{AB}^*) + \Delta E_{exc}(\overline{AB}^*)$) is the value $I_p(AB) - D_0(AB)$, above which the excited states become auto-ionizing.

The total kinetic energy \overline{E}_K released in the dissociation process is shared among the products inversely proportionally to their masses. If the number of reaction products is N , and their masses are M_1, M_2, \dots, M_N , then the kinetic energy of the product j with mass M_j is given by

$$\overline{E}_{Kj} = \frac{\mu}{M_j} \overline{E}_K \quad (26)$$

where μ is the reduced mass of the products. (In all previous discussions by reaction products we meant only the fragmented particles of the target molecular species; not the scattered or ejected electrons.)

The energetics of dissociative recombination (DR) process



is characterized by the absence of a threshold. Even electrons with zero kinetic energy, accelerated in the Coulomb field of AB^+ ion, can be captured on a doubly excited dissociative state (AB^{**}) of the parent molecule, that dissociates producing (normally) an excited product. The total kinetic energy of the products from the DR process (27) induced by an electron with kinetic energy (in the center-of-mass system of reference) E^{el} is

$$E_K = E^{el} + E_K^{(0)} - E_{exc}(B^*) \quad (28)$$

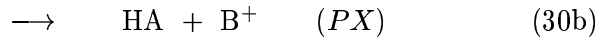
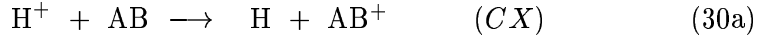
where $E_{exc}(B^*)$ is the excitation energy of B^* product, and

$$E_K^{(0)} = \Delta H_f^0(AB^+) - (\Delta H_f^0(A) + \Delta H_f^0(B)) \quad (29)$$

with $\Delta H_f^0(X)$ being the heat of formation of particle X in its ground state. The dissociation products share the energy E_K according to Eq. (26). It should be noted that evolving along the repulsive state (AB^{**}), the system passes through regions of inter-nuclear distance of A and B (or, in the multi-product case, regions on a hyper-surface) where the state AB^{**} is strongly coupled with other excited states of AB (including its Rydberg series), resulting in possible production of many excited B^* (or A) products. Some of these states may be bound and, through pre-dissociation, may even lead to ground state products, $A+B$.

2.3 General properties of collision cross sections

The charge exchange (CX) process of H^+ with all studied hydrocarbon molecules are exothermic, but some particle rearrangement (PX) channels may be endothermic. The exothermicity ΔE_{fi} of reactions



can be expressed as

$$\Delta E_{fi} = \sum_{\text{reactants}} \Delta H_f^0(X) - \sum_{\text{products}} \Delta H_f^0(Y) \quad (31)$$

where the first and second sum include all reactants and products, respectively and i and f in ΔE_{fi} indicate the initial and final arrangement of the particles involved in the reaction. We note that the molecular species in Eq. (31) are assumed to be in their ground vibrational (and rotational) state. If molecular particle X is vibrationally excited after the process, the value of its vibrational energy has to be subtracted from the value of $\Delta H_f^0(X)$. The possibility of vibrational excitation of molecular products in reactions (30) can considerably reduce the reaction exothermicity, and may even bring the initial and final reaction particle arrangement into an energy resonance ($\Delta E_{fi} = 0$). The establishment of energy resonance between the entrance and exit channel of a charge exchange reaction has dramatic consequences for the magnitude of its cross section (see Sects. 3.6 and 4.6. The reaction exothermicity ΔE_{fi} (after its correction for the possible vibrational excitation of reaction products) is released in the kinetic energy of products, which share this energy in accordance with Eq. (26).

The question of energy distribution of ejected electrons in I, DI, and DI^+ processes will not be discussed here. We refer to Ref. [18] for information on this subject.

Regarding the angular distribution of heavy-particle reaction products, it is generally assumed that it is isotropic. This assumption is based on the consideration that for plasma temperatures higher than ~ 0.5 eV, the molecules and their ions in the plasma are rotationally highly excited, so that averaging over the rotation of a selected molecular axis (with respect to the electron velocity vector) results in an isotropic angular distribution of dissociation products.

2.3 General properties of collision cross sections

2.3.1 Energy behaviour of cross sections

Both total and partial (for individual channels) cross sections for electron-impact processes considered in the present work that exhibit a threshold (such as I, DI, DE, DE^+ and DI^+) have similar energy behaviour. This

2.3 General properties of collision cross sections

behaviour is characterized by a relatively sharp rise of the cross section immediately after the threshold, a broad maximum in the energy region 70–100 eV (but ~ 30 –50 eV for DE^+), and a decrease beyond the maximum in the form $E^{-1} \ln(E)$, in accordance with the Bethe-Born theory. Only for those individual reaction channels, in which a dipole transition is not involved, the high energy decrease of the cross section is faster ($\sim E^{-1}$ or $\sim E^{-3}$). Hence, except for dissociative recombination, the total and partial cross sections for studied electron-impact processes have the general form

$$\sigma = A \left(1 - \frac{E_{th}}{E}\right)^\alpha \frac{1}{E} \ln(e + cE) \quad (32)$$

where E is the collision energy, E_{th} is the threshold energy, A , α and c very weakly depend on E and can be considered as constants, and $e = 2.71828\dots$ is the base of natural logarithm, introduced in Eq. (32) for convenience. The parameter α determines the near-threshold behaviour of the cross section and is different for different types of processes. The range of its values is between $\alpha = 1.55$ (for DI^+) to $\alpha = 3.0$ (for I, DI, DE) [2]. The previous studies of electron-impact processes of hydrocarbon molecules ([2, 6]), have shown that for a given process the parameter α and c remain to a high degree constant when C_xH_y varies, while the parameter A changes. The changes of values of A , when the number of C and H atoms in C_xH_y varies, follow certain rules, meaning that the cross sections of electron-impact processes of C_xH_y satisfy certain scaling relationships.

2.3.2 Cross section scaling relationships

As early as in 1966, it was experimentally observed [19] that the cross sections for total electron-impact ionization of hydrocarbon molecules C_xH_y , with x and y ranging up to $x = 5$ and $y = 12$, show a striking linearity with the number x of C atoms in C_xH_y for the high collision energies (≥ 600 eV) at which the experiments were performed. The analysis of more recent total ionization cross section data for C_xH_y molecules has showed that the x -linearity of these cross sections can be extended down to very low (~ 20 –30 eV) energies [6]. Moreover, this analysis has also showed that the total ionization cross sections (σ_{ion}^{tot}) for C_xH_y molecules ($x = 1 - 3$; $1 \leq y \leq 2x + 2$) obey a similar linearity with respect to the number y of H atoms in C_xH_y for any fixed value of x . It was demonstrated in [6] that the y -linearity of $\sigma_{ion}^{tot}(\text{C}_x\text{H}_y)$ is also strictly preserved down to collision energies of ~ 20 –30 eV.

The observed x -linearity of $\sigma_{ion}^{tot}(\text{C}_x\text{H}_y)$ was related in Ref. [9] to the additivity rules for the strengths of chemical bonds in poly-atomic molecules. These rules, discovered many years ago [20], do not lose their validity when the molecule is subjected to a long-range force (e.g. a multi-pole interaction) or to de-localization of its free charge (as it happens during the collisions)

2.3 General properties of collision cross sections

[21]. Because of their "stability" with respect to external perturbations, or to de-localization of the free molecular charge, the additivity rules remain valid irrespective of the type of process the molecule (or molecular ion) undergoes in a collision. Indeed, it was shown in Ref. [6] that the experimental partial ionization cross sections (both I and DI) of C_xH_y ($x = 1-2$; $1 \leq y \leq 2x+2$) also exhibit linear dependences on x and y , while in Ref. [2] the x - and y -linearity was demonstrated for the DE process of C_xH_y (see also Section 3.2). Therefore, the additivity rules for the strengths of chemical bonds should manifest themselves in linear x - and y -dependences of total and partial cross sections of other electron-impact processes studied here. Hence, the energy independent factor A in Eq. (32) for the cross section of an inelastic electron-impact process with C_xH_y or $C_xH_y^+$ can be written as

$$A = A_0 L(x, y) \quad (33)$$

where A_0 very weakly depends on E (and can be replaced by a numerical constant) and $L(x, y)$ is a function that linearly depends on both x (for fixed y) and y (for fixed x) for energies above 20 – 30 eV. The forms of $L(x, y)$ for specific processes will be determined in sections 3) and 4) where these processes are discussed, whereas the general forms of $L(x, y)$ for all studied types of processes will be given in section 5.

2.3.3 Cross section branching ratios for multichannel processes

As indicated by Eqs. (1)–(6), all studied processes in this work have many reaction channels, all of which (except the direct ionization, (1a), and the pure electron capture, (6a)) are related to the molecular dissociation (or particle rearrangement in the case of CX process). The total cross section of a given type of process for a given C_xH_y molecule is the sum of partial cross sections of individual reaction channels of that process for the considered molecule. The contribution of a particular reaction channel j to the total cross section σ_λ^{tot} of the process λ at a given collision energy E is given by the branching ratio

$$R_j^\lambda(E) = \frac{\sigma_j^\lambda(E)}{\sigma_\lambda^{tot}}, \quad (34)$$

where $\sigma_j^\lambda(E)$ is the partial cross section of channel j . Obviously, this relation can be used to determine $\sigma_j^\lambda(E)$ when $\sigma_\lambda^{tot}(E)$ and $R_j^\lambda(E)$ are known. Since the information for $\sigma_\lambda^{tot}(E)$ is much more available (experimentally or theoretically) in the literature than that for $\sigma_j^\lambda(E)$, determination of $R_j^\lambda(E)$ on the basis of theoretical or empirical arguments would be very useful for deriving the partial cross sections from the total one. We shall discuss here the branching ratios $R_j^\lambda(E)$ for the electron-impact processes I, DI, DE, DE⁺ and DI⁺ (Eqs. (1)–(4)) which show certain general properties.

2.3 General properties of collision cross sections

Direct measurements of $R_j^\lambda(E)$ (or of the "relative" partial cross sections $\sigma_j^\lambda(E)$) have been performed in the early sixties for the direct and dissociative ionization channels of C_2H_2 (7 channels), C_2H_4 (10 channels) and C_2H_6 (13 channels) at two electron impact energies: 75 eV and 3.5 MeV [22]. It was found that the values of $R_j^{ion}(7.5 \text{ eV})$ and $R_j^{ion}(3.5 \text{ MeV})$ for a given molecule are the same (within the experimental uncertainties). Using more recent experimental data for partial ionization cross sections of CH_4 (7 channels), C_2H_6 (13 channels) and C_3H_8 (23 channels) available in the energy range from threshold to 900 eV (200 eV for CH_4), it was shown in Ref. [6] that the cross section branching ratios R_j^{ion} for these molecules remain the same in the entire energy region above $\sim 20 - 30 \text{ eV}$ (within the uncertainties of the data, 8-10 %). The observed energy invariance of channel branching ratios for this process indicates that the basic dynamical mechanism for all ionization channels is the same, and the differences in the values of R_j^{ion} are related to structural factors.

The determination of R_j^{ion} in Ref. [6] for the reactions with unknown partial cross sections was based on the linear x - and y -dependences of both σ_{ion}^{tot} and σ_j^{ion} , and on the sufficient experimental information on both σ_{ion}^{tot} and σ_j^{ion} for normalization of these dependences. Similar procedures were used in Ref. [2] to determine R_j^λ for other processes. For the C_2H_y and C_3H_y molecules, however, for which the information on σ_j^λ is completely absent (except for ionization), we have to adopt another approach to determine R_j^λ . We first note that there is a strong correlation of the magnitude of partial cross section σ_j for the reaction channel j with the value of its threshold energy, $E_{th,j}$. From the Bethe-Born theory for ionization and excitation of atoms by charged particles, it follows that $\sigma_j \sim E_{th,j}^{-2}$. However, the dissociative processes have a more complex nature (for instance, in DI processes E_{th} is not related to the electron binding energy but to the appearance potential), and the dependence of σ_j on $E_{th,j}^{-2}$ can be quite different. In accordance with the energy invariance of R_j^λ (at least for $E \gtrsim 20 - 30 \text{ eV}$), we assume that the channel cross sections σ_j^λ have the same energy dependence as σ_λ^{tot} , given by Eq. (32), which extends down to the threshold. Very close to its threshold, the partial cross section behaves (see Eq. (32))

$$\sigma_j^\lambda \sim [(E - E_{th})/E]^{\alpha_\lambda} \simeq [(E - E_{th})/E_{th}]^{\alpha_\lambda}, \quad E \rightarrow E_{th}. \quad (35)$$

The ratio of two partial cross sections σ_1^λ and σ_2^λ with thresholds $E_{th,1}$ and $E_{th,2}$ respectively, in the vicinity of their thresholds is $\sigma_1^\lambda/\sigma_2^\lambda \simeq (E_{th,2}/E_{th,1})^{\alpha_\lambda}$. Since σ_λ^{tot} has the same type of threshold behaviour, then it follows that the branching ratios R_1^λ and R_2^λ in the threshold region are related by

$$\frac{R_1^\lambda}{R_2^\lambda} \simeq \left(\frac{E_{th,2}}{E_{th,1}} \right)^{\alpha_\lambda}. \quad (36)$$

2.3 General properties of collision cross sections

Assuming that the two branching ratios have the same energy dependence (if any), then the ratio (36) can be extended up to the region $\sim 20 - 30$ eV, when the energy invariance of R_1^λ/R_2^λ certainly holds. The assumption of the same energy dependence of all R_j^λ is highly plausible in view of the similarity of the basic mechanism that governs all reactions of a given type λ . The relation (36), together with the unitarity relation for the branching ratios,

$$\sum_j R_j^\lambda = 1, \quad (37)$$

is sufficient to determine all R_j^λ . If the reaction thresholds appear in the order

$$E_{th,1} < E_{th,2} < E_{th,3} < \dots < E_{th,k} < \dots \quad (38)$$

than the values of R_k^λ are given by

$$R_{k \geq 2}^\lambda = \left(\frac{E_{th,1}}{E_{th,k}} \right)^{\alpha_\lambda} R_1^\lambda, \quad R_1^\lambda = \frac{1}{1 + \sum_{k \geq 2} (R_k^\lambda/R_1^\lambda)} \quad (39)$$

The use of unitarity condition (37) in determination of R_k^λ ensures their validity at sufficiently large energies when all reaction channels are open. However, it is obvious that in the energy region $E_{th,1} < E \leq E_{th,2}$, when only the channel with lowest threshold is open, R_1^λ should be one, while Eq. (39) gives a smaller value. The partial cross section σ_1^λ calculated as $R_1^\lambda \sigma_\lambda^{tot}$ will be reduced. In other words, in any part of the energy region when not all reaction channels are open, the unitarity condition is not satisfied ($\sum_k \sigma_k^\lambda < \sigma_\lambda^{tot}$). In order to satisfy the unitarity condition at any collision energy, R_k^λ have to be modified. This requirement translates into a requirement that R_k^λ depend on energy.

One way to modify R_k^λ in order to account for unitarity in the threshold regions is the replacement of R_k^λ by

$$\tilde{R}_1^\lambda(E) = \frac{R_1^\lambda}{1 - \chi_1 (E_{th,1}/E)^\beta}, \quad \chi_1 = 1 - R_1 \quad (40a)$$

$$\tilde{R}_k^\lambda(E) = \frac{R_k^\lambda}{1 - \chi_k (E_{th,k}/E)^\beta}, \quad \chi_k = 1 - \frac{R_k^\lambda}{1 - \sum_{j=1}^{k-1} \tilde{R}_j^\lambda(E)} \quad (40b)$$

where β is a (positive) parameter. The $\tilde{R}_k^\lambda(E)$ defined by Eq. (40) have the following properties:

$$(i) \quad \tilde{R}_k^\lambda(E) \rightarrow R_k^\lambda, \quad \text{for } E \rightarrow \infty \quad (41a)$$

$$(ii) \quad \sum_{j=1}^k \tilde{R}_j^\lambda(E_k) = 1, \quad (41b)$$

$$(iii) \quad \tilde{R}_1^\lambda(E) \rightarrow 1, \quad \text{for } E \rightarrow E_{th,1} \quad (41c)$$

2.3 General properties of collision cross sections

Hence, the unitarity of \tilde{R}_k^λ is satisfied at every threshold (and for $E \gg E_{th,max}$), but, as evident from the expression for $\tilde{R}_1^\lambda(E)$, Eq. (40a), it is violated at energies between the thresholds. Except for $\tilde{R}_1^\lambda(E)$, however, this violation of unitarity for $E \neq E_{th,j}$ is relatively small, and for each specific reaction channel can be minimized by a suitable choice of parameter β . An optimum choice for β is $\beta \simeq 1.5(\pm 0.2)$. Decreasing β improves the unitarity at $E \neq E_{th,j}$, but the asymptotic values R_k^λ are then reached slowly.

If one slightly departs from the analyticity of this approach for rectifying R_k^λ , one can take $R_1(E) = 1$ in the interval $E_{th,1} < E \leq E_{th,2}$, and use Eq. (40a) only in the region $E > E_{th,2}$. This would result in a (small) discontinuity in the energy dependence of partial cross section $\sigma_1^\lambda(E)$ at $E = E_{th,2}$, which may not affect the continuity of corresponding rate coefficient at all.

We note that Eq. (40b) is a recursive relation for calculation of \tilde{R}_k^λ . The ordering of threshold values according to Eq. (38) is, therefore, essential. The described procedure for determining \tilde{R}_k^λ works best when the values of R_k^λ also follow the ordering of $E_{th,k}$ (i.e. $R_1^\lambda > R_2^\lambda > \dots > R_k^\lambda > \dots$). With the definition (39) for R_k^λ , this is always the case.

Another way of determining $\tilde{R}_k^\lambda(E)$ is to take

$$\tilde{R}_1^\lambda = 1, \quad \tilde{R}_{k \geq 2}^\lambda = 0, \quad \text{for } E_{th,1} \leq E < E_{th,2} \quad (42a)$$

$$\tilde{R}_1^\lambda(E) = \frac{R_1^\lambda}{1 - (1 - R_1^\lambda)(E_{th,2}/E)^\gamma}, \quad E \geq E_{th,2} \quad (42b)$$

$$\tilde{R}_k^\lambda(E) = R_k^\lambda \left[1 - \left(\frac{E_{th,k}}{E} \right)^\gamma \right], \quad E \geq E_{th,k}, \quad k \geq 2 \quad (42c)$$

where γ is a parameter. For $E \rightarrow \infty$, $\tilde{R}_k^\lambda \rightarrow R_k^\lambda$, and for $E = E_{th,k}$ $\tilde{R}_k^\lambda(E_{th,k}) = 0$, $k \geq 2$. The unitarity of $R_k^\lambda(E)$ is not preserved in this approach (except for $E_{th,1} \leq E \leq E_{th,2}$, and $E \gg E_{th,max}$), but the degree of its violation can be regulated by the choice of parameter γ . This parameter also determines how quickly the asymptotic values R_k^λ are reached when E increases. Values of $\gamma \simeq 1.5 - 1.8$ seem to provide an optimum choice. An attractive feature (besides its simplicity) of this approach is that $\tilde{R}_k^\lambda(E)$ are smooth monotonic functions (except for $\tilde{R}_1^\lambda(E)$ at $E = E_{th,2}$), ensuring that $\sigma_k^\lambda(E) = \tilde{R}_k^\lambda(E) \sigma_\lambda^{tot}(E)$ are also such functions.

Finally, the simplest way of improving the values of R_k^λ in the threshold regions is to re-normalize them in each energy interval between two thresholds, so that their unitarity in that interval is ensured, i.e.

$$\tilde{R}_j^\lambda = \frac{R_j^\lambda}{\sum_{i=1}^k R_i^\lambda}, \quad 1 \leq j \leq k, \quad E_{th,k} \leq E \leq E_{th,k+1} \quad (43)$$

Since the value of \tilde{R}_j^λ changes at each next threshold, the partial cross section $\sigma_j^\lambda(E) = \tilde{R}_j^\lambda \sigma_\lambda^{tot}$ experiences discontinuity also at each threshold. When the

2.3 General properties of collision cross sections

number of reaction channels is very large, and reaction thresholds are closely spaced, this approach for determining R_j^λ may not be so bad, especially for R_j^λ in the higher part of the threshold spectrum.

In closing the discussion on $\tilde{R}_k^\lambda(E)$, we would like to note that the unitarity ($\sum_k \tilde{R}_k^\lambda(E) = 1$) and continuity requirements for $\tilde{R}_k^\lambda(E)$ cannot be satisfied simultaneously. The above considered three possible ways for determination of $\tilde{R}_k^\lambda(E)$ demonstrate well this statement. The origin of the problem is the discreteness of the spectrum of threshold energies. The function $F(E_{th,k})$ is highly non-analytic, while the unitarity condition for $R_k^\lambda(E)$ at any energy requires its analyticity. Only at $E = E_{th,k}$ this requirement can be reconciled with the non-analyticity of $F(E_{th,k})$, preserving the analyticity of $\tilde{R}_k^\lambda(E)$ (as in the case of Eqs. (40)). If unitarity is enforced on $\tilde{R}_k^\lambda(E)$ for any E, then \tilde{R}_k^λ becomes also a non-analytic function of E (as in the case of Eqs. (43)).

The determination of branching ratios R_k^λ by Eq. (39) reflects only the role of the threshold on the magnitude of a partial cross section, but not other dynamical features that may characterize a specific reaction channel. Such features are related to the number and type of reaction products, types of chemical bonds broken in a reaction (e.g., C–H, C–C, C=C), etc. To include these specific aspects of a particular reaction channel into its branching ratio R_k^λ , we modify the value of R_k^λ given by Eq. (39) in the form

$$R_k^{\lambda'} = \xi_k^\lambda R_k^\lambda \quad (44a)$$

where the coefficient ξ_k^λ accounts, phenomenologically, for the non-threshold related dynamical aspects of the considered reaction channel. The determination of ξ_k^λ values will be discussed in the following sections when specific collision processes are considered. Generally speaking, for reactions in which only one C–H bond is broken, $\xi_k^\lambda \gtrsim 1$, while for reactions in which more than one C–H bond, or a C–C or C=C bond are broken, $\xi_k^\lambda < 1$. It is obvious that the modified branching ratios $R_k^{\lambda'}$ also must satisfy the unitarity condition

$$\sum_k R_k^{\lambda'} = 1 \quad (44b)$$

The values $R_k^{\lambda'}$ have to be used when calculating \tilde{R}_k^λ from Eqs. (40),(42) or (43). For all studied I/DI, DE⁺ and DI⁺ reactions in this work, the values $R_k^{\lambda'}$ are given in Table 5-7 and 12-14.

3 Collision Processes of C_2H_y and $C_2H_y^+$ with Electrons and Protons

3.1 Electron-impact ionization of C_2H_y (I,DI)

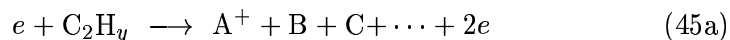
3.1.1 Cross section availability, reaction channels and energetics

The experimental and theoretical database for total and partial ionization cross sections in $e+C_2H_y$ collisions, as well as the procedures for determining the cross sections unavailable in the literature, were described in Ref. [6] in detail. We shall, therefore, present here only a brief account of them.

Absolute total cross section measurements for the electron-impact ionization of the C_2H_y family of molecules have been performed so far only for C_2H_2 [23, 24], C_2H_4 [19, 25, 26] and C_2H_6 [19, 26, 27]. The combined energy range of these experiments extends from threshold to 12 keV. The cross sections of Refs. [19, 25, 27] for C_2H_4 and C_2H_6 are consistent with each other (when shown on a Platzman plot) within 10%, while those of Ref. [26] are consistently somewhat higher. Total ionization cross section calculations have been done within the Binary-Encounter-Born (BEB) method for C_2H_2 [28], C_2H_3 [29], C_2H_4 [30] and C_2H_6 [30]. Generally, the BEB cross sections show good agreement with the experiment.

Extensive partial ionization cross sections measurements have been performed for C_2H_2 [22, 31, 32, 33], C_2H_4 [22], and C_2H_6 [22, 34, 35], which involve respectively 7 (6 in [32, 33]), 10 and 13 (11 in [34]) reaction channels. While in Ref. [22] the measurements were done for only two energies (75 eV and 3.5 MeV), in other measurements they cover the region from threshold up to ~ 1000 eV (~ 2000 in [31]). The experimental data of Ref. [33] (for C_2H_2) and Ref. [35] (for C_2H_6) have a very high (better than 10%) accuracy.

It should be emphasized that the measured partial cross sections in the experiments are related only to the ion-production channels, i.e. they are cross sections $\sigma_{DI}(A^+)$ for the processes



where A^+ is a well specified ion, but the other neutral products are unknown. This reflects the experimental difficulties for detection of neutral reaction products in coincidence with the ionic products. (The latter can be easily identified by mass spectrometry, and their numbers, or relative contribution to the positive ion current resulting from the collision event, easily determined.) Only in the case of direct ionization process, when $A^+=C_2H_y^+$ is the exit reaction channel in Eq. (45a) defined unambiguously. For determining the most important neutral fragmentation channels within a given ion-production channel, one can use the sensitive dependence of the magnitude of the channel cross section on the threshold energy for that

3.1 Electron-impact ionization of C_2H_y (I,DI)

channel. From Eq. (21), it follows that the threshold energies of dissociative ionization channels (or their appearance potentials A_p) are given by (for the reaction (45a))

$$E_{th}^{DI} \simeq A_p^{DI} = \Delta H_f^0(A^+) + \Delta H_f^0(B) + \Delta H_f^0(C) + \dots - \Delta H_f^0(C_2H_y) \quad (45b)$$

Of all possible fragmentation channels $B+C+\dots$ within a given ion(A^+)-production process, the largest cross sections have the channels with smallest thresholds, i.e. with smallest value of the sum of enthalpies of neutral reaction products. By applying this principle, and knowing the values ΔH_f^0 for all possible neutral fragments (see Table 1), one can easily determine the most important neutral fragmentation channels in reaction (44). It is obvious from Eq. (45b) that the ion-production channels with only one neutral fragment will have, in the general case, smaller threshold energies than the channels with more neutral fragments. Only in certain specific cases this general rule is violated.

The most important reaction channels in $e+C_2H_y$ ionization processes, identified by this method, are shown in Table 4. Included in this table is also the $e+C_2$ collision system, for reasons of completeness. Table 4 gives the values of E_{th} (calculated by using Eq. (45b)), mean electron energy loss $\overline{E_{th}^{(-)}}$ (calculated by using Eq. (20)) and mean total kinetic energy of all (heavy) products. The value of $\overline{E_K}$ was calculated from the equation (see Eq. (25))

$$\overline{E_K} = \chi D_0(C_2H_y^+ \rightarrow A^+ + B + C \dots) \quad (46)$$

D_0 is the dissociation energy of $C_2H_y^+$ ion for production of $A^+ + B + C + \dots$ products, and $\chi = 0.35$ (with a few exceptions; see discussion in Section 2.2). The values of $\overline{E_K}$ and $\overline{E_{el}^{(-)}}$ in Table 4 are related to each other by the relation $\overline{E_{el}^{(-)}} = E_{th} + \overline{E_K}$. The values of E_{th} for C_2H_2 and C_2H_6 in Table 4 are consistent with those determined experimentally for the appearance potentials of corresponding ion-production channels in Refs. [32, 36] and [34, 37], respectively. We see from Table 4 that for the more complex C_2H_y molecules, three (and even four)-body fragmentation DI channels become also important.

3.1.2 Cross section determination

A. Total cross sections

In the present database (as well as in Ref. [6]), as the basis for the recommended total ionization cross section of C_2H_2 , is taken that of Ref. [33] (uncertainty $\lesssim 10\%$), extended in the high-energy region (above 1000 eV) by using the BEB data [28], normalized to the experimental ones at $E \sim 300 - 500$ eV. For C_2H_4 , the experimental total ionization data of Ref. [25] (accuracy $\simeq 10\%$), available up to ~ 450 eV, were used, extended to higher energies by the data of Ref. [26], normalized to those of Ref. [25]

3.1 Electron-impact ionization of C_2H_y (I,DI)

at $E \sim 350 - 450$ eV, and the data of Ref. [19] (accuracy 10%) available from 600 eV up to 12 keV. For C_2H_6 , the mutually consistent experimental data of Refs. [19, 27, 35] were used in determining the recommended total ionization cross section from threshold to 12 keV. The total ionization cross sections for other C_2H_y molecules were derived from those of C_2H_2 , C_2H_4 and C_2H_6 by using the linear cross section scaling with the number of H atoms in C_2H_y (see the discussion in Section 2.3.1). As we mentioned before (Sect. 2.3.1), this scaling relationship is experimentally demonstrated down to 20-30 eV. Below these energies, the cross section is dominantly determined by its threshold behaviour, $\sigma_{ion}^{tot} \sim (1 - E_{th}/E)^\alpha$. The experimental total ionization cross sections for C_2H_2 , C_2H_4 and C_2H_6 show that the parameter α determining the near-threshold cross section behaviour for this process has the value $\alpha \simeq 3.0$. In view of the similarity of ionization mechanism for all C_2H_2 molecules, it can be safely assumed that the value $\alpha \simeq 3.0$ characterizes the near-threshold cross section behaviour also for the other molecules of C_2H_y family. In this way, the total ionization cross sections for C_2H , C_2H_3 and C_2H_5 have been uniquely determined. We note that the independently calculated σ_{ion}^{tot} for C_2H_3 [29] by using the BEB model agrees with $\sigma_{ion}^{tot}(C_2H_y)$ derived in the above described way better than 8% in the entire energy region (from threshold to ~ 10 keV).

B. Partial cross sections

As we have mentioned in the preceding sub-section, experimental ion-production cross sections are available only for C_2H_2 [33, 34, 35] (6 channels) and C_2H_6 [35] (13 channels). For C_2H_4 , they are available only at $E = 75$ eV and $E = 3.5$ MeV [22]. The experimentally studied ion-production channels for these systems are complemented in Table 4 with specification of the neutral products. As can be seen from this table, certain of ion-production channels (e.g $C_2H_2^+$ and C^+ channels in $e+C_2H_4$, or CH^+ channel in $e+C_2H_6$) are associated with two or more neutral fragmentation channels. The measured ion-production cross section is then distributed (partitioned) among the corresponding neutral fragmentation channels in accordance with the branching ratios for these channels determined from their threshold ratios (see Section 2.2).

The partial cross sections for the ionization channels of C_2H_2 were determined from the accurate (better than 10%) experimental ion-production cross sections of Ref. [33], extended to higher (>900 eV) energies by using the Bethe-Born scaling. The partial ionization cross sections for the $e+C_2H_6$ system were determined in a similar way, taking for a basis the ion-production cross sections of Ref. [35] (accuracy better than 10%). For the other $e+C_2H_y$ collision systems, the partial cross sections were determined by using the energy invariance of the branching ratios $R_j^{ion}(A^+/C_2H_y)$, and their linearity with respect to y . (For more details, see Ref. [6].) It has to be noted that in Ref. [5], beside the direct ionization, only the DI channels

3.1 Electron-impact ionization of C₂H_y (I,DI)

producing H and H₂ neutral products were included in the database.

3.1.3 Analytic representation of cross sections

The total and partial ionization cross section, determined by the procedures described in the preceding sub-section, can all be fitted to appropriate analytic expressions to facilitate their use in hydrocarbon transport modeling codes, or in other applications. For both total and partial cross sections, the following analytic expression was found appropriate

$$\sigma_{ion} = \frac{10^{-13}}{E \cdot I_c} \left[A_1 \ln \left(\frac{E}{I_c} \right) + \sum_{j=2}^N A_j \left(1 - \frac{I_c}{E} \right)^{j-1} \right] \quad (\text{cm}^2) \quad (47)$$

where I_c has a value close (or equal) to the appearance potential (expressed in eV), E is the collision energy (in eV) and A_j ($j = 1, \dots, N$) are fitting parameters. The number N of fitting parameters was determined from the condition that the r.m.s. of the fit is not larger than 2-3%. With $N = 6$, this condition was satisfied for all considered cross sections. The values of parameters I_c and A_j are given in Appendix A.1 for all reactions.

Note that expression (47) has the proper physical behaviour in the threshold and asymptotic regions. In contrast to this, the analytic expression used in Ref. [5] have a fixed $(E - E_{th})^2$ behaviour in the threshold region, and an exponential decay behaviour ($\sim \exp(-aE)$) in the high-energy region (beyond the cross section maximum). Such asymptotic behaviour of ionization cross section is completely unphysical.

As we have discussed in Section 2.3, the total ionization cross sections for all $e+\text{C}_2\text{H}_y$ systems should have the general energy behaviour given by Eq. (32), and have a linear dependence on y , i.e.

$$\sigma_{ion}^{tot}(\text{C}_2\text{H}_y) = A_0 F_2^{ion}(y) \left(1 - \frac{E_{th}}{E} \right)^\alpha \frac{1}{E} \ln(e + cE) \quad (\times 10^{-16} \text{cm}^2) \quad (48)$$

where A_0 , α and c are numerical constants, ($e = 2.71828\dots$), and

$$F_2^{ion}(y) = a + by \quad (49)$$

with E_{th} and E in Eq. (48) expressed in eV units. By fitting expression (48) to the values of total cross sections $\sigma_{ion}^{tot}(\text{C}_2\text{H}_y)$, we have found that in the energy region below $\sim 250 - 300$ eV, the expression (48) with

$$A_0 = 84.0, \quad \alpha = 3.0, \quad c = 0.09, \quad F_2^{ion}(y) = 2.97 + 0.073y \quad (50)$$

can represent the total cross sections with an accuracy better than 5%. Only at energies above ~ 500 eV, the parameters a and b in Eq. (49) begin slightly to depend on the energy, but the constants A_0 and c remain the same (with

3.2 Electron-impact dissociative excitation of C_2H_y to neutrals (DE)

an accuracy of 10%). (At high energies, the parameter α does not play any role.) Despite the fact that the parameters a and b in Eq. (49) attain a weak energy dependence at high energies (this dependence is much weaker for b than for a), the linearity of the function $F_2^{ion}(y)$ is preserved.

We note that the analytic expression (48), (50), describes (within an accuracy of 5–8%) also the $\sigma_{ion}^{tot}(C_2)$ cross section, calculated by the Deutsch-Märk model [38].

3.2 Electron-impact dissociative excitation of C_2H_y to neutrals (DE)

3.2.1 General remarks, reaction channels and energetics

There have been numerous experimental studies in the past of electron-impact dissociative excitation of C_2H_2 , C_2H_4 , and C_2H_6 molecules, [39]–[46], but all of them were concerned with the production of excited dissociation fragments in this process (optical measurements). Therefore, emission cross sections for various electronically excited dissociation products (such as H^* , C^* , CH^* , C_2^*) do exist in the literature, however they cannot be associated with a particular dissociation channel since several such channels (including cascade processes) may be involved (in general) in the production of a given excited fragment. Production of excited dissociation fragments obviously involves excitation of higher electronically excited states of C_2H_y molecule and, therefore, requires high collision energies. In the context of low-temperature fusion plasmas, most important are the dissociative excitation processes producing ground-state neutral fragments which are unattainable to optical measurements. Due to experimental difficulties of neutral particle detection, particularly coincident detection of several neutral fragments, total or partial cross section measurements of electron-impact dissociative excitation of C_2H_y (and C_xH_y in general) molecules have not been performed so far.

As mentioned earlier (see Section 2.2), the dominant mechanism of dissociative excitation of a molecule AB (not necessarily diatomic) by electron impact involves excitation of an electronically excited dissociative state AB^* . From the inverse proportionality of the excitation cross sections on the excitation energy (following, e.g., from the Born approximation) it is obvious that the dissociative excitation channels, associated with the lower excited dissociative states of AB and producing ground-state neutral fragments, will have the largest cross sections. Therefore, in our analysis of $e+C_2H_y$ dissociative excitation processes we shall concentrate primarily on these reaction channels. The dissociative molecular excited states of ground state neutral channels that have relatively small energies D_0 are likely to have energies in the Franck-Condon region of AB smaller than the ionization potential of AB. For the ground state neutral channels with large

3.2 Electron-impact dissociative excitation of C_2H_y to neutrals (DE)

energies, the corresponding dissociative excited molecular states AB^* may lie (in the Franck-Condon region of AB) energetically in the ionization continuum of AB . These states are obviously prone to auto-ionization, and the dissociative ionization (DI) becomes a competing process to dissociative excitation (DE). Apparently, the majority of dissociative excitation processes of C_xH_y producing excited fragments have dissociative states AB^* lying in the $(e + AB^+)$ continuum. The AB^* states lying deeply in the $(e + AB^+)$ continuum ("super-excited" states) contribute dominantly to the dissociative ionization. The competition of DI and DE processes in the continuum produces an isotope effect in the DE processes (but not in DI), since the probability of AB^* to survive the auto-ionization in the continuum depends on the velocity by which the dissociating system is passing the auto-ionizing part of the repulsive potential.

We also mention the fact that the excited dissociative states lying below the ionization continuum of AB (and producing mainly ground state fragments), may exhibit strong interactions with some of the stable (bound) excited states of AB at certain regions of inter-atomic distances (close to the equilibrium distance of the bound state), particularly when the dissociative and bound excited states have the same symmetry. This interactions (or non-adiabatic couplings) may lead to population of dissociative states through electron-impact excitation of bound excited states (pre-dissociation). An example of such pre-dissociation process is the transition from the bound $d^3\Pi_g$ excited state of C_2 to its dissociative $e^3\Pi_g$ excited state at the inter-nuclear distance $R \sim 1.7\text{\AA}$ [11].

In determining the most important dissociative excitation channels of C_2H_y to ground state neutrals (the channels producing excited neutrals are considered less important, but will nevertheless be discussed later on), we shall use the criterion resulting from the inverse proportionality of excitation cross section in the excitation (threshold) energy: the most important channels are those with small excitation threshold. The excitation threshold of AB^* dissociative state producing $A+B$ fragments is given by Eq. (16), in which $D_0(AB)$ is the energy of AB to produce the $A+B$ fragments with zero kinetic energy. For a $e+C_2H_y$ collision producing Y_i , ($i = 1, 2, \dots$) ground state fragments, D_0 is given by

$$D_0(\Sigma Y_i/C_2H_y) = \sum_i \Delta H_f^0(Y_i) - \Delta H_f^0(C_2H_y) \quad (51)$$

where $\Delta H_f^0(X)$ is the heat of formation of particle X . We assume that the most important channels are those for which the energy of dissociative excited state AB^* in the Franck-Condon region is smaller than the ionization potential of AB (i.e. which are not subject to dissociative ionization). Having in mind the discussion in Section 2.2 on the most probable (average) value of $\Delta E_{exc}(AB^*)$ we arrive at the condition

$$[I_p(C_2H_y) - D_0(\Sigma Y_i/C_2H_y)] < \Delta E_{exc}(\overline{AB^*}) \leq 0.35D_0(\Sigma Y_i/C_2H_y). \quad (52)$$

3.2 Electron-impact dissociative excitation of C_2H_y to neutrals (DE)

As discussed in Section 2.2, $\Delta E_{exc}(\overline{AB}^*)$ defines the mean total kinetic energy $\overline{E_K}$ of products Y_i . By choosing $\Delta E_{exc}(\overline{AB}^*)$ from the interval (52) (the value $0.35D_0$ is normally selected, unless other arguments dictate otherwise; see Section 2.2) and using Eq. (51), the excitation threshold energy $E_{th}^{DE} = E_{exc}(AB^*)$ for any dissociative excitation channel can be determined via Eq. (16).

In Table 5 we give the threshold energies and the mean total kinetic energies of products for the most important dissociative excitation channels to ground state neutrals in the $e+C_2H_y$ collisions satisfying the condition (52). It is interesting to note that the values of $\overline{E_K}$ for the H-production channels in $e+C_2H_2$, C_2H_4 , C_2H_6 collisions are consistent (within 0.5 eV) with the measured spectra of $H^*(n=4)$ products (obtained from the Doppler shift of $H^*(n=4)$ radiation) [46] after taking into account the increased value of the excitation threshold for $C_2H_{y-1}+H^*(n=4)$ production ($y=2,4,6$) and making use of the relation (27). This indicates that in order to include excited dissociation products in Table 5 in a relatively crude approximation, one has to add the excitation energy of the product(s) to the corresponding value of E_{th} in the table. The limit for such a reaction channel is shifted on the energy scale by the same amount, so that the mean total kinetic energy of the products remain the same as that given in Table 5.

In Table 5 are also given the "asymptotic" values (i.e., for $E \gtrsim 50$ eV) of the cross section branching ratios R'_{DE} for the individual dissociative excitation channels considered. The values of R'_{DE} were calculated by using the formulae (39) and (44a) with $\alpha=3$ (see next sub-section). The values of R'_{DE} in Table 5 show that for each C_2H_y molecule there are two - to - three dominant channels along which the molecule predominantly dissociates. The number of important DE channels decreases with increasing the number of H atoms in C_2H_y .

Finally, we mention that in the database of Ref. [5] only two reaction channels were included in the DE processes of C_2H_y : the H and the 2H production channels. Fixed branching ratios were used for these channels: 0.667 for H production and 0.333 for 2H production. (A value of $E_{th} \simeq 10$ eV was used for the thresholds of all DE channels.) Table 5 shows, however, that the H-production channel is not always the dominant one (in fact it is a minor channel for C_2H_6), and that the 2H production channel gives always a minor contribution (negligible in the case of C_2H_5 and C_2H_6) to the total DE cross section. The important contribution of H_2 production channel for all C_2H_y molecules was completely neglected in Ref. [5].

3.2.2 Determination of cross sections

A. Total cross sections

As mentioned earlier, total cross section measurements for electron-impact dissociative excitation of C_2H_y molecules have not been performed

3.2 Electron-impact dissociative excitation of C_2H_y to neutrals (DE)

so far. However, there is a measurement of the total σ_D^{tot} for C_2H_6 [47] which is the sum of the cross sections for all possible dissociative processes (DE, DI, ion-ion pair production, etc.). Assuming that the contribution of dissociative processes producing two or more ionized fragments, or multiply charged ion fragments, is small (the thresholds for these channels are above $\sim 50 - 60$ eV), the total dissociative excitation cross sections σ_{DE}^{tot} for production of neutrals can be expressed as

$$\sigma_{DE}^{tot} = \sigma_D^{tot} - \sigma_{DI}^{tot} \quad (53)$$

where σ_{DI}^{tot} is the total cross section for dissociative ionization discussed in Section 3.1.2. The cross section σ_D^{tot} for C_2H_6 has been measured in the energy range 15 - 600 eV [47], while $\sigma_{DI}^{tot}(C_2H_6)$ is known from the partial cross section measurements of Ref. [35] (up to 900 eV). Both σ_D^{tot} and σ_{DI}^{tot} exhibit broad maxima in the region around 80 eV. The relation (53), thus, determines the cross section $\sigma_{DE}^{tot}(C_2H_6)$ in the interval 15–600 eV. Above 600 eV, σ_{DE}^{tot} already attains a Bethe - Born behaviour, and below 15 eV it falls off according to the $(E - E_{th})^\alpha$ power law, with $\alpha \simeq 3$ ($E_{th} \simeq 7.45$ eV).

Total dissociation cross sections, σ_D^{tot} , have been measured also for CH_4 [48] and CF_4 , CHF_3 , C_2F_6 and C_3F_8 [49] in the energy range from around the threshold to 600 eV. The cross sections for C_2H_6 and C_2F_6 differ from each other by $\sim 10 - 20$ % for energies above ~ 50 eV. The measured cross section data for σ_D^{tot} show that the additivity rules for the strengths of chemical bonds manifest themselves also in the total dissociation (as linearity of $\sigma_D^{tot}(C_xH_y)$ with respect to both x and y for a given collision energy). Consequently, since the linearity of $\sigma_{DI}^{tot}(C_2H_y)$ has already been demonstrated (see Section 3.1.2), the cross sections $\sigma_{DE}^{tot}(C_2H_y)$ must also have a linear dependence on y . By virtue of additivity rules, one can expect that $\sigma_{DE}^{tot}(C_2H_y)$ and $\sigma_{ion}^{tot}(C_2H_y) \equiv \sigma_{I+DI}^{tot}(C_2H_y)$ are proportional to each other. Then, knowing the ratio $\sigma_{I+DI}^{tot}(C_2H_6)/\sigma_{ion}^{tot}(C_2H_6)$ one can determine σ_{DE}^{tot} for all other C_2H_y molecules, at least for $E \gtrsim 30$ eV where the additivity rules are strictly valid. For $E < 30$ eV, $\sigma_{DE}^{tot}(C_2H_y)$ ($y = 1-5$) is determined by its threshold behaviour $(1 - E_{th}/E)^\alpha$, with $\alpha \simeq 3$ (as derived from $\sigma_{DE}^{tot}(C_2H_6)$). (The proportionality of $\sigma_{DE}^{tot}(C_xH_y)$ and $\sigma_{ion}^{tot}(C_xH_y)$ follows also from the fact that both σ_{DE}^{tot} and σ_{ion}^{tot} are proportional to $\alpha_{pol}^{1/2}$, where α_{pol} is the polarizability of the C_xH_y molecule; see e.g. [6, 50].) All $\sigma_{DE}^{tot}(C_2H_y)$ cross sections derived by the above procedure can be represented by the analytic expression

$$\sigma_{DE}^{tot}(C_2H_y) = 34.6 F_2^{DE}(y) \left(1 - \frac{E_{th}}{E}\right)^3 \frac{1}{E} \ln(e + 0.15E) \quad (\times 10^{-16} cm^2) \quad (54)$$

where

$$F_2^{DE}(y) = 1.35 + 0.177y \quad (55)$$

3.3 Electron-impact dissociative excitation of $C_2H_y^+$ ions (DE^+)

E_{th} and E are expressed in eV units, and $e = 2.71828\dots$ is base of natural logarithm (introduced for convenience). E_{th} in Eq. (54) is obviously the smallest of the dissociative excitation thresholds. We note that the energy dependence of $\sigma_{DE}^{tot}(C_2H_y)$ is the same as for the DE process of CH_y molecules [2].

In analogy with the case of ionization (see previous sub-section), we expect that Eq. (55) also describes the cross section $\sigma_{DE}^{tot}(C_2)$.

B. Partial cross sections

The cross section for a particular DE channel $e + C_2H_y \rightarrow X + \dots$ can be obtained from the relation

$$\sigma_{DE}(X/C_2H_y) = \tilde{R}_{DE}(X/C_2H_y) \sigma_{DE}^{tot}(C_2H_y) \quad (56)$$

where $\tilde{R}_{DE}(X/C_2H_y)$ is the branching ratio for the considered DE channel, calculated by using Eqs. (40) of Section 2.3.3 (with $\beta \simeq 1.5$) and the "asymptotic" values of R'_{DE} in Table 5. (As discussed in Section 2.3.3, one can alternatively use for $\tilde{R}_{DE}(X/C_2H_y)$ also the prescriptions given by Eqs. (42), (43), depending on the desired balance between accuracy and simplicity of calculations.) It should be mentioned that when using σ_{DE}^{tot} in Eq. (56), the value of threshold energy E_{th} appearing in Eq. (54) should be taken the one that corresponds to the considered channel ($e + C_2H_y \rightarrow X + \dots$).

We note that in Ref. [5] a completely different analytic expression was used for $\sigma_{DE}(E)$, having an exponential decrease at large collision energies.

3.3 Electron-impact dissociative excitation of $C_2H_y^+$ ions (DE^+)

3.3.1 General remarks, reaction channels and energetics

Dissociative excitation of $C_2H_y^+$ ions (DE^+) has not been studied so far, neither theoretically nor experimentally. This is in contrast with the case of $e + CH_y^+$ collision system for which the H^+ , H_2^+ (and in the case of CH^+ also C^+) ion production DE^+ cross sections have been measured (see e.g. [2]). The process of dissociative excitation of an AB^+ ion by electron impact is governed by the same mechanism as the DE process for AB , except that now the intermediary dissociative excited state is AB^{+*} (see Eq. (17)). The energy threshold for the DE^+ process is given by Eq. (18) in which the dissociation energy $D_0(AB^+)$ for a given dissociation channel (say $e + C_2H_y^+ \rightarrow Y^+ + A + B + \dots$) is given by

$$D_0(Y^+/C_2H_y^+) = \Delta H_f^0(Y^+) + \sum \Delta H_f^0(\text{neutral products}) - \Delta H_f^0(C_2H_y^+) \quad (57)$$

where $\Delta H_f^0(X)$ is the heat of formation of particle X . The excitation energy $E_{exc}(AB^{+*})$ of the dissociative state AB^{+*} in the Franck - Condon region of ground vibrational state of AB^+ should be smaller than the ionization potential $I_p(AB^+)$ of the ion AB^+ , otherwise the dissociative state AB^{+*}

3.3 Electron-impact dissociative excitation of $C_2H_y^+$ ions (DE^+)

quickly auto-ionizes. For an "average" excited state \overline{AB}^{+*} (in the sense of the discussion in Section 2.2), the excitation energy $\Delta E_{exc}(\overline{AB}^{+*})$ appearing in Eq. (18) is given by (for the channel $e + C_2H_y^+ \rightarrow Y^+ + A + B + \dots$)

$$\Delta E_{exc}(\overline{AB}^{+*})_{FC} = \chi D_0(Y^+/C_2H_y^+), \quad \chi \simeq 0.35 \quad (58)$$

(with a few exceptions for the value of χ , discussed in Section 2.2)). The energy $E_{exc}(\overline{AB}^{+*})$ released in the dissociation processes is shared by the products Y^+, A, B, \dots according to Eq. (26). The requirement $E_{exc}(\overline{AB}^{+*}) < I_p(AB^+)$ defines all the DE^+ reaction channels for a given $C_2H_y^+$ molecular ion. The most important of them are those for which the threshold energy $E_{th} = \Delta E_{exc} + D_0$ is not very high (resulting from the inverse proportionality of σ_{DE^+} on E_{th}). Using this criterion, we have determined the most important DE^+ channels for each $C_2H_y^+$ molecules (including C_2^+) and they are listed in Table 6.

The values of thresholds energies (equal to the average electron energy losses, $\overline{E}_{el}^{(-)}$), and mean total kinetic energies of dissociation products (\overline{E}_K), are also given in Table 6 for each DE^+ channel. Moreover, in Table 6 are also given the "asymptotic" (i.e., for $E \gtrsim 30 - 40$ eV) values of cross section branching ratios R'_{DE^+} . These were calculated by using Eqs. (39) and (44a) of Section 2.3.3 with $\alpha = 2.5$ (see next sub-section). The values of R'_{DE^+} in Table 6 indicate that, like in the case of DE of C_2H_y , dominant in the electron-impact dissociative excitation of $C_2H_y^+$ molecular ions are only a few (two to three) channels. The number of important DE^+ channels is decreasing with increasing the number of H atoms in $C_2H_y^+$, as obvious from Table 6.

It has to be noted that the dissociation of an AB^+ ion by electron impact can proceed also via another mechanism: capture of incident electron on a doubly excited dissociative Rydberg state AB^{**} of C_2H_y molecule which can auto-ionize before its dissociation to neutral products, namely,



where $B^{(*)}$ indicates that (one of the) neutral product(s) may be excited. This "indirect", capture-auto-ionization dissociation (CAD) mechanism requires existence of "core-excited" states of the AB^+ ion with the same dissociation limit. The final products of the CAD process are the same as those of the proper ("direct") DE^+ process, but its threshold energy is expected to be much smaller (a few eV) than that for the proper DE^+ . The CAD process has been observed only in the $e + CH^+$ collision (producing C^+ ions), but its importance rapidly decreases for the CH_y^+ ions with $y \geq 2$ [2].

The CAD process has a signature in the oscillatory structure of dissociative recombination (DR) cross section σ_{DR} for collision energies above a few electrons, and σ_{CAD} can be related to the magnitude of oscillations of σ_{DR} .

3.3 Electron-impact dissociative excitation of $C_2H_y^+$ ions (DE^+)

Cross section information for the dissociative recombination of $C_2H_y^+$ with electrons is presently not available, and we do not have any basis for estimation of σ_{CAD} for these ions. In analogy with the case of CH_y^+ , one can expect that $\sigma_{CAD}(C_2H_y^+)$ should rapidly decrease with increasing y . The evidence with CH_y^+ also indicates that the CAD process is important only for those ion production channels for which the direct DE^+ process is weak. Table 6 indicates that none of the direct DE^+ channels for C_2H^+ is pronouncedly weak, i.e. for this ion the CAD process is not expected to be important. For the $C_2H_y^+$ ions with $y \geq 2$, its importance (compared to DE^+) should further decrease (as 2^y , if the analogy with CH_y^+ ions is used). Therefore, one can expect that CAD for $C_2H_y^+$ ions should not be an important process.

3.3.2 Determination of total and partial cross sections

As mentioned at the beginning of preceding sub-section, there are no total cross sections available for the DE^+ processes of $C_2H_y^+$ ions. However, as argued in Ref. [51], based on validity of additivity rules for the strengths of chemical bonds in all electron-impact processes for C_xH_y (and $C_xH_y^+$) systems, one can expect that dynamical (i.e. energy dependent) part of total cross section for a given process should depend dominantly only on the physical mechanism governing the process and not (or only weakly) on the structural properties of the molecule. This has been demonstrated in the case of DE processes for which the $\sigma_{DE}^{tot}(C_2H_y)$, Eq. (54), was found to have the same energy dependence as $\sigma_{DE}^{tot}(CH_y)$ obtained in Ref. [2] (see the remark following Eq. (55)). The only difference between $\sigma_{DE}^{tot}(CH_y)$ and $\sigma_{DE}^{tot}(C_2H_y)$ is the different structural factors $F_1^{DE}(y)$ for CH_y (see [2]) and $F_2^{DE}(y)$ for C_2H_y (see Eq. (55)). By using these arguments, and knowing the energy dependence of $\sigma_{DE^+}^{tot}(CH_y^+)$ from Ref. [2], we can write the expression for $\sigma_{DE^+}^{tot}(C_2H_y^+)$ in the form

$$\sigma_{DE^+}^{tot}(C_2H_y^+) = 29.4 F_2^{DE^+}(y) \left(1 - \frac{E_{th}}{E}\right)^{2.5} \frac{1}{E} \ln(e + 0.9E) (\times 10^{-16} cm^2), \quad (60)$$

where $F_2^{DE^+}(y)$ is the structural factor for DE^+ processes of $C_2H_y^+$, $e = 2.71828\dots$ is the base of the natural logarithm, and the collision and threshold energies, E and E_{th} , are expressed in eV units.

By virtue of validity of additivity rules for the DE^+ process, we know that $F_2^{DE^+}(y)$ should be a linear function of y . In order to determine this function, we shall use the fact that the DE^+ and dissociative ionization (DI) processes are governed by similar direct excitation mechanisms, and that in both processes the dissociating excited state AB^{+*} is the same for a given (common) ion + neutrals dissociation channel. Indeed, the excitation energy for a DI process is

$$E_{exc}^{DI}(AB^*) = I_p(AB) + D_0(AB^+) + \Delta E_{exc}(AB^{+*}),$$

3.3 Electron-impact dissociative excitation of $C_2H_y^+$ ions (DE^+)

while that for a DE^+ process is

$$\Delta E_{exc}^{DE^+}(AB^+) = D_0(AB^+) + \Delta E_{exc}(AB^{+*}),$$

i.e. they differ by the ionization potential $I_p(AB)$ only. If the state AB^{+*} is the same for DI and DE^+ processes, the corresponding dissociation products are also the same.) From the similarity of excitation mechanisms in DI and DE^+ processes, it follows that their total cross section should be proportional (for any C_xH_y , $C_xH_y^+$ pair, $x = 1, 2, 3$)

$$\sigma_{DE^+}^{tot}(C_xH_y^+) \sim \sigma_{DI}^{tot}(C_xH_y^+) \quad (x = 1, 2, 3) \quad (61)$$

The proportionality relation (61) immediately determines the slope of the function $F_2^{DE^+}(y)$ (equal to the slope of $F_2^{DI}(y)$ which is known from the $\sigma_{DI}^{tot}(C_2H_y)$ data of Section 3.1.2), while from its derived form

$$\frac{\sigma_{DI}^{tot}(C_2H_y)}{\sigma_{DI}^{tot}(CH_y)} = \frac{\sigma_{DE^+}^{tot}(C_2H_y^+)}{\sigma_{DE^+}^{tot}(CH_y^+)} \quad (62)$$

one can determine the other remaining parameter in $F_2^{DE^+}(y)$ for any fixed value of y (through the knowledge of $\sigma_{DI}^{tot}(C_{1,2}H_y)$ and $\sigma_{DE^+}^{tot}(CH_y)$ for any energy). Applying this procedure, we obtained the following expression for the structural function $F_2^{DE^+}(y)$

$$F_2^{DE^+}(y) = 0.74 + 0.90y \quad (63)$$

In analogy with the case of ionization of C_2H_y , we expect that Eqs. (60), (63) can also be extended to the case $y = 0$ (i.e., to $\sigma_{DE^+}^{tot}(C_2)$).

The cross section for a particular DE^+ channel $e + C_2H_y^+ \rightarrow X^+ + \dots$ can be obtained from $\sigma_{DE^+}^{tot}(C_2H_y^+)$ by using the relation

$$\sigma_{DE^+}(X^+/C_2H_y^+) = \tilde{R}_{DE^+}(X^+/C_2H_y^+) \sigma_{DE^+}^{tot}(C_2H_y^+) \quad (64)$$

where $\tilde{R}_{DE^+}(X^+/C_2H_y^+)$ is the branching ratio of the considered DE^+ channel, calculated by using either of the prescriptions given by Eqs. (40), (42) or (43) (with preference given to Eqs. (40) with $\beta = 1.5$, and the corresponding asymptotic values for R'_{DE^+} from Table 6).

We should note at the end of this section that the DE^+ processes have not been considered at all in the database of Ref. [5], although their cross sections are comparable to those for ionization of neutral hydrocarbons, and much larger than those for dissociative recombination in the energy range above $\sim 15 - 20$ eV.

3.4 Electron-impact dissociative ionization of $C_2H_y^+$ ions (DI^+)

3.4 Electron-impact dissociative ionization of $C_2H_y^+$ ions (DI^+)

3.4.1 General remarks, reaction channels and energetics

The electron-impact dissociative ionization (DI^+) processes of $C_2H_y^+$ ions are important only at high plasma temperatures (above $\sim 20 - 30$ eV) due to their large energy thresholds. There is no information in the literature about the cross sections for DI^+ processes of $C_2H_y^+$, but such information do exist for these processes for $e + CH_y^+$ collision systems [2]. As discussed in Section 2.2, the DI^+ process for a molecular ion AB^+ requires a vertical Franck-Condon transition to the ($A^+ + B^+$) repulsive state (see Eq. (22)), the transition energy of which (the energy threshold) is given by Eq. (24). The quantity ("ionization potential"):

$$I_p(AB^+) = D_0(AB^+ \rightarrow A + B^+) + I_p(A)$$

(or, equivalently, $= D_0(AB^+ \rightarrow A^+ + B) + I_p(B)$) can easily be calculated by using the relations given in Section 2.2 and the data in Table 1, for any DI^+ channel of $C_2H_y^+$. The Coulomb interaction energy of charged products in the Franck - Condon region of AB^+ is given by Eq. (24). Since the equilibrium distances for the various vibrational modes of $C_2H_y^+$ ions are not known, we shall (plausibly) assume that they are close to the equilibrium distance of CH^+ , which is $r_e(CH^+) \simeq 4.4\text{\AA}$. This gives for the Coulomb interaction energy of charged $A^+ + B^+$ products a value of $\Delta E_{exc}(A^+, B^+) \simeq 11.78$ eV. In view of the large values of $I_p(AB^+)$, the relatively small uncertainty in the $\Delta E_{exc}(A^+, B^+)$ value is of no significance for the value of $E_{th}^{DI^+}$.

The most important DI^+ channels in $e + C_2H_y^+$ collisions (including the case of $y = 0$) are given in Table 7, together with their threshold energies E_{th} . It is apparent from this table that the threshold energies of considered DI^+ channels are all close to each other not only for a given $C_2H_y^+$ ion but for the entire family of these ions. In Table 7 we also give the "asymptotic" values of the cross section branching ratios for the individual reaction channels, calculated by using Eqs. (39) and (44a) of Section 2.3.3, with $\alpha = 1.55$ (see next sub-section).

The total kinetic energy of reaction products in all DI^+ channels for any $C_2H_y^+$ ion is determined by the Coulomb interaction energy of repulsive ($A^+ + B^+$) state at $r_e(AB^+)$ (see Eq. (24)) and, as discussed above, is equal to 11.78 eV. Because of their strong repulsion, the charged reaction products carry most of this energy (sharing it in accordance with Eq. (26)), while the neutral products are left with almost zero kinetic energy.

3.4.2 Determination of total and partial cross sections

The total cross section $\sigma_{DI^+}^{tot}(C_2H_y^+)$ for electron-impact dissociation processes of $C_2H_y^+$ ion can be derived in a similar way as was done for $\sigma_{DE^+}^{tot}(C_2H_y^+)$ in Section 3.3.2. Using the argument on the separability of dynamical and structural part of the total cross section for electron-impact collision pro-

3.5 Dissociative electron recombination with $C_2H_y^+$ (DR)

cesses of C_xH_y and $C_xH_y^+$ systems, resulting from the additivity rules, (see for more details Ref. [51]), and knowing the cross section $\sigma_{DI^+}^{tot}(CH_y^+)$ for the CH_y^+ family of ions from Ref. [2], we write $\sigma_{DI^+}^{tot}(C_2H_y^+)$ in the form

$$\sigma_{DI^+}^{tot}(C_2H_y^+) = 30.1 F_2^{DI^+}(y) \left(1 - \frac{E_{th}}{E}\right)^{1.55} \frac{1}{E} \ln(e + 0.5E) (\times 10^{-16} cm^2) \quad (65)$$

where $F_2^{DI^+}(y)$ is the structural part of the cross section, $e = 2.71828\dots$ is the base of the natural logarithm, and the collision and threshold energies, E and E_{th} , are expressed in eV units. The linear function $F_2^{DI^+}(y)$ can be determined from similarity of the mechanism of DI^+ process with that for the dissociative ionization (DI) of neutral molecules. Indeed, the DI^+ process can be considered as excitation of an auto-ionization state in the continuum of AB^+ ion, as is the DI process excitation of an auto-ionizing state in the AB ionization continuum. On this basis, relations similar to [61] and [62] can be written for $\sigma_{DI^+}^{tot}(C_xH_y^+)$ and $\sigma_{DI}^{tot}(C_xH_y)$. From such relations, and with the knowledge of $\sigma_{DI^+}^{tot}(CH_y^+)$ and $\sigma_{DI}^{tot}(C_{1,2}H_y)$, one easily obtains

$$F_2^{DI^+}(y) = 1.31 + 0.33y \quad (66)$$

The cross section for a particular DI^+ channel $e+C_2H_y^+ \rightarrow X^+ + Y^+ + \dots$ is now obtained from $\sigma_{DI^+}^{tot}(C_2H_y^+)$ as

$$\sigma_{DI^+}(X^+, Y^+/C_2H_y^+) = \tilde{R}_{DI^+}(X^+, Y^+/C_2H_y^+) \sigma_{DI^+}^{tot}(C_2H_y^+) \quad (67)$$

where $\tilde{R}_{DI^+}(X^+, Y^+/C_2H_y^+)$ is the corresponding branching ratio. \tilde{R}_{DI^+} is calculated by using one of the prescriptions in Section 2.3.2). (Eqs. (40), (42) or (43)), and the corresponding asymptotic value R'_{DI^+} from Table 7. In view of close values of energy thresholds $E_{th}^{DI^+}$, the simple prescription given by Eq. (43) for determining \tilde{R}_{DI^+} is perhaps adequate for obtaining sufficiently accurate σ_{DI^+} in the threshold region.

3.5 Dissociative electron recombination with $C_2H_y^+$ (DR)

3.5.1 Data availability, reaction channels and energetics

The total cross section for dissociative electrons recombination (DR) with $C_2H_y^+$ ions was performed only for $C_2H_2^+$ [52] and $C_2H_3^+$ [53] ions, in the collision energy range up to ~ 1.0 and ~ 0.1 eV, respectively. The branching cross section ratios for the individual dissociation channels have also been determined in these references. For the higher members of $C_2H_y^+$ family of ions, such as $C_2H_5^+$ and $C_2H_7^+$, only the thermal rate coefficients have been measured [54]–[56]. Extrapolation of these data to higher temperatures will be discussed in the next sub-section.

3.5 Dissociative electron recombination with $C_2H_y^+$ (DR)

The important question of branching ratios for different channels of dissociative recombination on poly-atomic molecular ions has been discussed in the past on the basis of statistical phase space theory [57] and rearrangement and breaking the valence bonds during the DR process [58], in conjunction with the original curve-crossing concept for the DR mechanism proposed by Bates [59]. The proposed models, however, failed to provide correct predictions of DR branching ratios for most of the poly-atomic molecules considered, or even appropriate guidance for their determination.

The approach that will be followed here in determining the dominant DR channels for $C_2H_y^+$ ions is based on the assumption that the "direct" mechanism of the DR process (namely, capture of incident electron on a doubly excited dissociative state of parent molecule, the potential energy surface of which intersects the ground-state potential energy surface of the ion in the region of its minimum) is the dominant one, and with each dissociation channel having a dissociation limit below the bottom of ground-state ion potential, a sufficiently large number of such doubly excited states is associated. The direct DR mechanism obviously implies that at least one of the dissociation products is excited. It is also evident that the continuum wave function of dissociation products will have a stronger overlap with the vibrational wave functions of the ion if the (asymptotic) dissociation limit of a particular DR channel is close to (but below) the bottom of potential energy well of the ion (due to the smaller slope of repulsive potential of dissociative state). Therefore, the population of such DR channel should be, generally speaking, the strongest one, as observed experimentally in the case of $e + CH_y^+$ DR channels (see [2]).

However, an anti-bonding doubly excited state created by the direct DR mechanism, may experience strong (non-adiabatic) interactions with the bound excited states (having the same symmetry) of the molecule during the receding of dissociating fragments, which can lead to redistribution of initial populations. Such non-adiabatic couplings in the plethora of bound and dissociative excited states of the system (which includes also the entire Rydberg spectrum for each DR channel) may even lead to production of ground-state products (via population of corresponding repulsive states).

This indirect, non-adiabatic coupling mechanism may be responsible for the experimentally observed strong DR channel $e + C_xH_y^+ \rightarrow C_xH_{y-1} + H$ in all (studied) $C_xH_y^+$ systems.

Another indirect DR mechanism is the two-step process in which the initial step is formation (by the direct DR mechanism) of an unstable (electronically or vibrationally highly excited) product, $e + C_2H_y^+ \rightarrow C_2H_{y-1}^{**} + H$, followed by its prompt uni-molecular decay $C_2H_{y-1}^{**} \rightarrow C_2H_{y-2} + H$. Since formation of highly vibrationally (and electronically) excited molecular products by the direct DR mechanism is highly probable [60], it is believed that this two-step DR mechanism is responsible for the observed

3.5 Dissociative electron recombination with $C_2H_y^+$ (DR)

high branching ratios of the three-body fragmentation $C_2H_{y-2} + 2H$ in the $C_2H_2^+$ and $C_2H_3^+$ systems [53]. It is plausible to assume that the two-step DR mechanism should be equally effective also in the $e+C_3H_y^+$ collision systems.

Using these concepts and criteria (also tested on experimentally observed DR branching ratios for CH^+ , CH_2^+ , CH_3^+ [2], $C_2H_2^+$ [52], and $C_2H_3^+$ [53]) we have assigned the values of DR branching ratios for $C_2H_y^+$ $y \neq 2, 3$ molecular ions given in Table 8. In this table, the DR channels, that become open when incident electron has energy (in the centre-of-mass system) $\lesssim 1$ eV are also included. The excited states of dissociation products expected to be populated (only one of them) in each of DR channels at centre of mass (c.m.) collision energies below ~ 1 eV (see Table 3), are also given in the table. As a general criterion for determining the open DR channels given in the Table 8, the following relation was used ($e + C_2H_y^+ \rightarrow A + B^* + \dots$)

$$D_0(C_2H_y \rightarrow A + B + \dots) + E_{exc}(B^*) < I_p(C_2H_y) + E_{c.m.}^{el}, \quad E_{c.m.}^{el} \lesssim 1eV \quad (68)$$

where $E_{exc}(B^*)$ is the excitation energy of excited product.

The small values of branching ratios for the $C_2H_{y-2} + H_2$ DR channel in Table 8 are consistent with the observations of the $C_2H_2^+$ [52] and $C_2H_3^+$ [53] systems, and are believed to be due to the specific physical mechanism of this DR channel (formation H_2 molecules from two dissociating H atoms [53]). The small values of the branching ratios for all DR channels in which one C–C bond is broken are associated with the higher strength of C–C bonds with respect to the C–H bond, and with the necessity of either a molecular isomerization prior to the C–C bond cleavage, or an H-atom transfer between the transient fragments after the cleavage. These arguments hold also for the $C_3H_{y-2} + H_2$ and C–C bondage breaking dissociation channels of $e+C_3H_y^+$ systems.

The database in Ref. [5] for $C_2H_y^+$ ($y = 3 - 6$) assumes only two DR channels ($C_2H_{y-1} + H$ and $C_2H_{y-2} + H_2$), assigning to both of them a branching ratio of 0.5. This is in severe disagreement with the values given in Table 8. For $C_2H_2^+$, the DR channels $C_2H + H$, $CH + CH$ and $2C + 2H$ were assumed as dominant, with equal branching ratios ($=0.333$). The experimental values for these branching ratios [52], given in Table 8, are different from those adapted in Ref. [5]. The dissociation limit of the $2C + 2H$ channel lies far away in the $C_2H_2^+$ continuum, and this DR channel can never be populated. In Ref. [61], also a small number of DR channels for $C_2H_y^+$ were assumed, having, generally, same branching ratios.

It should be emphasized that with increasing the electron energy $E_{c.m.}$ above ~ 1 eV, other DR channels may become open which could lead to redistribution of DR channel populations. A similar effect is produced if the ion $C_2H_y^+$ is vibrationally excited. The DR branching ratios can exert significant changes particularly at energies above 8–10 eV, when different dissociative excitation channels of $C_2H_y^+$ become also open (see Table 6 for

3.5 Dissociative electron recombination with $C_2H_y^+$ (DR)

the thresholds of DE^+ channels). In this energy region, however, the DE^+ dominates over the DR process and the question of DR branching ratios becomes irrelevant. In this context it is also worthwhile to mention that the DR branching ratios determined at low (even thermal) energies tend to retain their energy invariance (as observed experimentally for the CH^+ [62] and CH_2^+ [63] ions up to 0.1–0.3 eV), as follows from the break-up mechanism proposed by Wigner [64] for the fragmentation of (excited) complex systems. Only when additional mechanisms start to interfere with the basic break-up mechanism (such as electron capture to doubly excited Rydberg dissociative states), or new channels become open with the increase of c.m. collision energy (as mentioned above), the DR branching ratios change their values.

The total kinetic energy $E_K^{(0)}$ of ground state products for zero electron impact energy (in c.m. system) is also given in Table 8 for each DR channel. $E_K^{(0)}$ has been calculated by using Eq. (29), and the data for ΔH_f^0 from Table 1. If $E_{c.m.}^{el}$ is the electron kinetic energy in the c.m. system and $E_{exc}(B^*)$ is the energy of excited DR product, the real total kinetic energy E_K of dissociation products is then given by Eq. (28) of Section 2.2. This energy is shared by the reaction products in accordance with Eq. (26).

3.5.2 Total and partial rate coefficients for DR

As we have mentioned at the beginning of proceeding sub-section, DR cross section measurements have not been performed for $C_2H_y^+$ ions except for $C_2H_2^+$ [52] and $C_2H_3^+$ [53] at thermal energies. Total thermal rate coefficients $\langle \sigma v \rangle_{DR}^{tot}$ have been measured for $C_2H_3^+$, $C_2H_5^+$ and $C_2H_7^+$ [54]–[56]. All available data for $\langle \sigma v \rangle_{DR}^{tot}(C_2H_y^+)$ show a remarkable linearity with y , including the value for $\langle \sigma v \rangle_{DR}^{tot}(C_2H^+)$ quoted in Ref. ([61]). Another common feature of $\langle \sigma v \rangle_{DR}^{tot}(C_2H_y^+)$ thermal data is their approximate $T^{-1/2}$ dependence on electron temperature T . This dependence follows directly from the E^{-1} dependence of their cross sections, σ_{DR}^{tot} , in the thermal energy region, predicted by Wigner [64] for any break-up reaction. In the case of CH_y^+ systems, where cross section measurements exist up to ~ 20 eV (see [2]), the approximate $T^{-1/2}$ dependence of calculated rate coefficients extends up to $T \sim 1$ eV. In the energy region above $\sim 1 - 2$ eV the $\sigma_{DR}^{tot}(CH_y^+)$ cross sections start to oscillate (due to the coupling of DR and CAD channels) and to decrease faster than E^{-1} . This decrease of $\sigma_{DR}^{tot}(CH_y^+)$ is even more pronounced for energies above 8–10 eV, when then DE^+ process starts to compete with the DR process. This enhanced decrease of $\sigma_{DR}^{tot}(CH_y^+)$ is reflected in a faster decrease of $\langle \sigma v \rangle_{DR}^{tot}(CH_y^+)$ with respect to $T^{-1/2}$ for temperatures above $T \sim 1$ eV. The enhanced decrease of $\langle \sigma v \rangle_{DR}^{tot}(CH_y^+)$ for $T \gtrsim 1$ eV with respect to $T^{-1/2}$ can be represented

3.6 Charge exchange and particle rearrangement reactions of protons with C_2H_y , (CX)

(for all CH_y^+ ions) by the function (when T is expressed in eV units)

$$f_{corr}(T) = \frac{1}{1 + 0.27 T^{0.55}} \quad (69)$$

We shall assume that the energy behaviour of $\sigma_{DR}^{tot}(C_2H_y^+)$ is similar to that of $\sigma_{DR}^{tot}(CH_y^+)$ (based on the common basic mechanism for DR processes in both systems) and apply the above corrective function also to the $T^{-1/2}$ dependence of $\sigma_{DR}^{tot}(C_2H_y^+)$. Therefore, $\sigma_{DR}^{tot}(C_2H_y^+)$ can be written as

$$\langle \sigma v \rangle_{DR}^{tot}(C_2H_y^+) = \frac{F_2^{DR}(y)}{T^{1/2} (1 + 0.27 T^{0.55})} (\times 10^{-8} cm^3/s) \quad (70)$$

where T is expressed in eV, and the scale factor 10^{-8} gives the typical magnitude of DR rate coefficients at $T \sim 1$ eV. The "structural" function $F_2^{DR}(y)$ can easily be obtained from the available experimental values of $\sigma_{DR}^{tot}(C_2H_y^+)$ at thermal temperatures, and its form is

$$F_2^{DR}(y) = 3.105 (1 + 0.45y). \quad (71)$$

This linearity is broken only for the $y = 0$ case (C_2^+ ion), when $F_2^{DR}(C_2^+) \simeq 1.87$ [61].

The validity of temperature dependence (70) of σ_{DR} can be extended up to 20 – 30 eV, where the DR process becomes already insignificant with respect to the DE^+ process.

The rate coefficient for an individual DR channel $e + C_2H_y^+ \rightarrow A + B^* + \dots$ is given by

$$\langle \sigma v \rangle_{DR}^{tot}(A, B^*/C_2H_y^+) = R_{DR}(A, B^*/C_2H_y^+) \langle \sigma v \rangle_{DR}^{tot}(C_2H_y^+), \quad (72)$$

where $R_{DR}(A, B^*/C_2H_y^+)$ is the corresponding branching ratio given in Table 8.

We note that in Ref. [5] the uncorrected $T^{-1/2}$ dependence of $\sigma_{DR}^{tot}(C_2H_y^+)$ was used for all temperatures. At $T = 10$ eV, the use of uncorrected $T^{-1/2}$ behaviour overestimates the value of $\langle \sigma v \rangle_{DR}^{tot}$ by a factor of 2.

3.6 Charge exchange and particle rearrangement reactions of protons with C_2H_y , (CX)

3.6.1 Data availability, reaction channels and energetics

The cross section database for charge exchange (Eq. (6a)) and particle rearrangement (Eqs. (6b),(6c)) processes of protons with the C_xH_y ($x = 1 - 3$; $1 \leq y \leq 2x + 2$) molecules was established in Ref. [7]. Here we shall give a refinement of its part pertinent to C_2H_y molecules, discuss in more detail the reaction channels and their energetics, and present new analytic fits for

3.6 Charge exchange and particle rearrangement reactions of protons with C_2H_y , (CX)

the cross sections.

Experimental charge exchange cross section measurements have been performed for C_2H_2 [65] (in the energy range 0.1–20 eV), C_2H_4 [66, 67] (for energies above 40 keV) and C_2H_6 [65],[67] - [70] (for energies above 0.1 keV). The cross section measurements for $C^+ + C_2H_4$ and $O^+ + C_2H_6$ [71], systems that have similar electronic energy properties as $H^+ + C_2H_4$ and $H^+ + C_2H_6$, respectively (especially the latter one), extend the energy ranges of the experimental data down to 0.017 keV/amu (for C_2H_4) and 0.012 keV/amu (for C_2H_6).

Quantum-mechanical cross section calculations were performed in the energy range 0.1 – 20 keV for the $H^+ + C_2H_2$, C_2H_6 collision systems [65], showing that good agreement with experimental data can be obtained only when vibrational excitation of $C_2H_2^+$ and $C_2H_6^+$ charge exchange products is taken into account.

We note that thermal rate coefficients, K_{CX}^{tot} , for the charge and particle exchange reactions (6a)–(6c) are known from astrophysical literature [61]. Converted into cross sections, these rates give for the (6a) and (6b),(6c) processes [7]

$$\sigma_{CX}^{(a)} = 7.26 \frac{R_{CX}^{(a)} K_{CX}^{tot}}{E^{1/2}} (\times 10^{-16} cm^2) \quad (73a)$$

$$\sigma_{CX}^{(b,c)} = 7.26 \frac{R_{CX}^{(b,c)} K_{CX}^{tot}}{E^{1/2} (1 + aE^\beta)} (\times 10^{-16} cm^2) \quad (73b)$$

where the K_{CX}^{tot} is expressed in units of $10^{-9} cm^3/s$, and the relative collision energy E is expressed in eV units. $R_{CX}^{(a)}$ and $R_{CX}^{(b,c)}$ in (73) are the branching ratios for the pure charge exchange (electron capture) and particle rearrangement channels of charge exchange process, respectively. The factor $(1 + aE^\beta)^{-1}$ in (73b) takes into account the fact that the cross section of particle exchange processes decreases much faster with the increase of collision energy than that for electron capture at energies above ~ 0.1 eV. The cross section expressions (73) follow directly from the Langevin mechanism for formation (polarization capture, or orbiting) and decay of the intermediary collision compound, (H^+, C_2H_y) . The branching factors, $R_{CX}^{(a)}$ and $R_{CX}^{(b,c)}/(1 + aE^\beta)$, have the meaning of decay probabilities of the (H^+, C_2H_y) compound in different channels. Implicit to the Langevin polarization capture model is the assumption of exothermicity of the compound formation process, i.e. the total internal energy E_{int} of the reactants (including both electronic and ro-vibrational motion) is larger than that of the products. This requirement defines the possible reaction channels for a given $H^+ + C_2H_y$ collision system.

In general, the reaction channels with higher exothermicity

3.6 Charge exchange and particle rearrangement reactions of protons with C_2H_y , (CX)

$$\Delta E = E_{int}(\text{products}) - E_{int}(\text{reactants})$$

or, equivalently, see Eq. (31):

$$\Delta E = \sum \Delta H_f^0(\text{reactants}) - \sum \Delta H_f^0(\text{products}),$$

will have larger decay probability (branching ratio). However, excessively large values of ΔE may reduce the reaction probability (especially at above-thermal collision energies) due to dynamic molecular effects. Using these criteria, we have determined the particle rearrangement charge exchange channels for the $H^+ + C_2H_y$ systems, and their respective exothermicities, ΔE , (using Eq. (35)). They are shown in Table 9. By using the above arguments for the relation between branching ratios and channel exothermicities, we have assigned the respective values of $R_{CX}^{(a)}$, or $R_{CX}^{(b,c)}$, for all channels of a given collision system, that are also given in Table 9. The values of K_{CX}^{tot} for C_2H , C_2H_2 and C_2H_3 are proportional to the square root of polarizability of these molecules, which is in accordance with the Langevin model (see [7],[72]), but K_{CX}^{tot} for C_2H_5 and C_2H_6 violate this proportionality.

This violation results from the resonant character of pure charge exchange (electron capture) processes which dominates in these collision systems, and extends down to thermal energy region (see next sub-section). In Table 9 are also given the values of parameters α and β that appear in Eq. (73b). These values were determined from the condition that the cross section $\sigma_{CX}^{(b,c)}$ constitutes a small fraction ($\leq 3\%$) of total charge exchange cross section in the energy region above ~ 1 eV. The particle rearrangement channel $H^+ + C_2 \rightarrow CH + H^+$ is endothermic (by 0.32 eV) and is excluded from Table 9.

In [5] the same CX reaction channels as in Table 9 were considered, except that the pure electron capture channel in $H^+ + C_2H_6$ system was omitted. This electron capture process in $H^+ + C_2H_6$ has a resonant character at above-thermal energies (see next sub-section), and there is no physical reason for it to be neglected in the thermal region. The branching ratios of CX reaction channels for a given $H^+ + C_2H_y$ collision system were chosen in [5] to be the same. The $H^+ + C_2$ collision system was also not included in Ref. [5].

3.6.2 Charge exchange cross sections

The validity of charge exchange cross sections $\sigma_{CX}^{(a)}$ and $\sigma_{CX}^{(b,c)}$, Eqs. (73), derived from the thermal rate coefficients is limited to energies below ~ 1 eV. At higher energies, the pure charge exchange (or electron capture) channel (6a) dominates the charge transfer process, and the discussions in the present sub-section will be devoted primarily to it.

The analysis of available experimental data on $\sigma_{CX}^{(a)}$ for C_2H_2 , C_2H_4 and C_2H_6 targets, performed in [7], has shown that the energy behaviour of $\sigma_{CX}^{(a)}(C_2H_6)$ has the typical features of a resonant electron capture reaction

3.6 Charge exchange and particle rearrangement reactions of protons with C_2H_y , (CX)

(slow, logarithmic increase with decrease the collision energy in the region below ~ 10 keV), $\sigma_{CX}^{(a)}(C_2H_4)$ has a similar "resonant" behaviour, but to a lesser extent, while $\sigma_{CX}^{(a)}(C_2H_2)$ has an energy behaviour typical for the non-resonant electron capture reactions (a broad maximum in the region 5.8 keV and a decrease for lower energies). For collision energies above 20 – 30 keV/amu, all charge exchange cross sections rapidly decrease with increasing energy. The resonant cross section behaviour was observed in [7] for all $H^+ + C_xH_y$ collision systems, with $y \geq 2x - 2$. It was further shown in [7] that in the energy region below ~ 20 keV, the cross sections of resonant CX reactions satisfy the scaling relationship (we hereafter omit the superscript(a))

$$\sigma_{CX}^{res}(C_xH_y) = \sigma_{0,l} \frac{y^{1/2}}{I_p} \quad (74)$$

where I_p is the ionization potential of C_xH_y and $\sigma_{0,l}$ is constant. On the other hand, in the energy region above ~ 50 keV, the cross sections for all CX reactions satisfy the scaling

$$\sigma_{CX}^{res}(C_xH_y) = \sigma_{0,h} \frac{y}{I_p^2} \quad (75)$$

which follows from the high-energy charge exchange theories (e.g. first Born approximation). The scaling relations (74), (75) were used in [7] to determine the resonant CX cross sections for the systems for which no data were available (with an appropriate interpolation in the range 20-50 keV). The cross sections for non-resonant CX reactions of $H^+ + C_xH_y$ systems with $y < 2x - 2$, can be fairly well estimated by using the Demkov two-state model (see [73]) with due account of the possible vibrational excitation of the product ion $C_xH_y^+$ [65]. The energy at which the broad cross section maximum of these reactions occurs satisfies the Massey relation [74]

$$c \Delta E / v_m \simeq 1 \quad (76)$$

where $\Delta E = I_p(H) - I_p(C_xH_y)$, v_m is the collision velocity at the position of σ_{CX}^{max} , and c is constant. (When ΔE is expressed in eV and v in atomic units $v_0 (= 2.19 \times 10^8 \text{ cm/s})$, the value of c for all C_xH_y exhibiting non-resonant CX with H^+ is $\simeq 7 - 9$.) Relation (76) shows that with increasing ΔE , the cross section maximum shifts towards larger collision energies. In the case of non-resonant CX reactions of C_xH_y , the exponential decrease of σ_{CX} for $v < v_m$, predicted by the theory [73], is hampered by the effects of polarization electron capture mechanism (due to the large values of polarizabilities of C_xH_y ; see e.g. [5]). Therefore, the non-resonant CX cross section for these collision systems exhibits a broad minimum in the energy range $\sim 10 - 100 \text{ eV}$, before starting to increase with the further decrease of collision energy and approach its thermal energy behaviour given by Eq.

3.6 Charge exchange and particle rearrangement reactions of protons with C_2H_y , (CX)

(73a).

The CX cross section for $H^+ + C_2H_y$ systems obtained in [7] by using the available experimental data, applying the above mentioned scaling procedures and performing Demkov-type cross section assessments (for non-resonant CX reactions), were fitted in that reference to analytic expressions containing a finite number of Chebishev polynomials. Although the number of polynomials was fairly large (about ten), the cross section of resonant CX reactions show small artificial oscillations in the low energy region. In the present work we use a different type, non-polynomial analytic expression to represent the total charge exchange (electron capture + particle exchange, $\sigma_{CX}^{(a)} + \sigma_{CX}^{(b,c)}$) cross sections, namely

$$\sigma_{CX}^{tot} = \frac{c_1}{E^{1/2} + c_2 E^{c_3}} + \frac{c_4 \exp(-c_5/E^{c_6})}{E^{c_7} + c_8 E^{c_9} + c_{10} E^{c_{11}}} (\times 10^{-15} \text{ cm}^2) \quad (77)$$

where c_i , ($i = 1 - 11$) are fitting parameters, and the collision energy E is expressed in eV units. The values of fitting parameters c_i are given in Table 10. The parameters c_i given in Table 10 for the $H^+ + C_2H$ system refer only to the pure electron capture channel, $H^+ + C_2H \rightarrow H + CH^+$, while the cross section for the particle exchange channel $H^+ + C_2H \rightarrow H_2 + C_2$ is given by the expression (73b), with the value of $R_{CX}^{(b)}$ given in Table 9. The cross section for pure electron capture channels of other $H^+ + C_2H_y$ ($y \geq 2$) systems, are obtained by subtracting from (77) the sum of particle exchange cross sections given by (73b) with the values of $R_{CX}^{(b,c)}$ given in Table 9. The first term in (77), although similar in form with (73b), should not be identified with it. However, this term has been indeed introduced in (77) to account for the cross section behaviour in the thermal energy region and to ensure the proper thermal energy limit of σ_{CX}^{tot} . The analytic expression (77) also ensures the correct energy behaviour of σ_{CX}^{tot} up to collision energies $E \simeq 300 - 400$ keV. As well known from the theory of charge exchange processes, the energy behaviour of σ_{CX} in the high-energy asymptotic limit should be $\sim E^{-5.5}$ [75].

We note that the coefficients c_5 and c_6 in Table 10 have zero values for CX reactions of C_2H_4 , C_2H_5 and C_2H_6 . This indicates the resonant character of these reactions. While the CX reaction for C_2H_4 has a rather flat cross section behaviour ($c_7 = 0.06$) in the energy range $\sim 1 \text{ eV} - 10 \text{ keV}$, the cross section slope defined by the value $c_7 = 0.14$ for C_2H_5 and C_2H_6 is typical for the resonant CX reactions in this energy range. For CX reactions of C_2H_y , $y \leq 3$, the coefficients c_5 and c_6 have non-zero values, indicating the non-resonant character of these reactions. We finally note that in Ref. [5], the thermal constant value of K_{CX}^{tot} (or equivalently, the $E^{-1/2}$ dependence of $\sigma_{CX}^{(a)}$ and $\sigma_{CX}^{(b,c)}$ cross sections) has been extended up to $T = 10 \text{ eV}$, which represents a significant overestimation of CX rate coefficients, particularly for particle re-arrangement reaction channels.

4 Collision Processes of C_3H_y and $C_3H_y^+$ with Electrons and Protons

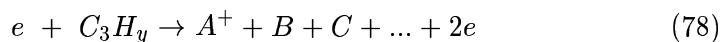
4.1 Electron-impact ionization of C_3H_y (I, DI)

4.1.1 Data availability, reaction channels and energetics

The cross section database for electron-impact ionization of C_3H_y ($1 \leq y \leq 8$) was thoroughly discussed in [6], where the procedures for deriving the unavailable cross sections in the literature were also described. We shall, therefore, confine ourselves in the present section to a brief review of existing experimental and theoretical data and discuss in more detail the energetics of individual reaction channels.

Total ionization cross section measurements for the $e+C_3H_8$ collision system have been performed in [19, 26, 27] jointly covering the energy range from the reaction threshold to 12 keV. The cross section of [19] and [27] are believed to be accurate to within 10%. Theoretical total cross section calculations have also been performed for this system within the binary-encounter Bethe (BEB) model [30] and the classical Deutsch-Märk (DM) model [76]. Total cross section measurements were done in [78] for 23 ion production channels of $e+C_3H_8$ collision system in the energy range from threshold to 950eV.

The accuracy of these cross sections (their sum was normalized to the total cross section of Ref. [27] at $E=100$ eV) is 10%, or better. For the other $e+C_3H_y$ ($1 \leq y \leq 7$) collision systems, no partial cross section data are presently available. The number of ionization channels in a $e+C_3H_y$ collision system is obviously significantly larger than for the $e+C_2H_y$ system, particularly for the higher -y members of the C_3H_y family. In determining the most important (with large cross sections) dissociative ionization (DI) channels in a $e+C_3H_y$ collision, i.e.



we have used the general criterion that the channels with smaller energy threshold have larger cross sections. In accordance with Eq. (21), the threshold of reaction (78) is given by

$$E_{th}^{DI} \simeq A_p^{DI} = \Delta H_f^0(A^+) + \Delta H_f^0(B) + \Delta H_f^0(C) + \dots - \Delta H_f^0(C_3H_y), \quad (79)$$

where $\Delta H_f^0(X)$ is the heat of formation of particle X (see Table 1). As obvious from Eq. (79), the most important DI channels are those with production of only one neutral fragment. However, exceptions from this general rule do exist due to variety of ΔH_f^0 values. In the case of direct

4.1 Electron-impact ionization of C₃H_y (I, DI)

ionization, the threshold energy, of course, is identical to the ionization potential, I_p .

The values of E_{th}^I ($=I_p$) and E_{th}^{DI} for the most important DI channels in $e+C_3H_y$ collisions (including also the case $y=0$) are given in Table 11. The values of mean total kinetic energies, \overline{E}_K , of DI fragments are also given in this table. These were calculated from the equation (see Section 2.2)

$$\overline{E}_K = \chi D_0(C_3H_y \rightarrow A^+ + B + C + \dots) \quad (80)$$

with $\chi = 0.35$. In a few cases the value of χ was chosen to be different than 0.35 in order to account for the specific physical situation (see Section 2.2). The values of average electron energy losses, $\overline{E}_{el}^{(-)} = E_{th} + \overline{E}_K$ in each ionization channel, are also given in Table 11.

In Table 11, we give also the "asymptotic" (at $E \geq 80$ eV) cross section branching ratios, $R'_{I/DI}$ for the various ionization channels for each $e+C_3H_y$ collision system. For the $e+C_3$ system, $R'_{I/DI}$ were calculated according the prescription given by Eqs. (39) and (44a) of Section 2.3.2 with $\alpha = 3.0$ (see next sub-section), while for the $e+C_3H_y$ ($1 \leq y \leq 7$) systems, they were determined in Ref. [6]. With respect to the DI channels considered in Ref. [6], Table 11 includes also some less important channels, which slightly affects the $R'_{I/DI}$ values given in Ref. [6]. The ion-production cross sections for $e+C_3H_8$ collision system are experimentally known, and their decomposition into specific neutral fragmentation channels was done in Ref. [6]. Therefore, the information on $R'_{I/DI}$ of the I/DI channels for $e + C_3H_8$ does not appear in Table 11. Some footnotes are given in Table 11, however, to indicate certain differences in the R'_{DI} values adopted in the present work for a few reactions.

In the database of Ref. [5] only the hydrocarbons C₃H_y with $1 \leq y \leq 6$ were included. As dominant ionization channels in this reference were considered the direct ionization (I) and the $C_3H_y \rightarrow C_3H_{y-1}^+ + H$ and $C_3H_y \rightarrow C_3H_{y-2}^+ + 2H$ DI channels, for $3 \leq y \leq 6$. The branching ratios of these three channel were taken the same (0.20, 0.13 and 0.67, respectively, at $E \simeq 70 - 100$ eV).

Table 11 shows that for direct ionization and H-production DI channels, the branching ratios adopted in Ref. [5] for these systems are reasonable (except for C₃H₃, where the difference is about a factor 2), but the branching ratio for 2H-production channel is highly erroneous. Due to its high energy threshold, this channel in fact does not appear at all in Table 11. Instead the H₂-production channel in these systems appears among the dominant ones. It has been shown in Ref. [6], that the 2H-production channel is usually about 20 % of the total H₂- and 2H- production cross section for all C_xH_y systems ($x = 1 - 3$, $1 \leq y \leq 2x + 2$). It is also interesting to note that for the $e + C_3H_8$ collision system, the dominant ionization channels at all energies are not the direct ionization and H-production DI channels,

4.1 Electron-impact ionization of C_3H_y (I, DI)

but rather the $C_2H_5^+$, $C_2H_4^+$ and $C_2H_3^+$ ion- production channels [78].

4.1.2 Total and partial cross sections

The total ionization cross sections for $e+C_3H_y$ systems ($1 \leq y \leq 8$) have been determined in Ref. [6] by using the experimental data for C_3H_8 [19, 26, 27, 78] and C_3H_6 [19, 26], theoretical data for C_3H_4 [77] and the semi-empirical cross section relationships following from the additivity rules for the strengths of chemical bonds in C_xH_y systems. These cross sections have been represented by the analytic expression

$$\sigma_{ion}^{tot} = \frac{10^{-13}}{E \cdot I_c} \left[A_1 \ln(E/I_c) + \sum_{j=2}^N A_j \left(1 - \frac{I_c}{E} \right)^{j-1} \right] (cm^2) \quad (81)$$

where I_c has a value close (or equal) to the reaction energy threshold (expressed in eV units), E is the collision energy (in eV units), and A_j ($j = 1, \dots, N$) are fitting parameters. The number N of fitting parameters was taken $N=6$, sufficient to achieve a fit accuracy with r.m.s. of 2-3 %. The analytic expression (81) has correct physical behaviour both in the threshold and high-energy (asymptotic) energy region. The values of parameters I_c and A_j are given in Appendix A.2 for all collision systems ($1 \leq y \leq 8$).

The partial cross sections for the individual ionization channels in the $e+C_3H_8$ system, determined in Ref. [6], can also be represented by an analytic expression of the form given by Eq. (81). The values of I_c and A_j fitting parameters for these cross sections are also given in Appendix A.2.

Based on the validity of additivity rules for total ionization cross sections, demonstrated in Ref. [6] for all $e+C_xH_y$ collision systems in the energy region above ~ 30 eV, and the fact that for $E < 30$ eV the ionization cross sections are essentially determined by their $(1 - E_{th}/E)^3$ behaviour (see Eqs. (48),(49), and Ref. [2] for $\sigma_{ion}(CH_y)$), by using a simple fitting procedure one can derive from the known $\sigma_{ion}^{tot}(C_3H_y)$ cross sections (given in Appendix A.2) a unified expression

$$\sigma_{ion}^{tot}(C_3H_y) = 84.0 F_3^{ion}(y) \left(1 - \frac{E_{th}}{E} \right)^3 \frac{1}{E} \ln(e+0.09E) (\times 10^{-16} cm^2) \quad (82)$$

where

$$F_3^{ion}(y) = 4.45 + 0.065y \quad (83)$$

where the collision and threshold energies, E and E_{th} , are expressed in eV units, and $e=2.71828\dots$ is the base of natural logarithm. The function (82),(83) represents the $\sigma_{ion}^{tot}(C_3H_y)$ data with an accuracy better than 5-8 % for energies below ~ 300 eV, and $\sim 10\%$ for energies above ~ 500 eV. Within the same accuracy these equations describe the cross section $\sigma_{ion}^{tot}(C_3^+)$, calculated by the Deutsch-Märk model.

4.2 Electron-impact dissociative excitation of C_3H_y to neutrals (DE)

The partial cross section for a particular ionization channel $e+C_3H_y \rightarrow A^+ + B + \dots 2e$ for the systems with $y \leq 7$ can now be obtained as

$$\sigma_{ion}(A^+, B/C_3H_y) = \tilde{R}_{I/DI}(A^+, B/C_3H_y) \sigma_{ion}^{tot}(C_3H_y), \quad (84)$$

where the branching ratio $\tilde{R}_{I/DI}$ is calculated by using Eqs. (40) with $\beta = 1.5$, (or Eqs. (42) with $\gamma \simeq 1.5$, or Eq. (43), if more appropriate) and the data of asymptotic values R'_{DI} given in Table 11.

We note that $\sigma_{ion}^{tot}(C_3H_y)$ cross sections in Ref. [5] also linearly increase with increasing y . They, however, have a weaker energy dependence in the threshold region ($\sim (E - E_{th})^2$), and an incorrect $exp(-aE)$ ($a = \text{constant}$) behaviour in the energy region above the energy at which the cross section maximum occurs. As we mentioned in Section 3.1.3, there is no physical basis for prescribing such high-energy behaviour of an electron-impact ionization cross section.

4.2 Electron-impact dissociative excitation of C_3H_y to neutrals (DE)

4.2.1 General remarks, reaction channels and energetics

As in the case of CH_y and C_2H_y hydrocarbon molecules, direct total or partial cross section measurements (or calculations) of the dissociative excitation (DE) reactions (2) for C_3H_y ($1 \leq y \leq 8$) have not been performed so far. The experimental difficulties are related to coincident detection of neutral fragments, while the theoretical ones lie in the complexity of electronic structure and dynamics of poly-atomic many-electron systems. The only related experimental result is the cross section σ_D for total dissociation of C_3H_8 [49] to both ionized and neutral fragments (in the energy range from ~ 20 to 600 eV), from which one can obtain the total DE cross section $\sigma_{DE}^{tot}(C_3H_8)$ by subtracting from $\sigma_D(C_3H_8)$ the sum of dissociative ionization cross sections for C_3H_8 , $\sigma_{DI}^{tot}(C_3H_8)$. This will be used as a starting point in the derivations of $\sigma_{DE}^{tot}(C_3H_y)$ in the next sub-section.

The dominant (direct excitation) mechanism of the DE process for C_3H_y molecules is the same as that for C_2H_y discussed in more detail in Section 3.2.1 (see also Section (2.2)). For determining the most important DE channels in $e+C_3H_y$ collisions, we shall, therefore, use the same criteria used also for $e+C_2H_y$ systems: Most important are the DE channels with relatively small threshold energies (see Eq. (16)), the mean excitation energy of which above the dissociation limit, $\Delta E_{exc}(\overline{AB}^*)$, satisfy the relations (analogous to Eq. (52))

$$[I_p(C_3H_y) - D_0(\Sigma Y_i/C_3H_y)] < \Delta E_{exc}(\overline{AB}^*) \leq \chi D_0(\Sigma Y_i/C_3H_y) \quad (85)$$

4.2 Electron-impact dissociative excitation of C_3H_y to neutrals (DE)

where

$$D_0(\Sigma Y_i/C_3H_y) = \sum_i \Delta H_f^0(Y_i) - \Delta H_f^0(C_3H_y) \quad (86)$$

is the dissociation energy of the channel $e+C_3H_y \rightarrow e + Y_1 + Y_2 + \dots$. The inequality (85) serves to determine the possible DE channels, with the value $\chi = 0.35$ taken as a rule, unless other considerations suggest another choice (see Section 2.2). For the dominant DE channels, determined on the basis of Eq. (85), the threshold energies E_{th}^{DE} were calculated by using Eq. (16), (with D_0 given by Eq. (86) and $\Delta E_{exc}(\overline{AB}^*) = 0.35D_0$, generally). The values of E_{th}^{DE} ($= \overline{E_{el}^{(-)}}$, the mean electron energy loss) and of the mean kinetic energy of dissociation products, $\overline{E_K} (= \overline{\Delta E_{exc}})$, are given in Table 12.

The asymptotic cross section branching ratios, R'_{DE} , calculated by using Eqs. (39) and (44a) with $\alpha = 3$ (see next sub-sections), are also given in this table. The values of R'_{DE} in Table 12 show that the electron-impact DE process of C_3H_y is dominated by a few channels only. This table also shows that the H- and H₂- production channels dominate the dissociation of C_3H_y molecules.

The DE database in Ref. [5] includes only the H- and 2H-production channels for the electron-impact dissociation of C_3H_y molecules with $3 \leq y \leq 6$, with the same branching ratios (0.666 and 0.333, respectively) for all molecules. We have found that the 2H-production channels does not satisfy the relation (85) for any of C_3H_y molecules ($y \geq 2$), and is not included in Table 12. The dissociation channel $e+C_3H \rightarrow 3C + H + e$ which in Ref. [5] is considered as dominant (the only important channel), was also not included in Table 12, because of its high energy threshold (above 15 eV) and negligible contribution to the total dissociation of C_3H .

It should also be noted that for all DE channels of all C_3H_y molecules considered in Ref. [5] ($1 \leq y \leq 6$), the value of threshold energy was taken to be the same, $\simeq 10$ eV. The values of E_{th} for the dominant DE channels in Table 12 are significantly different among themselves and from the value of 10 eV.

4.2.2 Total and partial cross sections

For determination of total DE cross section $\sigma_{DE}^{tot}(C_3H_y)$ for the $e+C_3H_y$ collision systems, we shall apply the same procedure used in determining $\sigma_{DE}^{tot}(C_3H_y)$ for C_2H_y (see section 3.2.2). From the experimental knowledge of total dissociation cross section $\sigma_D^{tot}(C_3H_8)$ [49] and of total cross section for dissociative ionization $\sigma_{DI}^{tot}(C_3H_8)$ [78], we can obtain $\sigma_{DE}^{tot}(C_3H_8)$ as the difference $\sigma_D^{tot}(C_3H_8) - \sigma_{DI}^{tot}(C_3H_8)$ up to $E = 600$ eV, the highest energy for which $\sigma_D^{tot}(C_3H_8)$ was measured. Since the maximum of $\sigma_{DE}^{tot}(C_3H_8)$ is in the region around $E \simeq 80-90$ eV, the extrapolation of $\sigma_{DE}^{tot}(C_3H_8)$ above 600 eV

4.3 Electron-impact dissociative excitation of $C_3H_y^+$ ions (DE^+)

can be done in accordance with the Bethe-Born formula. By using the arguments given in Section 3.2.2 about the proportionality of $\sigma_{DE}^{tot}(C_xH_y)$ with $\sigma_{ion}^{tot}(C_xH_y)$ and from the knowledge of the ratio $\sigma_{DE}^{tot}(C_3H_8)/\sigma_{ion}^{tot}(C_3H_8)$, one can determine σ_{DE}^{tot} for all other C_3H_y molecules, at least in the region $E > 30$ eV. For $E < 30$ eV, $\sigma_{DE}^{tot}(C_3H_y)(y = 1-7)$ is determined by its threshold behaviour $(1 - E_{th}/E)^\alpha$, with $\alpha = 3.0$ (as derived from $\sigma_{DE}^{tot}(C_3H_8)$). All $\sigma_{DE}^{tot}(C_3H_y)$ cross sections derived by the above procedure can be represented by the analytic expression

$$\sigma_{DE}^{tot}(C_3H_y) = 34.6 F_3^{DE}(y) \left(1 - \frac{E_{th}}{E}\right)^3 \frac{1}{E} \ln(e+0.15E) (\times 10^{-16} cm^2) \quad (87)$$

$$F_3^{DE}(y) = 2.20 + 0.190y \quad (88)$$

where the collision and threshold energies, E and E_{th} , are expressed in eV units, and $e = 2.71828\dots$ is the base of natural logarithm. $\sigma_{DE}^{tot}(C_3H_y)$ has the same form as that for $\sigma_{DE}^{tot}(C_2H_y)$ (see Eq. (54)), except for the difference between $F_3^{DE}(y)$ and $F_2^{DE}(y)$. In analogy with the case of ionization, one can use Eqs. (87), (88) also for the case $y = 0$ (i.e., to determine $\sigma_{DE}^{tot}(C_3)$)

The partial cross section for a particular DE channel $e + C_3H_y \rightarrow X + \dots$ can be obtained from $\sigma_{DE}^{tot}(C_3H_y)$ by using the relation

$$\sigma_{DE}(X/C_3H_y) = \tilde{R}_{DE}(X/C_3H_y) \sigma_{DE}^{tot}(C_3H_y) \quad (89)$$

where $\tilde{R}_{DE}(X/C_3H_y)$ is the branching ratio for the considered DE channel. It can be calculated by using Eqs. (40) (with $\beta \simeq 1.5$) and the asymptotic values of R'_{DE} given in Table 12. When using Eq. (89) to calculate $\sigma_{DE}(X/C_3H_y)$, one should use in the expression (87) for $\sigma_{DE}^{tot}(C_3H_y)$ the value of E_{th} that corresponds to the considered $e + C_3H_y \rightarrow X + \dots$ channel.

4.3 Electron-impact dissociative excitation of $C_3H_y^+$ ions (DE^+)

4.3.1 General remarks, reaction channels and energetics

As in the case of $C_2H_y^+$ ions, the process of dissociative excitation of $C_3H_y^+$ ions has not been studied so far, neither theoretically nor experimentally. As discussed in Section 3.3.1, the production of one ion and neutral products in the collision $e + C_3H_y^+$ can proceed via two mechanisms: direct excitation of a dissociative excited state of the $C_3H_y^+$ ion, and capture of the incident electron into a doubly excited (auto-ionizing) dissociative state, which after auto-ionization produces the same products as the direct process. Arguments have been given in Section 3.3.1 that for $C_2H_y^+$, and even more for $C_3H_y^+$ ions, the second mechanism (the CAD process) should not be effective. Therefore we shall discuss here only the direct DE^+ process.

4.3 Electron-impact dissociative excitation of $C_3H_y^+$ ions (DE^+)

We note that the DE^+ processes of $C_3H_y^+$ ions were not considered in Ref. [5].

In determining the most important channels for the DE^+ processes in a $e+C_3H_y^+$ collision system we shall use the same criteria as in Section 3.3.1 for $C_2H_y^+$:

1. σ_{DE^+} is large when $E_{th}^{DE^+}$ is smaller, and
2. the excitation energy $E_{exc}(AB^{+*})$ of intermediate excited dissociative state AB^{+*} should be smaller than ionization potential $I_p(AB^+)$ in the Franck-Condon region of ground-state AB^+ ion,

$$E_{exc}(AB^{+*})_{FC} < I_p(AB^+),$$
 otherwise the system auto-ionizes.

The threshold energy for a specific $e+C_3H_y \rightarrow Y^+ + A + B + \dots$ DE^+ channel is given by Eq. (18), in which $D_0(AB^+)$ and $\Delta E_{exc}(\overline{AB}^{+*})$ have the values

$$D_0(Y^+/C_3H_y^+) = \Delta H_f^0(Y^+) + \sum \Delta H_f^0(\text{neutral products}) - \Delta H_f^0(C_3H_y^+) \quad (90)$$

and

$$\Delta E_{exc}(\overline{AB}^{+*})_{FC} = \chi D_0(Y^+/C_3H_y^+), \quad \chi \simeq 0.35 \quad (91)$$

respectively (with a few exceptions for the value of χ , discussed in Section 2.2).

The energy $\Delta E_{exc}(\overline{AB}^{+*})$ is released during the DE^+ process as kinetic energy \overline{E}_x of dissociation products, and shared among them according to Eq. (26). The values of threshold energies (equal to average electron energy losses) and mean total kinetic energy of products \overline{E}_K for the most important DE^+ channels in $e+C_3H_y^+$ collisions are given in Table 13. The "asymptotic" (i.e. for $E > 30 - 40$ eV) values of cross section branching ratios, R'_{DE^+} , calculated by using Eqs. (39) and (44a), with $\alpha = 2.5$ (see next sub-section), are also given in this table.

We see from Table 13 that for the higher members of $C_3H_y^+$ family of ions ($y \geq 4$), only a small number of channels dominates the DE^+ process. The predominant role of certain channels in the DE^+ process (such the H - production channel in $e+C_3H_4^+$ system, or H_2 -production channel in $e+C_3H_5^+$, $C_3H_7^+$, $C_3H_8^+$ systems) has its origin in the very small value of dissociation energy of these channels. We further note that the threshold energies for the dominant DE^+ channels in $C_3H_y^+$ systems with $y \geq 4$ are fairly small (below ~ 3 eV; see Table 13). This indicates that DE^+ processes will strongly compete with the dissociative recombination (DR) process even at low plasma temperatures (< 5 eV).

4.4 Electron-impact dissociative ionization of $C_3H_y^+$ ions (DI^+)

4.3.2 Total and partial cross sections

As mentioned at the beginning of preceding sub-section, these are no total (or partial) cross section data available in the literature for the DE^+ process in $e+C_3H_y^+$ collision systems. The determination of total DE^+ cross section $\sigma_{DE^+}^{tot}(C_3H_y^+)$ for these systems will be done by the same procedure used in Section 3.3.2 for determining $\sigma_{DE^+}^{tot}(C_2H_y^+)$. Using the arguments given in Section 3.3.2 regarding the separability of dynamical (energy dependent) and structural factors in the cross sections of all electron-impact processes of C_xH_y molecules and their ions, and the known energy dependence of $\sigma_{DE^+}^{tot}$ for the $e+CH_y^+$ system [2], in analogy with Eq. (60) we write

$$\sigma_{DE^+}^{tot}(C_3H_y^+) = 29.4 F_3^{DE^+}(y) \left(1 - \frac{E_{th}}{E}\right)^{2.5} \frac{1}{E} \ln(e + 0.9E) (\times 10^{-16} cm^2), \quad (92)$$

where $F_3^{DE^+}(y)$ is the structural factor for DE^+ processes in $C_3H_y^+$, $e = 2.71828\dots$, and collision and threshold energies, E and E_{th} , are expressed in units of eV. The function $F_3^{DE^+}(y)$ can be determined by using the proportionality $\sigma_{DE^+}^{tot}(C_xH_y^+) \sim \sigma_{DI}^{tot}(C_xH_y^+)$ ($x = 1, 2, 3$), as discussed in Section 3.3.2, and the knowledge of $\sigma_{DE^+}^{tot}(CH_y)$ and $\sigma_{DI}^{tot}(C_{1,3}H_y)$, one obtains, on the basis of Eqs. (61) and (62) written for $C_3H_y^+$, the structural factor $F_3^{DE^+}(y)$ in the form

$$F_3^{DE^+}(y) = 1.19 + 0.91y. \quad (93)$$

Equations (92) , (93) can be also applied to the $y = 0$ case to determine $\sigma_{DE^+}^{tot}(C_3^+)$.

The partial cross section for a particular DE^+ channel $e+C_3H_y \rightarrow X^+ + \dots$ can now be obtained as

$$\sigma_{DE^+}(X^+/C_3H_y^+) = \tilde{R}_{DE^+}(X^+/C_3H_y^+) \sigma_{DE^+}^{tot}(C_3H_y^+) \quad (94)$$

where $\tilde{R}_{DE^+}(X^+/C_3H_y^+)$ is the branching ratio for the considered DE^+ channel, calculated by using Eqs. (40) with $\beta = 1.5$ (or, if more appropriately, Eqs. (42) with $\gamma = 1.5$, or Eqs. (43)), and the asymptotic values R'_{DE^+} from the Table 13.

4.4 Electron-impact dissociative ionization of $C_3H_y^+$ ions (DI^+)

4.4.1 General remarks, reaction channels and energetics

Due to their large thresholds (> 30 eV), the dissociative ionization processes of $C_3H_y^+$ ions (DI^+) should play a role only in the plasma regions with high ($> 20-30$ eV) temperatures. However, just because of their large thresholds, they can be an important plasma cooling mechanism ($\overline{E_{el}^-} = E_{th}$).

4.5 Dissociative electron recombination with $C_3H_y^+$ (DR)

The physical mechanism by which a DI^+ process in a $e + AB^+$ collision system proceeds was discussed in considerable detail in Section 3.4.1 (see also Section 2.2). We, therefore, omit here such discussion.

The most important DI^+ channels for the $e + C_3H_y^+$ collision systems are given in Table 14, together with the corresponding energy thresholds. The values of E_{th} given in this table have been calculated by using Eq. (23), with the value of $\Delta E_{exc}(A^+ + B^+) = 11.78$ eV. As discussed in Section 3.4.1, the total kinetic energy of the two charged products in DI^+ process is 11.78 eV, same for all DI^+ channels and $C_3H_y^+$ systems, while the kinetic energy of neutral products is zero (or close to zero).

In Table 14, the asymptotic values of branching ratios R'_{DI^+} of DI^+ channels are also given. They were calculated by using Eqs. (39) and (44a) with $\alpha = 1.55$ (see next sub-section).

4.4.2 Total and partial cross sections

The total DI^+ cross section for a $e + C_3H_y^+$ collision system, $\sigma_{DI^+}^{tot}(C_3H_y^+)$, can be derived in a similar way as in the case of $\sigma_{DI^+}^{tot}(C_2H_y^+)$ (see Section 3.4.2). Using the same arguments as in Section 3.4.2, one obtains

$$\sigma_{DI^+}^{tot}(C_3H_y^+) = 30.1 F_3^{DI^+}(y) \left(1 - \frac{E_{th}}{E}\right)^{1.55} \frac{1}{E} \ln(e + 0.5E) (\times 10^{-16} cm^2) \quad (95)$$

$$F_3^{DI^+}(y) = 1.71 + 0.41y \quad (96)$$

where the collision and threshold energies, E and E_{th} , are expressed in eV units, and $e=2.71828\dots$. Equations (95), (96) are also applicable to the $y = 0$ case, i.e., to determine $\sigma_{DI^+}^{tot}(C_3^+)$.

The partial cross section for a specific $e + C_3H_y^+ \rightarrow X^+ + Y^+ + \dots$ channel is given by

$$\sigma_{DI^+}(X^+, Y^+ / C_3H_y^+) = \tilde{R}_{DI^+}(X^+, Y^+ / C_3H_y^+) \sigma_{DI^+}^{tot}(C_3H_y^+) \quad (97)$$

where $\tilde{R}_{DI^+}(X^+, Y^+ / C_3H_y^+)$ is the corresponding branching ratio. \tilde{R}_{DI^+} can be calculated by using either of the prescriptions given in Section 2.3.2 (Eqs. (40), (42) or (43)) and the R'_{DI^+} data from Table 14. In view if the closeness of energy thresholds for considered DI^+ channels, the simple prescription given by Eqs. (43) is perhaps adequate for the purpose of obtaining sufficiently accurate description of the partial cross sections in the threshold region.

4.5 Dissociative electron recombination with $C_3H_y^+$ (DR)

4.5.1 Data availability, reaction channels and energetics

Total thermal rate coefficients $\langle \sigma v \rangle_{DR}$ for dissociative electron recombination with $C_3H_3^+$ and $C_3H_7^+$ ions have been reported in [54]–[56], together

4.5 Dissociative electron recombination with $C_3H_y^+$ (DR)

with $\langle \sigma v \rangle_{DR}^{tot}$ data for many other hydrocarbon ions (up to $C_8H_7^+$). By combining this information, the thermal rate coefficients for other $C_3H_y^+$ ions ($y \leq 8$) can be obtained (see next sub-section).

The determination of DR channel for a given $e + C_3H_y^+$ collision system can be done by employing the same approach used in Section 3.5.1 for the $e + C_2H_y^+$ systems. We assume that the "direct" DR mechanism is the dominant one, so that doubly excited dissociative states $C_3H_y^{**}$ energetically lying close (but below) the bottom of the $C_3H_y^+$ potential well, and whose repulsive energies intersect the $C_3H_y^+$ ground state potential energy in the region of its minimum, are associated with the dominant DR channels. The DR channels that satisfy this condition up to electron collision energies (in the c.m. system of reference) of ~ 1 eV, i.e., the relation (for, e.g., a $e + C_3H_y^+ \rightarrow A + B^* + \dots$)

$$D_0(C_3H_y \rightarrow A + B + \dots) + E_{exc}(B^*) < I_p(C_3H_y) + E_{c.m.}^{el}, \quad E_{c.m.}^{el} \simeq 1eV \quad (98)$$

are shown in Table 15 for all $C_3H_y^+$ ions. $E_{exc}(B^*)$ in Eq. (98) is the excitation energy of excited products. The excited DR products (that satisfy inequality (98)) are also given in Table 15. In addition, specific indirect (and two-step) mechanisms may strongly contribute to the $C_3H_{y-1} + H$ and $C_3H_{y-2} + 2H/H_2$ DR channels, as discussed in Section 3.5.1. In Table 15 we give also the values $E_K^{(0)}$ of the dissociation products, evaluated as if all of them would be in their ground state (calculated by using Eq. (29)).

The real total kinetic energy of dissociation products is $E_K = E_K^{(0)} - E_{exc}(B^*) + E_{c.m.}^{el}$, where $E_{c.m.}^{el}$ is the c.m. kinetic energy of incident electron, and the excitation energies of possible excited DR products are given in Table 3. The products share the total energy E_K in accordance with Eq. (26). In Table 15 we also give the estimated values of branching ratios of DR channels for each $e + C_3H_y^+$ collision system. These estimates were based on the above mentioned general criteria for selection of important DR channels, and its successful test on the observed branching ratio for CH_y^+ ($y = 1-3, 5$) [2] and $C_2H_2^+$ [52], $C_2H_3^+$ [53] systems.

In Ref. [5], only two DR channels were assumed in the electron recombination with $C_3H_y^+$ ($2 \leq y \leq 6$) ions: the H-, and H₂-production channels. An equal branching ratio ($R_{DR} = 0.5$) was assigned to these channels for all considered $C_3H_y^+$ ions. For the $e + C_3H^+$ system, three channels ($CH + 2C$, $C_2H + C$ and $3C + H$) were considered with equal ($=0.333$) branching ratio.

At electron energies $E_{c.m.} > 1$ eV, new DR channels may become open and the values R_{DR} given in Table 15 may change. These changes may particularly become significant at energies above the thresholds of DE^+ processes for a given $C_3H_y^+$ ion. The majority of DE^+ thresholds appear in the range 5–10 eV, (for $y \leq 3$) and 3–8 eV ($4 \leq y \leq 8$). Due to the competition of DR and DE^+ processes, the DR process becomes less important above these energies, and the question of energy variation of R_{DR} also loses its

4.5 Dissociative electron recombination with $C_3H_y^+$ (DR)

importance.

4.5.2 Total and partial DR rate coefficients

As mentioned in the preceding sub-section, total thermal DR rate coefficients $\langle \sigma v \rangle_{DR}^{tot}$ for $C_3H_3^+$ and $C_3H_7^+$ are available from the experiment [54]–[56]. In these references, thermal $\langle \sigma v \rangle_{DR}^{tot}$ data are also reported for a large number of $C_xH_y^+$ ions with x up to x=8. The available thermal $\langle \sigma v \rangle_{DR}^{tot}$ data for $C_xH_5^+$, ($x = 2, 4, 6$) show a remarkable linearity with x. When the data of Refs. [54]–[56] are combined with the $\langle \sigma v \rangle_{DR}^{tot}$ ($C_2H_y^+$) data of Section 3.5.2 and $\langle \sigma v \rangle_{DR}^{tot}$ (CH_y^+) data from Ref. [2], a x-linearity of $\langle \sigma v \rangle_{DR}^{tot}$ ($C_xH_y^+$) is observed also for other y=const series of $C_xH_y^+$ ions. By using interpolation / extrapolation procedures along these x-series of $\langle \sigma v \rangle_{DR}$ data, one can determine $\langle \sigma v \rangle_{DR}^{tot}$ for $C_3H_2^+$ and $C_3H_5^+$ ions, and confirm the $\langle \sigma v \rangle_{DR}$ value for $C_3H_3^+$ (within its experimental uncertainty).

It was found that the obtained $\langle \sigma v \rangle_{DR}^{tot}$ values for $C_3H_2^+$, and $C_3H_5^+$, together with the experimental data for $C_3H_3^+$ and $C_3H_7^+$, all lie on a straight line. (The experimental $\langle \sigma v \rangle_{DR}^{tot}$ data point for $C_3H_3^+$ is somewhat higher than that derived from inter- / extrapolation, but within its experimental uncertainty still follows the y linearity of $\langle \sigma v \rangle_{DR}^{tot}$ ($C_3H_y^+$)).

The T-dependence of $\langle \sigma v \rangle_{DR}^{tot}$ was discussed in Section 3.5.2 in detail. As discussed there, the T-dependence of $\langle \sigma v \rangle_{DR}^{tot}$ should be, to a large degree of accuracy, the same for all $C_xH_y^+$ systems. Therefore, in analogy with Eq. (70), the expression for $\langle \sigma v \rangle_{DR}^{tot}$ ($C_3H_y^+$) can be written in the form

$$\langle \sigma v \rangle_{DR}^{tot} (C_3H_y^+) = \frac{F_3^{DR}(y)}{T^{1/2}(1 + 0.27 T^{0.55})} (\times 10^{-8} cm^3/s) \quad (99)$$

where T is expressed in eV units. The "structural" function $F_3^{DR}(y)$ can be determined from the available thermal $\langle \sigma v \rangle_{DR}^{tot}$ data for $C_3H_2^+$, $C_3H_3^+$, $C_3H_5^+$ and $C_3H_7^+$ ions, discussed above. The linear fit of this data gives

$$F_3^{DR}(y) = 6.84 (1 + 0.15y). \quad (100)$$

Compared with Eq. (71) for $F_2^{DR}(y)$, Eq. (100) shows that $F_3^{DR}(y)$ increases with increasing y three times more slowly than $F_2^{DR}(y)$. This reflects the experimentally observed fact that thermal values of $\langle \sigma v \rangle_{DR}^{tot}$ ($C_xH_y^+$) tend to saturate with increasing both x and y [54], [55].

We also note that for the $e + C_3^+$ system, Ref. [61] gives a value $F_3^{DR}(y = 0)$ equal to that of $F_2^{DR}(y = 0)$. Consistent with the above observed y-linearity of $F_3^{DR}(y)$, we suggest a value $F_3^{DR}(y = 0) = 2.80$ for C_3^+ , which is 50% higher than the value given in Ref. [61].

The rate coefficient for an individual DR channel $e + C_3H_y^+ \rightarrow A + B^* + \dots$ is given by

$$\langle \sigma v \rangle_{DR}^{tot} (A, B^*/C_3H_y^+) = R_{DR}(A, B^*/C_3H_y^+) \langle \sigma v \rangle_{DR}^{tot} (C_3H_y^+), \quad (101)$$

4.6 Charge exchange and particle rearrangement reactions of protons with C_3H_y , (CX)

where $R_{DR}(A, B^*/C_3H_y^+)$ is the corresponding branching ratio for this channel, given in Table 15. While the validity of $\langle \sigma v \rangle_{DR}^{tot}(C_3H_y^+)$ extends to about 20 – 30 eV, the uncertainty of R_{DR} values above collision energies of ~ 5 eV, limits the validity of Eq. (101) to temperatures below ~ 10 eV.

We note that in Ref. [5] an uncorrected $T^{-1/2}$ dependence of $\langle \sigma v \rangle_{DR}^{tot}(C_3H_y^+)$ was used throughout. At $T=10$ eV this overestimates the value of $\langle \sigma v \rangle_{DR}^{tot}$ by a factor of 2.

4.6 Charge exchange and particle rearrangement reactions of protons with C_3H_y , (CX)

4.6.1 Data availability, reaction channels and energetics

Experimental cross section measurement for the pure charge exchange reaction (6a) in the $H^+ + C_3H_y$ systems have been performed only for the $H^+ + C_3H_8$ system in Refs. [65],[68],[70] in the energy range $\sim 0.1 - 200$ keV/amu. For the electronically similar system $O^+ + C_3H_8$ ($I_p(O) \simeq I_p(H)$), such cross section measurements were performed down to 0.01 keV/amu [71]. The charge exchange cross sections for $H^+ + C_3H_8$ and $O^+ + C_3H_8$ in the overlapping energy range (around ~ 0.1 keV/amu) coincide with each other and have the same energy behaviour.

Rate coefficients data for the total charge transfer process (both electron capture and particle exchange reactions (6a) and (6b),(6c), respectively) are known in the thermal region from astrophysical literature [61] for all $H^+ + C_3H_y$ systems. The experimental charge exchange cross section for $H^+ + C_3H_8$ system shows a typical behaviour for a resonant electron capture reaction (see Section 3.6.1), and smoothly tends towards its thermal energy limit with decreasing the energy. On the basis of electronic structure properties of $H^+ + C_3H_y$ collision systems, and their similarity with $H^+ + C_2H_y$ systems for which more experimental cross section data are available (see Section 3.6.1), it was argued in Ref. [7] that the charge exchange reaction of H^+ with C_3H_y , $4 \leq y \leq 8$, should also have resonant character.

As in the case of other C_xH_y molecules ($x = 1 - 3, y \leq 2x + 2$), their pure charge exchange (electron capture) process with H^+ is exothermic, ($I_p(H) > I_p(C_xH_y)$), which ensures large charge exchange cross sections in the thermal energy region. As discussed in Section 3.6.1, the reaction exothermicity is also required for particle rearrangement charge transfer channels, such as (6b) and (6c), for ensuring significant values of their thermal rate coefficients. By using this criterion, we have determined the particle rearrangement reaction channels for $H^+ + C_3H_y$ systems, as shown in Table 16. The reaction exothermicities, corresponding to each channel, are also shown in this table. They were calculated by using Eq. (31) of Section 2.2.

We note that particle re-arrangement channels $CH^+ + C_2$ and $CH + C_2^+$ of $H^+ + C_3$ collision systems are endothermic.

4.6 Charge exchange and particle rearrangement reactions of protons with C_3H_y , (CX)

In Table 16, the cross section branching ratios for the charge transfer channels in thermal energy region are also given. The estimates of these branching ratios were based partly on the proportionality of decay probability of intermediate Langevin complex (H^+ , C_3H_y) to the exothermicity of a given rearrangement channel, and partly on molecular dynamics consideration (favourable potential energy crossings, etc.). These branching ratios appear in the electron capture and particle exchange cross sections given by Eqs. (73a) and (73b), respectively. The total thermal charge exchange rate coefficients, K_{CX}^{tot} , taken from Ref. [61], are also given in Table 16. Furthermore, Table 16 gives also the values of parameters a and β appearing in the cross section (73b) for particle rearrangement reactions. These parameters were determined from the condition that particle rearrangement channels do not contribute more than 3-5% to the total charge exchange cross section for energies above ~ 1 eV.

The reaction exothermicities shown in Table 16 do not take into account that molecular products may be in vibrationally (or rotationally) excited states. If that is the case, the values of ΔE in Table 16 should be reduced by the amount of corresponding excitation energy. The remaining value of ΔE is then released as kinetic energy of the products. In the case of resonant charge reactions, most of ΔE (all of it in the case $\Delta E < D_0(C_3H_y^+)$) is absorbed in the ro-vibrational degrees of freedom of $C_3H_y^+$ product ion.

We note that in the database of Ref. [5], for all $H^+ + C_3H_y$ system with $3 \leq y \leq 6$, only the CX channels producing H, H_2 and $H + H_2$ neutral fragments were included. An equal branching ratio of 0.333 was assigned to these channels. No physical considerations were offered for this choice of R_{CX} . We note, however, that for the $H^+ + C_3H_3$ and $H^+ + C_3H_4$ systems, the $H + H_2$ channels are endothermic by 0.88 eV and 0.33 eV, respectively, and in the thermal energy region (e.g. below ~ 0.1 eV) they are not open at all. At the energies below their respective thresholds, the cross sections of these reaction channels should be exponentially small.

4.6.2 Charge exchange cross sections

The validity of the cross section (73a) and (73b) for the electron capture and particle rearrangement reactions in $H^+ + C_xH_y$ collision systems can be extended up to ~ 1 eV. Above this energy, the contribution of particle rearrangement channels to the total charge exchange cross section becomes (increasingly) negligible. The determination of charge exchange cross section for $H^+ + C_3H_y$ systems in this region was performed in Ref. [7], and the applied procedures in this determination were briefly discussed in Section 3.6.2 in connection with CX cross sections for $H^+ + C_2H_y$ systems. We shall omit here those discussions.

The total charge exchange cross section σ_{CX}^{tot} , i.e., the sum of electron capture (reaction (6a)) and particle rearrangement (reactions (6b),(6c))

5.1 General considerations

cross sections, for a specific $H^+ + C_3H_y$ collision systems determined in Ref. [7], will be presented here in the analytic form given by Eq. (77). As discussed in Section 3.6.2, this form ensures correct thermal and high energy behaviour of σ_{CX}^{tot} . With respect to σ_{CX}^{tot} of Ref. [7] some of the resonant cross sections have been slightly changed due to slightly different values of ionization potentials $I_p(C_3H_y)$ used here (based on Ref. [8]) from those used in Ref. [7]. We mention that in Ref. [7], an analytic expression employing Chebishev polynomials was used to fit the experimental or derived cross section data.

The fitting coefficients c_i , in the analytic expression (77) for the cross sections $\sigma_{CX}^{tot}(C_3H_y)$ are given in Table 17. The parameters c_i in this table for the $H^+ + C_3H_y$ system refer only to the cross section of the pure charge exchange channel, $H^+ + C_3H \rightarrow H + C_3H^+$. The particle exchange cross section for this system is given by Eq. (73b). The cross section for the pure electron capture channel in the other $H^+ + C_3H_y$ ($y \geq 2$) systems can be obtained by subtracting from $\sigma_{CX}^{tot}(C_3H_y)$, given by Eq. (77), the sum of the cross sections for all particle rearrangement channels. The analytic expression (77), with the fitting coefficients c_i given in Table 17, represents the $\sigma_{CX}^{tot}(C_3H_y)$ cross section from the thermal region ($E \sim 0.01$ eV) up to $E \simeq 300 - 400$ keV.

The zero values of the coefficients c_5 and c_6 for charge exchange reactions with $C_3H_4 - C_3H_8$ indicate that these reactions have resonant character. Their energy dependence in the energy range ~ 0.1 eV $- \sim 10$ keV is given by the c_4/E^{c_7} term only in Eq. (77). The different from zero values of c_5 and c_6 coefficients for $H^+ + C_3H_y$ reactions with $y \leq 3$, indicate the non-resonant character of these reactions. We note that the terms in the second denominator in Eq. (77) associated with the coefficients c_8 and c_{10} define the high-energy (above ~ 50 keV) behaviour of the CX cross section.

5 Unified Analytic Representation of Total Cross Sections

5.1 General considerations

We have already seen in Section 3) and (4) that all electron-impact processes in $C_xH_y / C_xH_y^+$ systems are governed by similar dynamical mechanisms. Except for the exothermic DR process, the total cross sections for all other processes of $C_xH_y / C_xH_y^+$, Eqs. (1)–(4), exhibit the same type of energy behaviour: sharp, power-law increase in the threshold region ($E_{th} < E < (2 - 3)E_{th}$), a broad maximum at $E_m \sim (6 - 10)E_{th}$, and a Born-type $E^{-1} \ln E$ behaviour at the high energies ($E \gg E_m$). The DR total cross section has a different energy behaviour ($\sim 1/E(1 + cE^\gamma)$, $c, \gamma = \text{const}$), and it is the same for all $C_xH_y^+$ ions. Moreover, we have seen in Sections 3

5.2 Unified total cross sections for electron-impact processes

and 4 that the total cross section for a specific type of process, λ , has the same energy behaviour for all $e+C_xH_y / C_xH_y^+$ collision systems, and that the difference between the cross sections for different $C_xH_y / C_xH_y^+$ species is introduced by a structural factor $F_x^\lambda(y)$. As discussed in Sections 3 and 4 (see also [51]), the separability of structural and dynamical effects in the total cross sections of electron-impact processes of $e+C_xH_y / C_xH_y^+$ collision systems results from the "stability" of additivity rules for the strength of chemical bonds with respect to external perturbations [21] (that the $C_xH_y / C_xH_y^+$ system experiences during a collision process). The observed linear dependences of structural factors $F_x^\lambda(y)$ for all considered electron-impact processes, $\lambda = (1) - (5)$, (x is the equation number of the process λ), are given in Sections 3 and 4 for $x = 2$ and $x = 3$, respectively. For $x = 1$, the functions $F_1^\lambda(y)$ are given in Ref. [2].

As mentioned in Section 2.3.2, the additivity rules should manifest themselves also with respect to the number x of C atoms in the $C_xH_y / C_xH_y^+$ systems, i.e., $F_x^\lambda(y)$, considered as function of x , should also have a linear behaviour. This has been demonstrated in Ref. [6] for total ionization cross sections, in Ref. [49] (implicitly) for total dissociation cross sections ($\sigma_{DI}^{tot} + \sigma_{DE}^{tot}$), and in Section 4.6.2 for $\langle \sigma v \rangle_{DR}^{tot}$. It is obvious that by combining the x - and y -dependences of $F_x^\lambda(y)$ into one functional form, $F_\lambda(x, y)$, one obtains a uniform representation of total cross sections for a specific process λ for all $C_xH_y / C_xH_y^+$ species. For the processes (1)–(3) and (5) ($\lambda = 1 - 3, 5$), as well as for the group of resonant reactions of charge exchange process (6a) ($\lambda = 6$), this was done in Ref. [51]. We shall present these results in the following sub-sections, and include also the result for the DI^+ process, Eq. (4) ($\lambda = 4$).

5.2 Unified total cross sections for electron-impact processes

The total cross sections for processes (1)–(4) have the following common form ($\lambda = 1 - 4$)

$$\sigma_\lambda^{tot}(E) = A_\lambda F_\lambda(x, y) \left(1 - \frac{E_{th_\lambda}^{x,y}}{E}\right)^{\alpha_\lambda} \frac{1}{E} \ln(e + c_\lambda E) (\times 10^{-16} cm^2) \quad (102)$$

where the collision and threshold energies, E and $E_{th_\lambda}^{x,y}$, are expressed in eV units, $e=2.71828\dots$, A_λ , α_λ , c_λ are known constants (see, e.g., Sections 3 and 4 for $x=2, 3$ and Ref. [2] for $x=1$). For any fixed value of x ($x = 1, 2, 3$), the functions $F_\lambda(x, y)$ are also known (Ref. [2] and Sections 3 and 4). In order to achieve a uniform representation of σ_λ^{tot} , we introduce the reduced energy $\varepsilon = E/E_{th_\lambda}^{x,y}$, after which Eq. (102) reads

$$\sigma_\lambda^{tot}(\varepsilon) = \frac{A_\lambda}{E_{th_\lambda}^{x,y}} F_\lambda(x, y) \left(1 - \frac{1}{\varepsilon}\right)^{\alpha_\lambda} \frac{1}{\varepsilon} \ln(e + a_\lambda \varepsilon) (\times 10^{-16} cm^2) \quad (103)$$

5.2 Unified total cross sections for electron-impact processes

where $a_\lambda = c_\lambda \langle E_{th,x}^{x,y} \rangle$, and $\langle E_{th,\lambda}^{x,y} \rangle$ is an average (e.g., the mean) value of $E_{th,\lambda}^{x,y}$. Since the dispersion of $E_{th,\lambda}^{x,y}$ values around $\langle E_{th,\lambda}^{x,y} \rangle$ is generally small (within a factor of two at the most), the replacement of $c_\lambda E_{th,\lambda}^{x,y}$ by $a_\lambda = \text{const}$ in the argument of the logarithm introduces an insignificant error only (smaller than $\ln 2/\varepsilon$) in the reduced energy region where the logarithmic factor in Eq. (103) considerably affects the cross section value (i.e. at $\varepsilon \gg 1$). Defining a reduced cross section $\tilde{\sigma}_\lambda^{tot}(\varepsilon)$ by the relation

$$\tilde{\sigma}_\lambda^{tot}(\varepsilon) = \frac{E_{th,\lambda}^{x,y}}{F_\lambda(x,y)} \sigma_\lambda^{tot}(\varepsilon) \quad (104)$$

we obtained from Eq. (103)

$$\tilde{\sigma}_\lambda^{tot}(\varepsilon) = A_\lambda \left(1 - \frac{1}{\varepsilon}\right)^{\alpha_\lambda} \frac{1}{\varepsilon} \ln(e + a_\lambda \varepsilon) (\times 10^{-16} \text{ cm}^2), \quad (105)$$

For a given process λ , $\tilde{\sigma}_\lambda^{tot}$ depends only on the reduced energy ε and not on structural specifics of the $C_x H_y / C_x H_y^+$ target. The values of parameters A_λ , α_λ and a_λ for processes I+DI, DE, DE⁺ and DI⁺ ($\lambda = 1, 2, 3, 4$, respectively) are:

$$A_1 = 84.0, A_2 = 34.6, A_3 = 29.4, A_4 = 30.1 \quad (106a)$$

$$\alpha_1 = 3.0, \alpha_2 = 3.0, \alpha_3 = 2.5, \alpha_4 = 1.55 \quad (106b)$$

$$a_1 = 0.96, a_2 = 1.27, a_3 = 7.02, a_4 = 14.5 \quad (106c)$$

The functional forms of $F_\lambda(x, y)$ for these processes are:

$$F_1(x, y) = (1 + 0.373y) + 0.47(x-1) \left[\left(1 + \frac{x+5.65}{x}\right) - \frac{0.655(1-\delta_{x,1})y}{(x-1)} \right], \quad (107a)$$

$$F_2(x, y) = (1 + 0.29y) + 1.25(x-1) \left[0.28(x-1) - \frac{0.36y}{x^2} \right], \quad (107b)$$

$$F_3(x, y) = 1 + 0.71(y-1) + (x-1) \left[0.45 + \frac{0.19(1-\delta_{x,y})y}{(x-1)} \right], \quad (107c)$$

$$F_4(x, y) = 1 + 0.086(y-1) + (x-1) \left[0.40 + \frac{0.488y}{x} \right], \quad (107d)$$

where $\delta_{i,j}$ is the Kronecker symbol.

The above expressions for $F_\lambda(x, y)$ were obtained as fits to the functions $F_x^\lambda(y)$ given in Sections 3 and 4, for $x = 2$ and 3 , respectively, and in Ref. [2], for $x = 1$. The x -linearity of $F_\lambda(x, y)$ for $\lambda = 1, 3, 4$ is obvious from the above expressions. $F_2(x, y)$ is also linear in the small $x = 1-3$ interval, but for higher x -values its linearity is violated. This is a consequence of the small number of x -values ($x = 1, 2, 3$ only) in the fitting procedure, and not a violation of additivity rules.

5.3 Unified cross section for resonant charge exchange reactions

The total rate coefficients $\langle \sigma v \rangle_{DR}^{tot}$ for dissociative recombination processes of $C_x H_y^+$ ions, Eq. (5), ($\lambda = 5$), can also be represented in a unified form. By combining the expressions $\langle \sigma v \rangle_{DR}^{tot}(C_2 H_y^+)$ and $\langle \sigma v \rangle_{DR}^{tot}(C_3 H_y^+)$ given in Sections 3.5.2) and (4.5.2, respectively, and deriving a similar expression for $\langle \sigma v \rangle_{DR}^{tot}(C H_y^+)$, one obtains (by a fitting procedure)

$$\langle \sigma v \rangle_{DR}^{tot}(C_x H_y^+) = \frac{4.15 F_5(x, y)}{T^{1/2}(1 + 0.27T^{0.55})} (\times 10^{-9} cm^3/s) \quad (108)$$

where T is expressed in eV units, and

$$F_5(x, y) = 1 + 6.48(x - 1) \left(1 + \frac{1.75(x - 2)}{x^2} \right) + 2 \left[1 + \frac{0.776(x - 1)}{(x - 0.95)^{2.62}} \right] y. \quad (109)$$

The reduces DR rate coefficient

$$\langle \tilde{\sigma} v \rangle_{DR}^{tot} = \frac{\langle \sigma v \rangle_{DR}^{tot}(C_x H_y^+)}{F_5(x, y)} = \frac{4.15}{T^{1/2}(1 + 0.27T^{0.55})} (\times 10^{-9} cm^3/s), \quad (110)$$

is obviously independent of the ion species and, together with the expression (109), defines the scaling of $\langle \sigma v \rangle_{DR}^{tot}(C_x H_y^+)$.

5.3 Unified cross section for resonant charge exchange reactions

As mentioned in Sections 3.6.2) and (4.6.2, the pure charge exchange reactions of H^+ with $C_{2,3}H_y$ have a resonant character when $2x - 1 \leq y \leq 2x + 2$. Similar resonant character have also the electron capture reactions of protons with CH_3 and CH_4 molecules [2]. In the collision energy range $0.1 < E(eV) < 10^4$, the cross sections of these reactions satisfy the simple scaling given by Eq. (74) [7]. For energies below ~ 0.1 eV, and above ~ 50 keV, this scaling is changed due to a change of the dominant electron capture mechanism in these regions. By using the relation (74) and the available experimental cross section data for resonant reactions $H^+ + CH_4, C_2H_6, C_3H_8, C_4H_{10}$ (see [7] and Sections 3.6.1) and (4.6.1), one can obtain the following expression for $\sigma_{ex,res}^{tot}$

$$\sigma_{CX,res}^{tot}(C_x H_y) = 2.76 \frac{Ry}{I_p(C_x H_y)} y^{1/2} E^{-0.14} (\times 10^{-15} cm^2) \quad (111)$$

where $I_p(C_x H_y)$ is the ionization potential of $C_x H_y$, $Ry = 13.605$ eV, and E and $I_p(C_x H_y)$ are expressed in eV units.

Equation (111) allows to obtain a reduced resonant charge exchange cross section for all $C_x H_y$ molecules

$$\tilde{\sigma}_{CX,res}^{tot} = \frac{I_p(C_x H_y)}{Ry y^{1/2}} \sigma_{CX,res}^{tot}(C_x H_y) = 2.76 E^{-0.14} (\times 10^{-15} cm^2) \quad (112)$$

6.1 Electron-impact collision processes

that is function only on the collision energy. Eq. (112) defines the scaling of $\sigma_{CX,res}^{tot}$ with respect to C_xH_y molecular species. The collisional dynamics of non-resonant charge exchange reactions, in the energy regions where they have large cross sections, is governed by strong coupling of many electronic states of the $H^+ + C_xH_y$ system. The absence of a single, dominant mechanism responsible for the electron capture process, makes it impossible to obtain a unifying analytic expression for the cross sections of non-resonant charge exchange reactions.

The accuracy of cross sections represented by the unified analytic formulae given in this section is (for all E):

- $\lambda=1$: better than 20% for $x=1$, 50% for $x=2$, and 70% for $x=3$,
- $\lambda=2$: better than 70% for all x ,
- $\lambda=3, 4$: better than 50% for all x ,
- $\lambda=5$: better than 30–40% for all x (and $E < 20 - 30$ eV).

The accuracy of Eq. (111) for $\sigma_{CX,res}^{tot}$ in the energy range of its validity, $0.1 < E(eV) < 10^4$ is within 15% (same as the experimental uncertainties).

The accuracies of individual total cross sections for $\lambda = 1-4$, determined in Section 3 and 4 are, however, significantly better than those quoted above.

6 Reaction Rate Coefficients

6.1 Electron-impact collision processes

The analytic forms of cross sections for electron-impact processes (1) - (4), which were given in Sections 3 and 4 for $C_2H_y / C_2H_y^+$ and $C_3H_y / C_3H_y^+$ molecular systems, respectively, and in Ref. [2] for CH_y / CH_y^+ systems, allow to obtain analytic (in some cases approximate) expressions also for the rate coefficients $\langle \sigma v \rangle_\lambda$ of these processes. Such expressions have already been obtained in [2] (FZ-Juel Report) for some of these processes related to the CH_y / CH_y^+ systems.

The rate coefficient for a reaction λ ($\lambda = 1 - 4$ for processes defined by Eqs. (1)–(4), respectively) with cross section $\sigma_\lambda(v)$, where v is the electron collision velocity ($v = (2E/m)^{1/2}$, E being the electron energy) is given by Maxwellian average of the product $\sigma(v) \cdot v$ (we take $m_e = 1$, $k_B = 1$, k_B being the Boltzmann constant)

$$\langle \sigma v \rangle_\lambda = \frac{4}{\pi^{1/2} u^3} \int_{v_{th}}^{\infty} v^3 \sigma_\lambda(v) \exp\left(-\frac{v^2}{u^2}\right) dv \quad (113)$$

where $u = (2T)^{1/2}$, T is the electron temperature, and $v_{th} = (2E_{th})^{1/2}$ is the collision velocity corresponding to threshold energy.

6.1 Electron-impact collision processes

We first consider the total rates $\langle \sigma v \rangle_{\lambda}^{tot}$ for the process $\lambda = 1 - 4$. As we have seen in the preceding section, for all processes $\lambda = 1 - 4$, the total cross section σ_{λ}^{tot} has the general form

$$\sigma_{\lambda}^{tot}(E) = B_0 \left(1 - \frac{E_{th}}{E}\right)^{\alpha} \frac{1}{E} \ln(e + cE) \quad (114)$$

where $e=2.71828\dots$, and the constant B_0 includes the structural dependence of σ_{λ}^{tot} (as well as the scale factor 10^{-16} , when E is expressed in eV). With the expression (114) for σ_{λ}^{tot} , the rate coefficient $\langle \sigma v \rangle_{\lambda}^{tot}$ takes the form

$$\langle \sigma v \rangle_{\lambda}^{tot} = \frac{8B_0 E_{th}}{\pi^{1/2} u^3} \int_1^{\infty} \left(1 - \frac{1}{x}\right)^{\alpha} \ln(e + ax) e^{-\beta x} dx \quad (115)$$

where $a = cE_{th}$ and $\beta = E_{th}/T$. The product ax in the argument of the \ln function in Eq. (115) is always larger than 0.7 (see, e.g., Eq. (105c)) and the function $\ln(e + ax)$ can be expressed as

$$\ln(e + ax) \simeq \frac{2.62}{1 + ax} + \ln(ax) \quad (116)$$

with an accuracy better than 4% for $x \leq 1$, and better than 1% for $x > 1$. Eq. (115) then becomes

$$\langle \sigma v \rangle_{\lambda}^{tot} = \frac{8B_0 E_{th}}{\pi^{1/2} u^3} (2.62\mathcal{I}_1 + \ln(a)\mathcal{I}_2 + \mathcal{I}_3) \quad (117)$$

where

$$\mathcal{I}_1 = \int_1^{\infty} \frac{1}{1 + ax} \left(1 - \frac{1}{x}\right)^{\alpha} e^{-\beta x} dx \quad (118a)$$

$$\mathcal{I}_2 = \int_1^{\infty} \left(1 - \frac{1}{x}\right)^{\alpha} e^{-\beta x} dx \quad (118b)$$

$$\mathcal{I}_3 = \int_1^{\infty} \left(1 - \frac{1}{x}\right)^{\alpha} \ln x e^{-\beta x} dx \quad (118c)$$

The integral \mathcal{I}_2 is given in Ref. [79] and has the form

$$\mathcal{I}_2 = \frac{1}{\beta} \Gamma(1 + \alpha) e^{-\beta/2} \mathcal{W}_{-\alpha; 1/2}(\beta) \quad (119)$$

where $\Gamma(x)$ is the Gamma function and $\mathcal{W}_{\lambda; \mu}(x)$ is the Whittaker function. The main contribution in integral \mathcal{I}_1 gives the region $x \simeq 1$, and the factor

6.1 Electron-impact collision processes

$(1 + ax)^{-1}$ in the integrand can be replaced by $(1 + a)^{-1}$. The integral \mathcal{I}_1 is then reduced to \mathcal{I}_2 and we have

$$\mathcal{I}_1 \simeq \frac{1}{1 + a} \mathcal{I}_2. \quad (120)$$

Finally, the main contribution in I_3 comes from the region of larger x . Retaining only the first term in the expansion of $(1 - \frac{1}{x})^\alpha$ in powers of $1/x$, we obtain

$$\mathcal{I}_3 \simeq \frac{1}{\beta} E_1(\beta) = -\frac{1}{\beta} E_i(-\beta) \quad (121)$$

where $E_1(\beta)$ is the exponential integral function. The neglected terms in Eq. (121) are related to higher order Schlömlich's exponential integrals, $E_n(\beta)$. The low temperature ($T \ll E_{th}$) dependence of $\langle \sigma v \rangle_\lambda^{tot}$ can be obtained by using the expansions of $\mathcal{W}_{\lambda,\mu}(\beta)$ and $E_1(\beta)$ for large values of β [79]

$$\mathcal{W}_{\lambda,\mu}(\beta) \simeq \beta^\lambda e^{-\beta/2} \left[1 + \frac{\mu^2 - (\lambda - 1/2)^2}{\beta} + \mathcal{O}(1/\beta^2) \right] \quad (122)$$

$$E_1(\beta) \simeq \frac{1}{\beta} e^{-\beta} \left[1 - \frac{1}{\beta} + \mathcal{O}(1/\beta^2) \right]. \quad (123)$$

Other rapidly converging expansions for $E_1(z)$ and $\mathcal{W}_{\lambda,\mu}(z)$ are given elsewhere [79], [80]. In order to obtain $\langle \sigma v \rangle_\lambda^{tot}$ in units of cm^3/s , one should express σ_λ^{tot} given by Eq. (114) in units of cm^2 (i. e. include in the constant B_0 the factor $10^{-16} cm^2$), express T and E_{th} in eV units, and multiply Eq. (115) by the atomic unit of velocity, $v_0 = 2.19 \cdot 10^8 cm/s$.

The rate coefficients $\langle \sigma v \rangle_\lambda^{(s)}$ for individual reaction channels (s) can be obtained from $\langle \sigma v \rangle_\lambda^{tot}$ as

$$\langle \sigma v \rangle_\lambda^{(s)} = \tilde{R}_\lambda^{(s)} \langle \sigma v \rangle_\lambda^{tot} \quad (124)$$

where $\tilde{R}_\lambda^{(s)}$ is the branching ratio for the channel (s). However, only energy independent values for $\tilde{R}_\lambda^{(s)}$, determined by the prescription given by Eqs. (43) of Section 2.3.2, can be used in Eq. (124). If the forms of $\tilde{R}_\lambda^{(s)}$ given by Eqs. (40) or Eqs. (42) are used, then

$$\langle \sigma v \rangle_\lambda^{(s)} = \langle \tilde{R}_\lambda^{(s)} \sigma_\lambda^{tot} v \rangle \quad (125)$$

has to be used.

The total partial ionization rate coefficients can be obtained by using the expression (47) (same for both C_2H_y and C_3H_y). The integration in

6.2 Charge exchange processes

Eq. (113) with this expression for $\sigma_\lambda(v)$ gives (after multiplication with v_0)

$$\begin{aligned} \langle \sigma v \rangle_{ion} &= 8.76 \frac{1}{I_c} \left(\frac{\beta}{2\pi I_c} \right)^{1/2} \cdot \\ &\cdot \left[A_1 E_1(\beta) + \sum_{j=2}^N A_j (j-1)! e^{-\beta/2} \mathcal{W}_{-(j-1); 1/2}(\beta) \right] \\ &(\times 10^{-5} \text{cm}^3/\text{s}) \end{aligned} \quad (126)$$

where I_c and A_i are the fitting parameters appearing in Eq. (47), $\beta = I_c/T$, and I_c and T are expressed in eV units.

6.2 Charge exchange processes

For the charge exchange reactions, we assume that the protons have a Maxwellian velocity distribution characterized by a temperature $T = m_p u^2/2$, and that the hydrocarbon molecules have a certain kinetic energy $E = MV^2/2$. The charge exchange rate coefficient is then defined as

$$\langle \sigma v \rangle_{CX} = \frac{1}{\pi^{1/2} u V} \int_0^\infty v_r^2 \sigma_{CX}(v_r) \left[e^{-(v_r-V)^2/u^2} - e^{-(v_r+V)^2/u^2} \right] dv_r \quad (127)$$

where $v_r = |\vec{u} - \vec{V}|$ is the relative collision velocity. In Eq. (127) it is taken into account that all CX processes are exothermic. Having in mind the complexity of analytic expression, Eq. (77), for the total charge exchange cross section (valid for both C_2H_y and C_3H_y systems), and the fact that hydrocarbon impurities entering the plasma from the walls possess certain kinetic energy, it becomes fairly clear that the integration in Eq. (127) cannot be carried out in a way so as to obtain a result in reasonably compact analytic form. Therefore, the calculations of $\langle \sigma v \rangle_{CX}$, with the analytic expression (77) for σ_{CX} , has to be carried out numerically. However, for the resonant CX reaction, the cross section of which is represented by the simple form given by Eq. (111), that is valid in the broad energy range from ~ 0.1 eV to ~ 10 keV (extendible down to ~ 0.05 eV and up to ~ 20 keV with an increased uncertainty from $\sim 15\%$ to $\sim 30\%$), a compact analytic expression for $\langle \sigma v \rangle_{CX}$ can be obtained assuming that hydrocarbon molecules have negligible kinetic energies, \mathcal{E} . The resulting rate coefficient is [79]

$$\langle \sigma v \rangle_{CX, res} = 4.03 B_0^{x,y} T^{1/2-\alpha} \Gamma(2-\alpha) (\times 10^{-9} \text{cm}^3/\text{s}) \quad (128)$$

where $\alpha = 0.14$, $B_0^{x,y} = y^{1/2} Ry/I_p(C_x H_y)$, $Ry = 13.605$ eV, $\Gamma(2-\alpha) = 0.9487$ and T and $I_p(C_x H_y)$ (the ionization potential of $C_x H_y$) are expressed in units of eV. The correction to Eq. (128) due to the finite kinetic energy

7 Concluding Remarks

\mathcal{E} of the hydrocarbon molecule can be obtained for $\mathcal{E} \lesssim 15$ eV from the $\langle \sigma v \rangle_{CX, res}(T, \mathcal{E})$ data in Ref. [7] in the form:

$$\Delta \langle \sigma v \rangle_{CX, res} \simeq 2 \left[\left(\frac{\mu_{3,8}}{\mu_{x,y}} \log(1 + \mathcal{E}) \right) \right]^{2.5} / (1 + 0.2T^{0.5} + T^{1.5}) (\times 10^{-9} cm^3/s) \quad (129)$$

where $\mu_{x,y}$ is the reduced mass of the $H^+ + C_xH_y$ collision system, and \mathcal{E} is expressed in eV units.

We further note that for temperatures larger than ~ 1 keV, the rate coefficient $\langle \sigma v \rangle_{CX}$ can simply be represented by the product

$$\langle \sigma v \rangle_{CX} = \sigma_{CX} \cdot v, \quad (130)$$

where v is the relative collision velocity. The expression (130) is valid (for $T > 1$ keV) also when the hydrocarbons are not at rest, and have kinetic energies below ~ 1 keV.

7 Concluding Remarks

In this work we present a collisional database for the most important electron and proton impact processes with C_2H_y ($y = 1 - 6$) and C_3H_y ($y = 1 - 8$) molecules and their $C_{2,3}H_y^+$ ions. These processes are given by Eqs. (1)–(6). Both total and partial (for individual reaction channels) cross sections have been determined in a wide energy range: For inelastic electron-impact processes (1)–(4), this range extends from energy threshold to several keV; for dissociative recombination processes (5) it covers the region from thermal (< 0.05 eV) energies to $\sim 10 - 20$ eV, while for the proton-impact charge exchange processes (6) the covered energy range extends from thermal to ~ 0.5 MeV energies. The selection of processes included in this present work was done on the basis of their expected importance for the kinetics of fusion edge plasmas with temperatures up to $\sim 100 - 200$ eV. On this basis, the electron-impact processes resulting in production of multiply charged ions (with large energy thresholds), or the high energy dissociative charge transfer, have been excluded from the scope of present database.

The present database is aimed mainly for hydrocarbon transport studies in fusion edge plasmas by kinetic (such as Monte-Carlo) modeling codes. The questions related to the production and collisions of excited (either electronically or ro-vibrationally) hydrocarbon species have, therefore not been addressed (except in connection with DR and resonant CX mechanisms). However, the questions of fragmentation paths (reaction channels), and reaction energetics for each fragmentation channel have been analyzed and quantified to full extent.

In view of the limited experimental or theoretical cross section information available in the literature, for determining the cross sections for

7 Concluding Remarks

majority of considered processes, and their individual reaction channels, semi-empirical cross section scaling relationships have been widely used. For electron-impact collision processes these cross section scaling relationships have their origin in the additivity rules for the strengths of chemical bonds in poly-atomic molecules, while in the case of charge exchange processes they have well established theoretical basis. All used cross section scaling relationships have firm experimental confirmation.

The observed cross section scalings with respect to structural parameters of collision systems were basis for establishing unified analytic representations for the cross sections (or reaction rate coefficients) for all studied collision processes (with the exception of the non-resonant charge exchange only) (Section 4).

The determination of reaction channels for a given process and for a particular collision system was done by applying certain well defined criteria. The determination of cross section branching ratios for the particular reaction channels was also performed on the basis of criteria derived from the cross section energy behaviour for the considered process in the threshold region. The uncertainty involved in these procedures is rather small. However, the unavailability of information regarding the energies of excited dissociative states of C_xH_y and $C_xH_y^+$ systems, makes the derived values for the quantities involved in the energetics of dissociative processes (such as electron energy loss, mean total kinetic energy of dissociative products) less certain. Nevertheless, the available information on the energy parameters of the reactants and products (heat of formation, ionization potentials, dissociation energy limits) significantly reduces the uncertainty of reaction energetics quantities (to about 0.5 – 1 eV).

The analytic expressions for total and partial cross sections of considered processes (1)–(4) allow to obtain also approximate analytic expressions for their rate coefficients (Section 6). For the total and partial ionization cross sections, as well as for the resonant charge exchange reactions, the $\langle \sigma v \rangle$ analytic expressions are exact. Only for the non-resonant charge exchange reactions, it was not possible to obtain compact analytic expression for $\langle \sigma v \rangle$.

The accuracy of provided cross sections varies for various of considered processes. The accuracy electron-impact ionization cross sections is believed to be within 20–30%, except for the cross sections of C_2H_2 , C_2H_4 , C_2H_6 and C_3H_8 , for which experimental data exist with an accuracy of 10–20%. The cross sections for DE, DE^+ and DI^+ processes, derived by using the semi-empirical scalings, may have uncertainties up to 50–100%. The rate coefficients of dissociative recombination are believed to be accurate to within 20–30 % in the temperature region below ~ 10 eV, and perhaps somewhat less accurate at higher temperatures. The cross sections of resonant charge exchange reactions of C_2H_4 , C_2H_6 and C_3H_8 , based on experimental measurement in a broad energy range, should be accurate

7 Concluding Remarks

to within 15–20%. An uncertainty up to 25–30% can be ascribed to all other resonant charge exchange reactions (of C_2H_5 , $C_3H_5 - C_3H_7$), and to the non-resonant reaction of C_2H_4 (for which a set of low-energy cross section measurements exists). The accuracy of cross sections for all other non-resonant reactions (of C_2H , C_2H_3 , $C_3H - C_3H_4$) is believed to be within 30 – 50 % for $E \lesssim 1$ eV and $E \gtrsim 1$ keV, where the cross sections are determined by well established scalings, and considerably smaller for the energies in between (except for the C_3H_4 molecule for which CX reaction should be almost resonant). The cross section and rate coefficient information provided in the present work is included in the Atomic and Molecular Data Section of the EIRENE code, and can be down-loaded from its web-domain (www.eirene.de).

8 References

References

- [1] A. A. Haasz, J. A. Stephens, E. Vietzke et al., *Atom Plasma-Mater. Interac. Data Fusion* 7 (part A), 5 (1998).
- [2] R. K. Janev and D. Reiter, *Phys. Plasmas* 9, 4071(2002); see also: R. K. Janev and D. Reiter: "Collision processes of hydrocarbon species in hydrogen plasmas: I. The methane family", Report FZ-Jülich Jül -3966, Forschungszentrum Jülich, Jülich Germany (Feb. 2002).
- [3] D. Reiter, in: *Atomic and Plasma-Material Interaction Processes in Controlled Thermonuclear Fusion*, edited by R. K. Janev and H.W. Drawin (Elsevier Science, Amsterdam) (1993), 243, see also: D. Reiter, "The EIRENE Code", <http://www.eirene.de>
- [4] A. B. Ehrhardt and W. D. Langer, "Collision processes of hydrocarbons in hydrogen plasmas", Report PPPL-2477, Princeton Plasma Physics Laboratory, Princeton, NJ (Sept. 1987).
- [5] D. A. Alman, D. N. Ruzic and J.N. Brooks, *Phys. Plasmas* 7, 1421 (2000).
- [6] R. K. Janev, J. G. Wang, I. Murakami and T. Kato, "Cross sections and rate coefficients for electron-impact ionization of hydrocarbon molecules", Report NIFS-DATA-68, National Institute for Fusion Science, Toki, Japan (Oct., 2001).
- [7] R. K. Janev, J. G. Wang and T. Kato, "Cross sections and rate coefficients for charge exchange reactions of protons with hydrocarbon molecules", Report NIFS-DATA-64, National Institute for Fusion Science, Toki, Japan(May,2001).
- [8] M. W. Chase, "NIST-JANAF Thermochemical Tables", 4th edition, *J. Phys. Chem. Ref. Data*, Monograph 9 (1998) pp. 1-1951, (See, also: [www.NIST Chemistry WebBook](http://www.NIST.Chemistry.WebBook), 2001).
- [9] H. M. Rosenstock, K. Draxl, B. M. Steiner, and J. T. Herron, *J. Phys. Chem. Ref. Data* 6 (Suppl. 1) 1 (1977).
- [10] H. D. P. Liu and G. Verhaegen, *J. Chem. Phys.* 53, 735 (1970); R. P. Saxon and B. Liu, *ibid.* 78, 1344 (1982).
- [11] A. A. Radzig and B. M. Smirnov, *Reference Data on Atoms, Molecules and Ions*, (Springer-Verlag, Berlin 1985).

REFERENCES

- [12] S. Green, P. S. Bagns, B. Liu, A. D. McLean, and M. Yoshimine, *Phy. Rev. A* *5*, 1614 (1972).
- [13] A. J. Lorquet, J. C. Lorquet, H. Wankenne, J. Monigny, and H. Lefebvre-Brion, *J. Chem. Phys.* *55*, 4053 (1971).
- [14] H. Tawara, Y. Itikawa, H. Nishimura, H. Tanaka, and Y. Nakamura, "Collision data involving hydro-carbon molecules", Report NIFS-DATA-6, National Institute for Fusion Science, Toki, Japan (July, 1990).
- [15] N. Djurić, Y.-S. Chung, B. Walbank, and G. H. Dunn, *Phys. Rev. A* *56*, 2887 (1997).
- [16] N. Djurić, S. Zhou, G. H. Dunn, and M. E. Bannister, *Phys. Rev. A* *58*, 304 (1998).
- [17] R. Loch and J. Momigny, *Chem. Phys.* *49*, 173 (1980).
- [18] Y.-K. Kim, in: *Atomic and Molecular Processes in Fusion Edge Plasmas*, edited by R. K. Janev (Plenum Press, New York, 1995) p.263.
- [19] B. L. Schram, M. J. van der Wiel, F. J. de Heer, and H. R. Moustafa, *J. Chem. Phys.* *44*, 49 (1966).
- [20] S. W. Benson and J. H. Buss, *J. Chem. Phys.* *29*, 546 (1958).
- [21] D. R. Bates, *Int. J. Mass-Spectrom. Ion Processes* *8*, 1 (1987).
- [22] C. E. Melton, *J. Chem. Phys.* *37*, 562 (1962).
- [23] J. T. Tate and P. T. Smith, *Phys. Rev.* *39*, 270 (1932).
- [24] A. Gaudin and R. Hageman, *J. Chim. Phys.* *64*, 917 (1967).
- [25] D. Rapp and P. Englander-Golden, *J. Chem. Phys.* *43*, 1464 (1965).
- [26] H. Nishimura and H. Tawara, *J. Phys. B* *27*, 2063 (1994).
- [27] N. Durić, I. Cadez, and M. Kurepa, *Int. J. Mass Spectrom, Ion Process* *108*, R1 (1991)
- [28] Y.-K. Kim, M. A. Ali, and M. E. Rudd, *J. Res NIST* *102*, 693 (1997).
- [29] K. K. Irikura and Y.-K. Kim (private communication, 2000).
- [30] W. Hwang, Y.-K. Kim, and M. E. Rudd, *J. Chem. Phys.* *104*, 2956 (1996).
- [31] A. Gaudin and R. Hageman, *J. Chim. Phys.* *64*, 1209 (1967).
- [32] S.-H. Zheng and S. K. Srivastava, *J. Phys. B* *29*, 3235 (1996).

REFERENCES

- [33] C. Tian and C. R. Vidal, *J. Phys. B* *31*, 895 (1998).
- [34] H. Chatham, D. Hills, R. Robertson, and A. Gallagher, *J. Chem. Phys.* *81*, 1770 (1984).
- [35] V. Grill, G. Walder, P. Scheir, M. Krudel, and T. D. Märk, *Int. J. Mass Spectrom. Ion Processes* *129*, 31 (1993).
- [36] P. Plessis and P. Marmet, *Int. J. Mass Spectrom. Ion Processes* *70*, 23 (1986).
- [37] P. Plessis and P. Marmet, *Can. J. Chem.* *65*, 1424 (1987).
- [38] H. Deutsch, K. Becker, S. Matt and T. D. Märk, *Int. J. Mass Spectrom. Ion Processes* *197*, 37 (2000).
- [39] D. A. Vroom and F. J. de Heer, *J. Chem. Phys.* *50*, 573 (1969).
- [40] J. F. M. Aarts, C. I. M. Beenakker, and F. J. de Heer, *Physica* *53*, 32 (1971).
- [41] C. I. M. Beenakker and F. J. de Heer, *chem. Phys.* *6*, 291 (1974).
- [42] C. I. M. Beenacker, P. J. F. Verbeek, G. R. Möhlmann and F. J. de Heer, *J. Quant. Spectrosc. Radiat. Transfer* *15*, 265 (1974).
- [43] R. S. Freund, S. M. Tarr, and J. A. Schiavone, *J. Chem. Phys.* *79*, 213 (1983).
- [44] T. Ogawa, Y. Ueda, and M. Higo, *Bull. Chem. Soc. Jpn.* *56*, 3033 (1983).
- [45] K. D. Pang, J. M. Ajello, B. Franklin, and D. E. Shemansky, *J. Chem. Phys.* *86*, 2750 (1987).
- [46] N. Yonekura, T. Tsuboi, H. Tomura, K. Nakashima, J. Kurawaki, and T. Ogawa, *Jpn. J. Appl. Phys.* *32*, 3296 (1993)
- [47] H. F. Winters, *J. Chem. Phys.* *36*, 353 (1979).
- [48] H. F. Winters, *J. Chem. Phys.* *63*, 3462 (1975).
- [49] H. F. Winters, and M. Inokuti, *Phys. Rev. A* *25*, 1420 (1982).
- [50] Cz. Szmytkowski, *Z. Phys. D* *13*, 69 (1989).
- [51] R. K. Janev, and D. Reiter, *J. Nucl. Mater.* *313-316*, 1202 (2003).
- [52] A. M. Derktatch, A. Al-Khalili, L. Viktor et al., *J. Phys. B* *32*, 3391 (1999).

REFERENCES

- [53] S. Kalhori, A. A. Viggiano, S. T. Arnold et al., *Astron. Astrophys.* *391*, 1159 (2002).
- [54] H. Aboulaziz, J. C. Gomet, D. Pasquerault, B. R. Rowe, and J. B. A. Mitchell, *J. Chem. Phys.* *99*, 237 (1993).
- [55] L. Lehfaoui, C. Rebrion-Rowe et al., *J. Chem. Phys.* *106*, 1 (1997).
- [56] J. B. A. Mitchell, and C. Rebrion-Rowe, *Int. Rev. Phys. Chem.* *16*, 201 (1997).
- [57] E. Herbst, *Astrophys. J.*, *222*, 508 (1978); S. Green, and E. Herbst, *ibid* *229*, 121 (1979).
- [58] D. R. Bates, *Astrophys. J.*, *306*, L 45 (1986) and *344*, 531 (1989).
- [59] D. R. Bates, *Phys. Rev.* *78*, 492(1950).
- [60] D. R. Bates, *Monthly Notices Roy. Astron. Soc.* *262*, 260 (1993)
- [61] T. J. Millar, P. R. A. Facquhar, and K. Willacy, *Astron. Astrophys. Suppl. Ser.* *121*, 139 (1997).
- [62] Z. Amitay, D. Zajfman, P. Fork et al., *Phys. Rev. A* *54*, 4032 (1996).
- [63] A. Larson, A. Le Padellec, J. Semaniak et al., *Astrophys. J.* *505*, 459 (1998).
- [64] E. P. Wigner, *Phys. Rev.* *73*, 1002 (1948).
- [65] T. Kusakabe, K. Asahina, A. Iida et al., *Phys. Rev. A* *62*, 062715 (2000).
- [66] J. G. Collins, and P. J. Kebarle, *J. Chem. Phys.* *46*, 1082(1967).
- [67] L. H. Toburen, Y. Nakai, and R. A. Langley, *Phys. Rev.* *171*, 114 (1968).
- [68] M. Elliot, *J. Phys.(France)* *38*, 24 (1977).
- [69] S. L. Varghese, G. Bissinger, M. J. Joyce, and R. Laubert, *Nucl. Instr. Meth.*, *170*, 269 (1980).
- [70] M. L. Jones, B. Dougherty, and M. Dillingham, *Nucl. Instrum. Meth. Phys. Res. B* *10 / 11*, 142 (1985).
- [71] T. Kusakabe, R. Buenker, and M. Kimura, *At. Plasma-Mater. Interact. Data Fusion* *10*, 151 (2002).
- [72] G. Gioumouisis, and D. P. Stevenson, *J. Chem. Phys.* *29*, 294 (1958).
- [73] B. M. Smirnov, “*Asymptotic Methods in the Theory of Slow Atomic Collisions*”, (Nauka, Moscow, 1973).(in Russian).

REFERENCES

- [74] E. E. Nikitin and S. Ya. Umanskii, “*Theory of Slow Atomic Collisions*”, (Springer-Verlag, Berlin, Heidelberg, 1985).
- [75] B. H. Bransden, and M. R. C. McDowell, “*Charge Transfer and the Theory of Ion-Atom Collisions*”, (Clarendon Press, Oxford, 1992).
- [76] H. Deutsch, K. Becker, R. K. Janev, M. Probst, and T. D. Märk, J. Phys. B *33*, 4872 (2002).
- [77] H. Deutsch, and T. D. Märk (private communication, 2000).
- [78] V. Grill, G. Walder, D. Margreiter, T. Rauth, H. U. Poll, P. Scheir, and T. D. Märk, Z. Phys. D *25*, 217(1993).
- [79] I. S. Gradshteyn and I. M. Ryzhik, “*Tables of Integrals, Series and Products*”, (Academic Press, New York, 1965).
- [80] M. Abramowitz and I. Stegun, “*Handbook of Mathematical Functions*”, (NBS Math. Ser., Washington 1964).

9 Tables

9 Tables

Table 1: Heat of formation (ΔH_f^0) and ionization potential (I_p) of C_xH_y ($0 \leq x \leq 3$; $0 \leq y \leq 2x + 2$). Only C_xH_y isomers with the lowest value of ΔH_f^0 are included. (Refs.: [8, 9]) *

CH_y	ΔH_f^0 (eV/mol)	I_p (eV)	C_2H_y	ΔH_f^0 (eV/mol)	I_p (eV)	C_3H_y	ΔH_f^0 (eV/mol)	I_p (eV)
H	2.277	13.595	H ₂	0.015	15.427	-	-	-
C	7.428	11.26	C ₂	8.628	11.41	C ₃	8.499	12.60
CH	6.16	10.64	C ₂ H	4.943	11.61	C ₃ H	4.40	12.70
CH ₂	4.005	10.396	C ₂ H ₂	2.350	11.40	C ₃ H ₂	5.40	10.43
CH ₃	1.43	9.84	C ₂ H ₃	3.10	8.25	C ₃ H ₃	2.72	8.34
CH ₄	-0.775	12.704	C ₂ H ₄	0.544	10.51	C ₃ H ₄	1.92	10.36
			C ₂ H ₅	1.233	8.12	C ₃ H ₅	1.77	8.13
			C ₂ H ₆	-0.87	11.52	C ₃ H ₆	0.23	9.72
						C ₃ H ₇	0.933	7.55
						C ₃ H ₈	-1.085	10.96

*The heat of formation for an ion $C_xH_y^+$ is given by $\Delta H_f^0(C_xH_y^+) = \Delta H_f^0(C_xH_y) + I_p(C_xH_y)$.

9 Tables

Table 2: C_xH_y isomers: their heat of formation (ΔH_f^0) and ionization potential (I_p), Ref. [8].

C_xH_y	Name	ΔH_f^0 (eV/mol)	I_p (eV)
C_2H_2	Acetylene	2.35	11.40
	$CH_2=C$?	?
C_2H_5	Allyl	1.233	8.12
	Cyclopropyl	(1.17)*	8.18
$C_3H_2^\dagger$	Propadienylidene	5.40	10.43
	Cyclopropenylidene	6.78	9.15
C_3H_3	Propargil	2.72	8.66
	Cyclopropenyl	(4.8)*	6.60
$C_3H_4^\dagger$	Propyne	1.92	10.36
	1,2 - Propadiene	2.65	9.62
	Cyclopropene	3.16	9.67
C_3H_5	Allyl	1.77	8.13
	Cyclopropyl	2.05	8.18
C_3H_6	Propene	0.23	9.72
	Cyclopropane	0.76	9.86
C_3H_7	Iso-propyl	0.933	7.55
	n-propyl	1.036	8.10

* ΔH_f^0 value obtained from the observed "sum rule" that $\Delta H_f^0 + I_p$ for different isomers of the same C_xH_y are approximately equal (to within 0.5 eV).

$^\dagger C_3H_2$ has also two other isomers, $HCCCH$ and $HCCH=C$, the values of ΔH_f^0 and I_p of which are unknown (see [8]). Similarly, C_3H_4 has an additional isomer, H_2CCHCH , with unknown values of ΔH_f^0 and I_p [8].

9 Tables

Table 3: Low-lying bound electronic excited states of C_xH_y molecules ($x=1-3$; $0 \leq y \leq 2x + 2$) [8].

Molecule	State	E_{exc} (eV)	Transition	Comment
C ($I_p = 11.260$ eV)	$2p^2$ (1D_2)	1.264		Transitions according to selection rules
	$2p^2$ (1S_0)	2.684		
	$2s2p^3$ ($^5S_2^0$)	4.182		
	$2p3s$ (3P_0)	7.480		
CH ($I_p = 10.64$ eV)	a $^4\Sigma^-$	0.725	—	Metastable
	A $^2\Delta$	0.363	$A - X$	
	B $^2\Sigma^-$	3.23	$B - X$	
	C $^2\Sigma^-$	3.94	$C - X$	
	D $^2\Pi$	7.49	$D \leftarrow X$	
	E $^2\Pi$	8.14	$E \leftarrow X$	
	F $^2\Pi$	8.18	$F \leftarrow X$	
	G	9.22	$G \leftarrow X$	Rydberg series on G
CH ₂ ($I_p = 10.396$ eV)	a	0.390	$a - b$	
	b	1.425	$b - a$	
	c	$\simeq 3.58$	$c - a$	
	$3p$	7.95	?	
	$3d^3A_2$	8.76	$A_2 - X$	
	C	8.79	$C - X$	
	D	8.88	$D - X$	
	$4p$	9.21	?	
CH ₃ ($I_p = 9.84$ eV)	$3s$ $^2A'_1$	5.73	$^2A'_1 - X$	
	$3p$ $^2A''_2$	7.435	?	
	$3d$ $^2E''$	8.25	$^2E'' - X$	
	$3d$ $^2A'_1$	8.28	$^2A'_1 - X$	
	$4p$ $^2A''_2$	8.66	?	
	$4f$ $^2E'$ (?)	8.99	?	
CH ₄ ($I_p = 12.704$ eV)				No excited states listed in [8]

Table 3: (continued)

Molecule	State	E_{exc} (eV)	Transition	Comment
C ₂ ($I_p = 11.41$ eV)	a $^3\Pi_u$	0.0089	—	Metastable
	b $^3\Sigma_g^-$	0.798	b \rightarrow a	
	A $^1\Pi_g$	1.040	A — X	
	c $^3\Sigma_u^-$	1.650	—	Metastable (?)
	d $^3\Pi_g$	2.482	d \rightarrow a	
	C $^1\Pi_g$	4.248	C \rightarrow A	
	e $^3\Pi_g$	5.058	e \rightarrow a	
	D $^1\Sigma_u^-$	5.361	D — X	
	E $^1\Sigma_g^-$	6.823	E — A	
C ₂ H ($I_p = 11.61$ eV)	A	4.58	A — X	
	B'	3.64	?	
	B	4.85	B — X	
	C(?)	6.37	?	
	3ps (Ryd)	8.94	?	
C ₂ H ₂ (acetylene)				No excited states listed in [8]
CH ₂ =C ($I_p \approx 11.6$ eV)	a	2.07	a — b	
	b	2.75	a — b	
	?	7.92	?	
	?	9.03	?	
C ₂ H ₃ ($I_p = 8.25$ eV)	A	2.48	A — X	
	B	5.21	B — X	$E_{exc} = E_{diss}$
	Ryd (?)	7.37	Ryd — X	
C ₂ H ₄ ($I_p = 10.51$ eV)				No excited states listed in [8]
C ₂ H ₅ ($I_p = 8.12$ eV)	3s	5.03	3s — X	
	3p	6.05	3p — X (?)	repulsive state (?)
C ₂ H ₆ ($I_p = 11.52$ eV)				No excited states listed in [8]

Table 3: (continued)

Molecule	State	E_{exc} (eV)	Transition	Comment
C ₃ ($I_p = 12.60$ eV)	a	2.19	a — b	The I_p value quoted in [8] is 13.0 eV
	b	2.92	a — b	
	A	3.06	A — X	
	B	≈ 3.71	B — X	
	$^1S_u^+$	6.55	?	
C ₃ H ($I_p = 12.70$ eV)				No excited states listed in [8]
C ₃ H ₂ (propadienylidene) ($I_p = 10.43$ eV)	A	1.29	A — X (?)	repulsive state (?)
	B	2.32	B — X	
	C	4.79	C — X	
C ₃ H ₂ (cyclopropenylidene) ($I_p = 9.15$ eV)	?	3.45	?	$E_{exc} = E_{ph\ diss}$
C ₃ H ₃ (propargyl) ($I_p = 8.34$ eV)				No excited states listed in [8]
CH ₂ CCH ($I_p = ?$)	?	3.73	?	
	?	5.12		
C ₃ H ₄ ($I_p = 10.36$ eV)				No excited states listed in [8] for any isomer
C ₃ H ₅ (allyl) ($I_p = 8.13$ eV)	A	3.04	A — X	
	B	4.97	B — X	
	C	5.00	C — X	
	D	5.13	?	
	3d	5.15	?	
	4s	6.66	?	
	6s	7.60	?	
	7s	7.76	?	
8s	7.86	?		

Table 3: (continued)

Molecule	State	E_{exc} (eV)	Transition	Comment
C_3H_6 ($I_p = 9.72$ eV)				No excited states listed in [8] for any isomer
C_3H_7 (isopropyl) ($I_p = 7.55$ eV)	3s	4.59	3s — X	} $E_{exc} = \overline{E}_{exc}^{(v)}$
	3p	5.27	3p — X	
	3d	5.99	3d — X	
C_3H_7 (n-propyl) ($I_p = 8.10$ eV)				No excited states listed in [8]
C_3H_8 ($I_p = 10.96$ eV)				No excited states listed in [8]

9 Tables

Table 4: Main electron-impact ionization channels of C_2H_y , their threshold energies (E_{th} , Ref. [8]), mean electron energy losses ($\overline{E}_{el}^{(-)}$) and mean total kinetic energies of reaction fragments (\overline{E}_K).

Reaction channel	E_{th} (eV)	$\overline{E}_{el}^{(-)}$ (eV)	\overline{E}_K (eV)*
$e + C_2 \rightarrow C_2^+ + 2e$	11.41	11.41	—
$\rightarrow C^+ + C + 2e$	17.44	19.55	2.11
$e + C_2H \rightarrow C_2H^+ + 2e$	11.61	11.61	—
$\rightarrow C_2^+ + H + 2e$	17.43	19.82	2.39
$\rightarrow CH^+ + C + 2e$	19.29	21.98	2.69
$\rightarrow C^+ + CH + 2e$	19.92	22.83	2.91
$\rightarrow H^+ + C_2 + 2e$	19.62	22.42	2.80
$e + C_2H_2 \rightarrow C_2H_2^+ + 2e$	11.40	11.40	—
$\rightarrow C_2H^+ + H + 2e$	16.48	18.26	1.78
$\rightarrow C_2^+ + H_2 + 2e$	17.76	19.99	2.23
$\rightarrow CH^+ + CH + 2e$	20.61	23.83	3.22
$\rightarrow C^+ + CH_2 + 2e$	20.35	23.48	3.13
$\rightarrow H^+ + C_2H + 2e$	18.46	20.93	2.47
$e + C_2H_3 \rightarrow C_2H_3^+ + 2e$	8.25	8.25	—
$\rightarrow C_2H_2^+ + H + 2e$	12.92	14.56	1.64
$\rightarrow C_2H^+ + H_2 + 2e$	14.23	16.06	1.83
$\rightarrow C_2H^+ + 2H + 2e$	16.02	19.79	3.77
$\rightarrow C_2^+ + H_2 + H + 2e$	19.78	23.82	4.04
$\rightarrow CH_2^+ + CH + 2e$	17.41	20.75	3.24
$\rightarrow CH^+ + CH_2 + 2e$	18.24	21.94	3.50
$\rightarrow C^+ + C_2H_3 + 2e$	17.04	20.11	3.07
$\rightarrow H^+ + C_2H_2 + 2e$	15.12	17.52	2.40

* $\overline{E}_K = 0.35D_0$ ($C_2H_y^+$), unless otherwise indicated by specifying the value of χ ($\overline{E}_K = \chi D_0$).

Table 4: (continued)

Reaction channel	E_{th} (eV)	$\overline{E}_{el}^{(-)}$ (eV)	\overline{E}_K (eV)
$e + C_2H_4 \rightarrow C_2H_4^+ + 2e$	10.51	10.51	—
$\rightarrow C_2H_3^+ + H + 2e$	13.09	13.99	0.90
$(a_1)^* \rightarrow C_2H_2^+ + H_2 + 2e$	13.23	14.18	0.95
$(a_2)^* \rightarrow C_2H_2^+ + H + H + 2e$	17.76	20.30	2.54
$\rightarrow C_2H^+ + H_2 + H + 2e$	19.06	21.76	2.70
$\rightarrow C_2^+ + 2H_2 + 2e$	20.09	23.44	3.35
$\rightarrow CH_3^+ + CH + 2e$	16.91	19.14	2.23
$\rightarrow CH_2^+ + CH_2 + 2e$	17.94	20.34	2.60
$\rightarrow CH^+ + CH_3 + 2e$	18.20	20.71	2.51
$(b_1)^\dagger \rightarrow C^+ + CH_3 + H + 2e$	21.87	25.54	3.67
$(b_2)^\dagger \rightarrow C^+ + CH_2 + H_2 + 2e$	22.22	26.00	3.78
$(b_3)^\dagger \rightarrow C^+ + CH_4 + 2e$	18.94	21.34	2.40
$e + C_2H_5 \rightarrow C_2H_5^+ + 2e$	8.12	8.12	—
$\rightarrow C_2H_4^+ + H + 2e$	12.10	13.49	1.39
$(c_1)^\ddagger \rightarrow C_2H_3^+ + H_2 + 2e$	10.14	11.15	1.01($\chi = 0.5$)
$(c_2)^\ddagger \rightarrow C_2H_3^+ + 2H + 2e$	14.67	16.93	2.26
$\rightarrow C_2H_2^+ + H_2 + H + 2e$	14.81	17.16	2.35
$\rightarrow C_2H^+ + 2H_2 + 2e$	15.35	17.88	2.53
$\rightarrow CH_3^+ + CH_2 + 2e$	14.04	16.11	2.07
$\rightarrow CH_2^+ + CH_3 + 2e$	14.60	16.87	2.27
$\rightarrow CH^+ + CH_4 + 2e$	14.79	17.13	2.34
$(d_1)^\S \rightarrow C^+ + CH_4 + H + 2e$	18.97	22.77	3.80
$(d_2)^\S \rightarrow C^+ + CH_3 + H_2 + 2e$	18.92	22.70	3.78

*The channels (a_1) , (a_2) share the total cross section for $C_2H_2^+$ production weighting factors 0.85, 0.15, respectively.

† The channels (b_1) , (b_2) and (b_3) share the $\sigma(C^+)$ ion production cross section by the weighting factors 0.3, 0.3 and 0.4, respectively.

‡ The channels (c_1) and (c_2) share the $\sigma(C_2H_3^+)$ ion production cross section by the weighting factors 0.8 and 0.2, respectively.

§ The channels (d_1) and (d_2) share equally the $\sigma(C^+)$ ion production cross section.

Table 4: (continued)

Reaction channel	E_{th} (eV)	$\overline{E}_{el}^{(-)}$ (eV)	\overline{E}_K (eV)
$e + \text{C}_2\text{H}_6 \rightarrow \text{C}_2\text{H}_6^+ + 2e$	11.52	11.52	—
$\rightarrow \text{C}_2\text{H}_5^+ + \text{H} + 2e$	12.50	13.09	0.59($\chi = 0.6$)
$\rightarrow \text{C}_2\text{H}_4^+ + \text{H}_2 + 2e$	11.43	11.85	0.42($\chi = 1$)
$\rightarrow \text{C}_2\text{H}_3^+ + \text{H}_2 + \text{H} + 2e$	14.51	15.53	1.02
$\rightarrow \text{C}_2\text{H}_2^+ + 2\text{H}_2 + 2e$	14.65	15.75	1.10
$\rightarrow \text{C}_2\text{H}^+ + 2\text{H}_2 + \text{H} + 2e$	17.73	20.59	2.86
$\rightarrow \text{C}_2^+ + 3\text{H}_2 + 2e$	21.01	24.33	3.32
$\rightarrow \text{CH}_3^+ + \text{CH}_3 + 2e$	13.51	14.23	0.72
$\rightarrow \text{CH}_2^+ + \text{CH}_4 + 2e$	16.05	17.09	1.04
$\rightarrow \text{CH}^+ + \text{CH}_3 + \text{H}_2 + 2e$	19.10	21.76	2.66
$\rightarrow \text{CH}^+ + \text{CH}_4 + \text{H} + 2e$	19.86	22.54	2.68
$\rightarrow \text{C}^+ + \text{CH}_4 + \text{H}_2 + 2e$	18.77	21.32	2.55

9 Tables

Table 5: Main electron-impact dissociative excitation channels of C_2H_y , their threshold energies (E_{th}), mean total kinetic energies of products ($\overline{E_K}$) and cross section branching ratios (R'_{DE}) at $E \simeq 80$ eV.

Reaction channel	$E_{th} = \overline{E_{el}^{(-)}} \text{ (eV)}$	$\overline{E_K} \text{ (eV)}^*$	R'_{DE}
$e + C_2 \rightarrow C(^3P) + C(^1D)$	7.68	0.25	0.75
$e + C_2 \rightarrow C(^3P) + C(^3P)^\dagger$	(7.68)	1.50	0.25
$e + C_2H \rightarrow C_2 + H + e$	8.8	2.8	0.73
$\rightarrow C + CH + e$	11.0	3.3	0.27
$e + C_2H_2 \rightarrow C_2H + H + e$	7.5	2.6	0.51
$\rightarrow C_2 + H_2 + e$	8.7	2.3	0.18
$\rightarrow C_2 + 2H + e$	11.38	0.50	0.11
$\rightarrow CH + CH + e$	10.6	0.6	0.09
$\rightarrow C + CH_2 + e$	9.8	0.7	0.11
$e + C_2H_3 \rightarrow C_2H_2 + H + e$	4.60	1.7	0.49
$\rightarrow C_2H + H_2 + e$	5.58	1.6	0.20
$\rightarrow C_2H + 2H + e$	7.14	0.8	0.11
$\rightarrow C_2 + H_2 + H + e$	8.10	0.15	0.07
$\rightarrow CH_2 + CH + e$	7.61	0.5	0.06
$\rightarrow C + CH_3 + e$	6.87	1.1	0.07
$e + C_2H_4 \rightarrow C_2H_3 + H + e$	6.9	2.1	0.32
$\rightarrow C_2H_2 + H_2 + e$	5.8	2.4	0.24
$\rightarrow C_2H_2 + 2H + e$	6.5	2.1	0.16
$\rightarrow C_2H + H_2 + H + e$	8.4	1.8	0.08
$\rightarrow CH_3 + CH + e$	8.7	1.6	0.06
$\rightarrow CH_2 + CH_2 + e$	8.9	1.5	0.06
$\rightarrow C + CH_4 + e$	8.1	2.0	0.08

* $\overline{E_K}$ is chosen from the interval $[I_p(C_2H_y) - D_0(C_2H_y)] < \overline{E_K} \leq 0.35D_0(C_2H_y)$.

† Population of $C(^3P) + C(^3P)$ channel is due to the nonadiabatic coupling of the molecular state $d^3\Pi_g$ with the state $e^3\Pi_g$ (at $R \simeq 1.7\text{\AA}$) which dissociates to $C(^3P) + C(^1D)$ fragments.

Table 5: (continued)

Reaction channel	$E_{th} = \overline{E_{el}^{(-)}} \text{ (eV)}$	$\overline{E_K} \text{ (eV)}$	R'_{DE}
$e + \text{C}_2\text{H}_5 \rightarrow \text{C}_2\text{H}_4 + \text{H} + e$	4.45	2.86	0.44
$\rightarrow \text{C}_2\text{H}_3 + \text{H}_2 + e$	5.36	2.83	0.19
$\rightarrow \text{C}_2\text{H}_3 + 2\text{H} + e$	8.67	2.25	0.04
$\rightarrow \text{C}_2\text{H}_2 + \text{H}_2 + \text{H} + e$	5.47	2.05	0.11
$\rightarrow \text{CH} + 2\text{H}_2 + e$	5.98	2.24	0.10
$\rightarrow \text{CH}_4 + \text{CH} + e$	6.5	2.4	0.06
$\rightarrow \text{CH}_3 + \text{CH}_2 + e$	6.6	2.4	0.06
$e + \text{C}_2\text{H}_6 \rightarrow \text{C}_2\text{H}_5 + \text{H} + e$	7.45	3.07	0.24
$\rightarrow \text{C}_2\text{H}_4 + \text{H}_2 + e$	4.00	2.57	0.46
$\rightarrow \text{C}_2\text{H}_3 + \text{H}_2 + \text{H} + e$	9.40	3.13	0.04
$\rightarrow \text{C}_2\text{H}_2 + 2\text{H}_2 + e$	6.20	2.93	0.11
$\rightarrow \text{CH}_4 + \text{CH}_2 + e$	6.95	2.86	0.07
$\rightarrow \text{CH}_3 + \text{CH}_3 + e$	6.38	2.65	0.08

9 Tables

Table 6: Main electron-impact dissociative excitation channels of $C_2H_y^+$, their threshold energies ($E_{th} = \overline{E_{el}^{(-)}}$), mean total kinetic energies of products ($\overline{E_K}$) and cross section branching ratios (R'_{DE^+}) at $E \simeq 30\text{--}40$ eV.

Reaction channel	$E_{th} = \overline{E_{el}^{(-)}} \text{ (eV)}$	$\overline{E_K} \text{ (eV)}^*$	R'_{DE^+}
$e + C_2^+ \rightarrow C^+ + C + e$	8.14	2.11	1.00
$e + C_2H^+ \rightarrow C_2^+ + H + e$	9.21	2.39	0.38
$\rightarrow C_2 + H^+ + e$	10.80	2.80	0.36
$\rightarrow CH^+ + C + e$	10.37	2.69	0.14
$\rightarrow CH + C^+ + e$	11.22	2.91	0.12
$e + C_2H_2^+ \rightarrow C_2H^+ + H + e$	6.86	1.78	0.42
$\rightarrow C_2H + H^+ + e$	9.53	2.47	0.22
$\rightarrow C_2^+ + H_2 + e$	8.59	2.23	0.16
$\rightarrow C_2 + H_2^+ + e$	14.00	3.63	0.03
$\rightarrow CH^+ + CH + e$	12.43	3.22	0.05
$\rightarrow CH_2^+ + C + e$	10.91	2.83	0.07
$\rightarrow CH_2 + C^+ + e$	12.08	3.13	0.05
$e + C_2H_3^+ \rightarrow C_2H_2^+ + H + e$	6.32	1.64	0.38
$\rightarrow C_2H_2 + H^+ + e$	9.27	2.40	0.21
$\rightarrow C_2H^+ + H_2 + e$	7.05	1.83	0.19
$\rightarrow C_2H + H_2^+ + e$	10.97	2.84	0.06
$\rightarrow CH_2^+ + CH + e$	12.50	3.24	0.04
$\rightarrow CH_2 + CH^+ + e$	13.48	3.49	0.03
$\rightarrow CH_3^+ + C + e$	9.93	2.58	0.06
$\rightarrow CH_3 + C^+ + e$	11.86	3.08	0.03

* $\overline{E_K} = 0.35D_0$ ($C_2H_y^+$), unless otherwise indicated by specifying the value of χ in the relation $\overline{E_K} = \chi D_0$.

Table 6: (continued)

Reaction channel	$E_{th} = \overline{E_{el}^{(-)}} \text{ (eV)}$	$\overline{E_K} \text{ (eV)}$	R'_{DE+}
$e + C_2H_4^+ \rightarrow C_2H_3^+ + H + e$	4.64	2.06	0.44
$\rightarrow C_2H_2^+ + H_2 + e$	4.90	2.18 ($\chi = 0.8$)	0.32
$\rightarrow C_2H_2 + H_2^+ + e$	9.10	2.36 ($\chi = 0.8$)	0.07
$\rightarrow CH_3^+ + CH + e$	8.61	2.23	0.05
$\rightarrow CH_3 + CH^+ + e$	9.69	2.51	0.04
$\rightarrow CH_2^+ + CH_2 + e$	10.03	2.60	0.04
$\rightarrow CH_4 + C^+ + e$	9.27	2.40	0.04
$e + C_2H_5^+ \rightarrow C_2H_4^+ + H + e$	6.18	2.20 ($\chi = 0.55$)	0.25
$\rightarrow C_2H_3^+ + H_2 + e$	4.04	2.02 ($\chi = 1.0$)	0.55
$\rightarrow C_2H_3^+ + 2H + e$	8.71	2.26	0.08
$\rightarrow CH_3^+ + CH_2 + e$	7.99	2.07	0.07
$\rightarrow CH_3 + CH_2^+ + e$	8.75	2.27	0.05
$e + C_2H_6^+ \rightarrow C_2H_5^+ + H + e$	1.76	0.78 ($\chi = 0.8$)	0.23
$\rightarrow C_2H_4^+ + H_2 + e$	1.05	0.63 ($\chi = 1.5$)	0.73
$\rightarrow CH_3^+ + CH_3 + e$	2.77	0.72	0.04

Table 7: Main electron-impact dissociative ionization channels of $C_2H_y^+$, their threshold energies (E_{th}), and cross section branching ratios (R'_{DI+}). (The mean total kinetic energy of products for all channels is $\overline{E_K} = 11.8$ eV.)

Reaction channel	$E_{th} = \overline{E_{el}^{(-)}} \text{ (eV)}$	R'_{DI+}
$e + C_2^+ \rightarrow C^+ + C^+ + 2e$	28.63	1.00
$e + C_2H^+ \rightarrow C_2^+ + H^+ + 2e$	31.20	0.64
$\rightarrow CH^+ + C^+ + 2e$	30.75	0.36
$e + C_2H_2^+ \rightarrow C_2H^+ + H^+ + 2e$	30.47	0.27
$\rightarrow C_2^+ + H_2^+ + 2e$	33.58	0.16
$\rightarrow C_2^+ + H + H^+ + 2e$	36.29	0.11
$\rightarrow CH^+ + CH^+ + 2e$	31.65	0.13
$\rightarrow CH^+ + C^+ + H + 2e$	35.83	0.10
$\rightarrow CH_2^+ + C^+ + 2e$	31.19	0.13
$e + C_2H_3^+ \rightarrow C_2H_2^+ + H^+ + 2e$	30.07	0.28
$\rightarrow C_2H^+ + H_2^+ + 2e$	32.44	0.19
$\rightarrow C_2H^+ + H + H^+ + 2e$	35.15	0.14
$\rightarrow CH_2^+ + CH^+ + 2e$	31.65	0.14
$\rightarrow CH_3^+ + C^+ + 2e$	30.42	0.15
$e + C_2H_4^+ \rightarrow C_2H_3^+ + H^+ + 2e$	27.97	0.26
$\rightarrow C_2H_2^+ + H_2^+ + 2e$	29.94	0.17
$\rightarrow C_2H_2^+ + H + H^+ + 2e$	32.65	0.12
$\rightarrow CH_3^+ + CH^+ + 2e$	28.98	0.12
$\rightarrow CH_2^+ + CH_2^+ + 2e$	29.55	0.12
$\rightarrow CH_4^+ + C^+ + 2e$	31.37	0.11

Table 7: (continued)

Reaction channel	$E_{th} = \overline{E_{el}^{(-)}} \text{ (eV)}$	R_{DI}^+
$e + \text{C}_2\text{H}_5^+ \rightarrow \text{C}_2\text{H}_4^+ + \text{H}^+ + 2e$	29.38	0.31
$\rightarrow \text{C}_2\text{H}_3^+ + \text{H}_2^+ + 2e$	29.34	0.15
$\rightarrow \text{C}_2\text{H}_3^+ + \text{H} + \text{H}^+ + 2e$	31.85	0.10
$\rightarrow \text{C}_2\text{H}_2^+ + \text{H}_2 + \text{H}^+ + 2e$	32.09	0.10
$\rightarrow \text{C}_2\text{H}_2^+ + \text{H}_2^+ + \text{H} + 2e$	33.92	0.09
$\rightarrow \text{C}_2\text{H}^+ + \text{H}_2 + \text{H}_2^+ + 2e$	34.46	0.08
$\rightarrow \text{CH}_4^+ + \text{CH}^+ + 2e$	31.17	0.08
$\rightarrow \text{CH}_3^+ + \text{CH}_2^+ + 2e$	28.12	0.09
$e + \text{C}_2\text{H}_6^+ \rightarrow \text{C}_2\text{H}_5^+ + \text{H}^+ + 2e$	26.37	0.34
$\rightarrow \text{C}_2\text{H}_4^+ + \text{H}_2^+ + 2e$	27.64	0.17
$\rightarrow \text{C}_2\text{H}_4^+ + \text{H} + \text{H}^+ + 2e$	30.25	0.10
$\rightarrow \text{C}_2\text{H}_3^+ + \text{H}_2 + \text{H}^+ + 2e$	28.39	0.11
$\rightarrow \text{C}_2\text{H}_2^+ + \text{H}_2 + \text{H}_2^+ + 2e$	30.36	0.08
$\rightarrow \text{CH}_4^+ + \text{CH}_2^+ + 2e$	27.47	0.08
$\rightarrow \text{CH}_3^+ + \text{CH}_3^+ + 2e$	23.69	0.12

9 Tables

Table 8: Main dissociative recombination channels of $C_2H_y^+$, their cross section branching ratios (R_{DR}), total kinetic energy of products ($E_K^{(0)}$) in their ground states and for zero electron impact energy, and possible excited products.

Reaction channel	R_{DR}	$E_k^{(0)}$ (eV)	Excited products for $E \lesssim 1$ eV
$e + C_2^+ \rightarrow C + C$	1.0	5.22	$C(^1D)$, $C(^1S)$
$e + C_2H^+ \rightarrow C_2 + H$	0.85	5.59	$C_2(a; b; A; c; d; C)$
$\quad \rightarrow CH + C$	0.15	2.96	$CH(A; a)$, $C(^1D; ^1S)$
$e + C_2H_2^+ \rightarrow C_2H + H$	0.50	6.33	$C_2H(A; B^1; B)$
$\quad \rightarrow C_2 + H + H$	0.30	0.52	$C_2(a; b)$
$\quad \rightarrow CH + CH$	0.13	1.42	$CH(a; A)$
$\quad \rightarrow CH_2 + C$	0.05	2.32	$C(^1D; ^1S)$
$\quad \rightarrow C_2 + H_2$	0.02	5.05	$C_2(a; b; A; c; d; c)$
$e + C_2H_3^+ \rightarrow C_2H_2 + H$	0.29	6.72	
$\quad \rightarrow C_2H + H + H$	0.59	1.91	
$\quad \rightarrow C_2H + H_2$	0.06	6.39	$C_2H(A; B; B^1)$
$\quad \rightarrow CH_2 + CH$	0.03	1.14	$CH_2(a; b;)$, $CH(A; a)$
$\quad \rightarrow C_2 + H_2 + H$	0.024	0.46	$C_2(a; b; A)$
$\quad \rightarrow CH_3 + C$	0.006	1.91	$C(^1D; ^1S)$
$e + C_2H_4^+ \rightarrow C_2H_3 + H$	0.28	5.64	$C_2H_3(A; B)$
$\quad \rightarrow C_2H_2 + H + H$	0.48	4.15	
$\quad \rightarrow C_2H_2 + H_2$	0.08	8.64	
$\quad \rightarrow C_2H + H + H_2$	0.03	7.23	$C_2H(A; B'; B; C)$
$\quad \rightarrow CH_2 + CH_2$	0.10	2.97	$CH_2(a; b)$
$\quad \rightarrow CH_3 + CH$	0.03	3.44	$CH(a; A; B)$

Table 8: (continued)

Reaction channel	R_{DR}	$E_k^{(0)}$ (eV)	Excited products for $E \lesssim 1$ eV
$e + \text{C}_2\text{H}_5^+ \rightarrow \text{C}_2\text{H}_4 + \text{H}$	0.32	6.53	
$\rightarrow \text{C}_2\text{H}_3 + \text{H} + \text{H}$	0.50	1.69	$\text{C}_2\text{H}_3(\text{A})$
$\rightarrow \text{C}_2\text{H}_3 + \text{H}_2$	0.06	6.23	$\text{C}_2\text{H}_3(\text{A}; \text{B})$
$\rightarrow \text{C}_2\text{H}_2 + \text{H}_2 + \text{H}$	0.05	4.70	
$\rightarrow \text{CH}_4 + \text{CH}$	0.04	3.97	$\text{CH}(\text{A}; \text{a}; \text{B})$
$\rightarrow \text{CH}_3 + \text{CH}_2$	0.03	3.92	$\text{CH}_2(\text{a}; \text{b}; \text{c})$
$e + \text{C}_2\text{H}_6^+ \rightarrow \text{C}_2\text{H}_5 + \text{H}$	0.30	7.14	$\text{C}_2\text{H}_5(3\text{s}; 3\text{p})$
$\rightarrow \text{C}_2\text{H}_4 + \text{H} + \text{H}$	0.46	5.55	
$\rightarrow \text{C}_2\text{H}_4 + \text{H}_2$	0.08	10.09	$\text{H}_2(\text{B})$
$\rightarrow \text{C}_2\text{H}_3 + \text{H}_2 + \text{H}$	0.03	2.22	$\text{C}_2\text{H}_3(\text{A})$
$\rightarrow \text{CH}_4 + \text{CH}_2$	0.04	7.43	$\text{CH}_2(\text{C}; 3\text{p})$
$\rightarrow \text{CH}_3 + \text{CH}_3$	0.08	7.79	$\text{CH}_3(3\text{s}; 3\text{p}; 3\text{d})$

9 Tables

Table 9: Charge exchange reaction channels in $H^+ + C_2H_y$ thermal collisions: total rate coefficients (K_{CX}^{tot}) [61], channel branching ratios (R_{CX}), reaction exothermicities (ΔE) and values of parameters a and β in Eq. 73b

Reaction channel	K_{CX}^{tot} ($10^{-9} \text{cm}^3/\text{s}$)	R_{CX}	ΔE (eV)	a	β
$H^+ + C_2 \rightarrow H + C_2^+$	3.1	0.65	2.19	—	—
$\rightarrow CH^+ + C$		0.35	0.32	20.0	2.5
$H^+ + C_2H \rightarrow H + C_2H^+$	3.0	0.65	1.99	—	—
$\rightarrow H_2 + C_2^+$		0.35	0.71	35.0	2.5
$H^+ + C_2H_2 \rightarrow H + C_2H_2^+$	3.5	0.65	2.20	—	—
$\rightarrow H_2 + C_2H^+$		0.35	1.65	25.0	2.5
$H^+ + C_2H_3 \rightarrow H + C_2H_3^+$	4.0	0.65	5.35	—	—
$\rightarrow H_2 + C_2H_2^+$		0.25	5.20	20.0	2.5
$\rightarrow H + H_2 + C_2H^+$		0.10	2.28	20.0	2.5
$H^+ + C_2H_4 \rightarrow H + C_2H_4^+$	4.8	0.65	3.09	—	—
$\rightarrow H_2 + C_2H_3^+$		0.20	5.05	40.0	2.5
$\rightarrow H + H_2 + C_2H_2^+$		0.15	0.37	40.0	2.5
$H^+ + C_2H_5 \rightarrow H + C_2H_5^+$	4.5	0.60	5.49	—	—
$\rightarrow H_2 + C_2H_4^+$		0.15	6.04	335	2.5
$\rightarrow H + H_2 + C_2H_3^+$		0.15	3.46	335	3.0
$\rightarrow 2H_2 + C_2H_2^+$		0.10	3.33	335	3.0
$H^+ + C_2H_6 \rightarrow H + C_2H_6^+$	4.2	0.65	2.08	—	—
$\rightarrow H_2 + C_2H_5^+$		0.15	5.63	160	2.5
$\rightarrow H + H_2 + C_2H_4^+$		0.10	1.65	160	3.0
$\rightarrow 2H_2 + C_2H_3^+$		0.10	3.62	160	3.0

9 Tables

Table 10: Values of coefficients c_i in Eq. 77 for total charge exchange cross section in $H^+ + C_2H_y$ collisions.

c_i	C_2	C_2H^\dagger	C_2H_2	C_2H_3	C_2H_4	C_2H_5	C_2H_6
c_1	2.62	1.42	2.54	2.90	3.28	3.06	2.41
c_2	0.22	2.35	0.21	0.03	3.85	335.0	160.0
c_3	1.05	1.30	1.05	1.27	1.25	1.65	1.75
c_4	8.34	40.22	8.26	9.35	4.26	10.34	7.98
c_5	6.38	11.76	6.38	3.68	0.0	0.0	0.0
c_6	0.16	0.14	0.16	0.12	0.0	0.0	0.0
c_7	0.00	0.0	0.0	0.0	0.06	0.14	0.14
c_8	$2.06(-7)^\ddagger$	$4.84(-6)$	$2.06(-7)$	$1.81(-6)$	$1.40(-4)$	$1.51(-4)$	$1.16(-4)$
c_9	1.58	1.40	1.58	1.36	0.91	0.89	0.96
c_{10}	$2.52(-21)$	$7.92(-18)$	$2.55(-21)$	$4.85(-22)$	$3.65(-19)$	$2.83(-18)$	$2.80(-19)$
c_{11}	4.40	3.88	4.40	4.50	3.96	3.80	4.00

[†]The cross section for $H^+ + C_2H$ system refers only to the electron capture channel (i.e. particle exchange contribution is excluded).

[‡] $a(-x)$ denotes $a \times 10^{-x}$.

9 Tables

Table 11: Main electron-impact ionization channels of C_3H_y ($0 \leq y \leq 8$), their threshold energies (E_{th}) (Refs. [8, 9]), mean electron energy losses ($\overline{E_{el}^{(-)}}$), mean total kinetic energy of products $\overline{E_K}$ and cross section branching ratios at $E = 80$ eV ($R'_{I,DI}$).

Reaction channel	E_{th} (eV)	$\overline{E_{el}^{(-)}}$ (eV)	$\overline{E_K}$ (eV)	$R'_{I,DI}$
$e + C_3 \rightarrow C_3^+ + 2e$	12.60	12.60	—	0.82
$\rightarrow C_2^+ + C + 2e$	19.02	21.26	2.24	0.08
$\rightarrow C^+ + C_2 + 2e$	18.88	21.08	2.20	0.10
$e + C_3H \rightarrow C_3H^+ + 2e$	12.70	12.70	—	0.916
$\rightarrow C_3^+ + H + 2e$	18.98	21.18	2.20	0.010
$\rightarrow C_2H^+ + C + 2e$	19.58	21.99	2.41	0.007
$\rightarrow C_2^+ + CH + 2e$	21.85	25.05	3.20	0.004
$\rightarrow CH^+ + C_2 + 2e$	21.08	24.01	2.93	0.006
$\rightarrow C^+ + C_2H + 2e$	19.24	21.53	2.29	0.016
$\rightarrow H^+ + C_3 + 2e$	19.97	22.51	2.54	0.041
$e + C_3H_2 \rightarrow C_3H_2^+ + 2e$	10.43	10.43	—	0.700
$\rightarrow C_3H^+ + H + 2e$	13.91	15.15	1.24	0.030
$\rightarrow C_3^+ + H_2 + 2e$	15.72	17.57	1.85	0.050
$\rightarrow C_2H_2^+ + C + 2e$	15.78	17.65	1.87	0.040
$\rightarrow C_2H^+ + CH + 2e$	17.31	19.72	2.41	0.013
$\rightarrow C_2^+ + CH_2 + 2e$	18.69	20.58	1.89	0.007
$\rightarrow CH_2^+ + C_2 + 2e$	17.68	20.22	2.54	0.010
$\rightarrow CH^+ + C_2H + 2e$	16.34	18.41	2.07	0.015
$\rightarrow C^+ + C_2H_2 + 2e$	15.65	17.47	1.82	0.045
$\rightarrow H^+ + C_3H + 2e$	14.87	16.42	1.55	0.090

Table 11: (continued)

Reaction channel	E_{th} (eV)	$\overline{E}_{el}^{(-)}$ (eV)	\overline{E}_K (eV)	$R'_{I,DI}$
$e + C_3H_3 \rightarrow C_3H_3^+ + 2e$	8.34	8.34	—	0.541
$\rightarrow C_3H_2^+ + H + 2e$	15.39	17.86	2.47	0.082
$\rightarrow C_3H^+ + H_2 + 2e$	14.40	16.50	2.10	0.204
$\rightarrow C_2H_3^+ + C + 2e$	16.06	18.76	2.70	0.020
$\rightarrow C_2H_2^+ + CH + 2e$	17.19	20.29	3.10	0.018
$\rightarrow C_2H^+ + CH_2 + 2e$	17.83	21.15	3.32	0.013
$\rightarrow C_2^+ + CH_3 + 2e$	18.80	22.46	3.66	0.009
$\rightarrow CH_3^+ + C_2 + 2e$	17.23	20.34	3.11	0.012
$\rightarrow CH_2^+ + C_2H + 2e$	16.62	19.52	2.90	0.016
$\rightarrow CH^+ + C_2H_2 + 2e$	16.43	19.26	2.83	0.018
$\rightarrow C^+ + C_2H_3 + 2e$	19.08	22.53	3.45	0.024
$\rightarrow H^+ + C_3H_2 + 2e$	18.55	22.12	3.57	0.042
$e + C_3H_4 \rightarrow C_3H_4^+ + 2e$	10.36	10.36	—	0.350
$\rightarrow C_3H_3^+ + H + 2e$	11.42	12.27	0.85 ($\chi = 0.8$)	0.145
$\rightarrow C_3H_2^+ + H_2 + 2e$	13.92	15.16	1.24	0.300
$\rightarrow C_3H^+ + H_2 + H + 2e$	17.48	19.97	2.49	0.047
$\rightarrow C_2H_4^+ + C + 2e$	16.56	18.73	2.17	0.008
$\rightarrow C_2H_3^+ + CH + 2e$	15.59	17.42	1.83	0.034
$\rightarrow C_2H_2^+ + CH_2 + 2e$	15.83	17.74	1.91	0.027
$\rightarrow C_2H^+ + CH_3 + 2e$	16.06	18.05	1.99	0.016
$\rightarrow C_2^+ + CH_4 + 2e$	17.39	19.85	2.46	0.005
$\rightarrow CH_4^+ + C_2 + 2e$	17.68	20.24	2.56	0.006
$\rightarrow CH_3^+ + C_2H + 2e$	14.29	15.66	1.37	0.024
$\rightarrow CH_2^+ + C_2H_2 + 2e$	14.83	16.39	1.56	0.021
$\rightarrow CH^+ + C_2H_3 + 2e$	17.98	20.64	2.66	0.014
$\rightarrow C^+ + C_2H_4 + 2e$	17.32	19.75	2.43	0.005
$\rightarrow H^+ + C_3H_3 + 2e$	16.67	18.88	2.21	0.008

Table 11: (continued)

Reaction channel	E_{th} (eV)	$\overline{E}_{el}^{(-)}$ (eV)	\overline{E}_K (eV)	$R'_{I,DI}$
$e + C_3H_5 \rightarrow C_3H_5^+ + 2e$	8.13	8.13	—	0.282
$\rightarrow C_3H_4^+ + H + 2e$	12.79	14.42	1.63	0.192
$\rightarrow C_3H_3^+ + H_2 + 2e$	9.31	10.25	0.94 ($\chi = 0.8$)	0.272
$\rightarrow C_3H_2^+ + H_2 + H + 2e$	16.36	19.24	2.88	0.083
$\rightarrow C_3H^+ + 2H_2 + 2e$	15.36	17.89	2.53	0.005
$\rightarrow C_2H_5^+ + C + 2e$	14.01	16.42	2.41	0.006
$\rightarrow C_2H_4^+ + CH + 2e$	15.44	18.00	2.56	0.020
$\rightarrow C_2H_3^+ + CH_2 + 2e$	13.58	15.48	1.90	0.061
$\rightarrow C_2H_2^+ + CH_3 + 2e$	13.41	15.26	1.85	0.034
$\rightarrow C_2H^+ + CH_4 + 2e$	14.00	16.05	2.05	0.019
$\rightarrow CH_4^+ + C_2H + 2e$	15.09	17.52	2.43	0.014
$\rightarrow CH_3^+ + C_2H_2 + 2e$	11.85	13.15	1.30	0.033
$\rightarrow CH_2^+ + C_2H_3 + 2e$	15.73	18.39	2.66	0.015
$\rightarrow CH^+ + C_2H_4 + 2e$	15.57	18.17	2.60	0.010
$e + C_3H_6 \rightarrow C_3H_6^+ + 2e$	9.72	9.72	—	0.206
$\rightarrow C_3H_5^+ + H + 2e$	11.95	13.06	1.11 ($\chi = 0.5$)	0.152
$\rightarrow C_3H_4^+ + H_2 + 2e$	12.07	13.24	1.17 ($\chi = 0.5$)	0.137
$\rightarrow C_3H_3^+ + H_2 + H + 2e$	13.13	14.32	1.19	0.125
$\rightarrow C_3H_2^+ + 2H_2 + 2e$	15.62	17.68	2.06	0.036
$\rightarrow C_2H_5^+ + CH + 2e$	15.28	17.22	1.94	0.045
$\rightarrow C_2H_4^+ + CH_2 + 2e$	14.82	16.60	1.78	0.065
$\rightarrow C_2H_3^+ + CH_3 + 2e$	12.55	13.96	1.41 ($\chi = 0.5$)	0.093
$\rightarrow C_2H_2^+ + CH_4 + 2e$	12.74	14.25	1.51 ($\chi = 0.5$)	0.044
$\rightarrow CH_4^+ + C_2H_2 + 2e$	14.04	15.55	1.51	0.022
$\rightarrow CH_3^+ + C_2H_3 + 2e$	14.14	15.68	1.54	0.042
$\rightarrow CH_2^+ + C_2H_4 + 2e$	14.71	16.45	1.74	0.010
$\rightarrow CH^+ + C_2H_5 + 2e$	17.80	20.63	2.83	0.006

Table 11: (continued)

Reaction channel	E_{th} (eV)	$\overline{E}_{el}^{(-)}$ (eV)	\overline{E}_K (eV)	$R'_{I,DI}$
$e + C_3H_7 \rightarrow C_3H_7^+ + 2e$	7.55	7.55	—	0.184
$\rightarrow C_3H_6^+ + H + 2e$	10.30	11.40	1.10 ($\chi = 0.4$)	0.100
$\rightarrow C_3H_5^+ + H_2 + 2e$	8.99	9.71	0.72 ($\chi = 0.5$)	0.106
$\rightarrow C_3H_4^+ + H_2 + H + 2e$	13.65	15.78	2.13	0.077
$\rightarrow C_3H_3^+ + 2H_2 + 2e$	10.16	11.20	1.04 ($\chi = 0.4$)	0.103
$\rightarrow C_2H_5^+ + CH_2 + 2e$	12.42	14.12	1.70	0.084
$\rightarrow C_2H_4^+ + CH_3 + 2e$	11.55	12.95	1.40	0.094
$\rightarrow C_2H_3^+ + CH_4 + 2e$	9.64	10.48	0.84 ($\chi = 0.4$)	0.122
$\rightarrow C_2H_2^+ + CH_4 + H + 2e$	14.32	16.81	2.49	0.013
$\rightarrow C_2H_2^+ + CH_3 + H_2 + 2e$	14.26	16.76	2.50	0.014
$\rightarrow CH_4^+ + C_2H_3 + 2e$	13.09	15.03	1.94	0.030
$\rightarrow CH_3^+ + C_2H_4 + 2e$	10.88	12.04	1.16	0.051
$\rightarrow CH_2^+ + C_2H_5 + 2e$	14.70	17.20	2.50	0.019
$\rightarrow CH^+ + C_2H_6 + 2e$	15.40	19.25	2.85	0.003
$e + C_3H_8 \rightarrow C_3H_8^+ + 2e$	10.94	10.94	—	†
$\rightarrow C_3H_7^+ + H + 2e$	11.84	12.72	0.88 ($\chi = 1$)	
* $\rightarrow C_3H_6^+ + H_2 + 2e$	11.05	11.23	0.18 ($\chi = 2$)	
* $\rightarrow C_3H_6^+ + 2H + 2e$	15.59	16.21	1.62	
$\rightarrow C_3H_5^+ + H_2 + H + 2e$	13.28	14.44	1.16 ($\chi = 0.5$)	
$\rightarrow C_3H_4^+ + 2H_2 + 2e$	13.39	14.60	1.21 ($\chi = 0.5$)	
$\rightarrow C_3H_3^+ + 2H_2 + H + 2e$	14.45	15.67	1.22	
$\rightarrow C_3H_2^+ + 3H_2 + 2e$	16.96	19.06	2.10	
$\rightarrow C_3H^+ + 3H_2 + H + 2e$	20.51	23.85	3.34	
$\rightarrow C_2H_5^+ + CH_3 + 2e$	11.86	12.76	0.90	
$\rightarrow C_2H_5^+ + CH_2 + H + 2e$	16.71	18.72	2.01	
$\rightarrow C_2H_5^+ + CH + H_2 + 2e$	16.61	18.59	1.98	
$\rightarrow C_2H_4^+ + CH_4 + 2e$	10.35	10.74	0.39	
$\rightarrow C_2H_4^+ + CH_3 + H + 2e$	14.85	16.56	1.71	

*H₂ and 2H channels contribute 80% and 20% to $\sigma(C_3H_6^+)$, respectively.†The analytic fits for C₃H₈ partial ionization cross sections are given in Appendix 1.

Table 11: (continued)

Reaction channel	E_{th} (eV)	$\overline{E}_{el}^{(-)}$ (eV)	\overline{E}_K (eV)	$R'_{I,DI}$
$\rightarrow C_2H_4^+ + CH_2 + H_2 + 2e$	15.15	16.97	1.82	
$\rightarrow C_2H_4^+ + CH + H_2 + H + 2e$	19.59	22.96	3.37	
$\rightarrow C_2H_3^+ + CH_3 + H_2 + 2e$	13.88	15.34	1.46 ($\chi = 0.5$)	
$\rightarrow C_2H_3^+ + CH_4 + H + 2e$	13.93	15.41	1.48 ($\chi = 0.5$)	
$\rightarrow C_2H_2^+ + CH_4 + H_2 + 2e$	14.08	15.63	1.55 ($\chi = 0.5$)	
$\rightarrow C_2H_2^+ + CH_3 + H_2 + H + 2e$	18.58	21.24	2.66	
$\rightarrow C_2H_2^+ + CH_2 + 2H_2 + 2e$	17.79	20.55	2.76	
$\rightarrow C_2H^+ + CH_4 + H_2 + H + 2e$	19.16	22.03	2.87	
$\rightarrow C_2H^+ + CH_3 + 2H_2 + 2e$	19.09	21.94	2.85	
$\rightarrow CH_3^+ + C_2H_5 + 2e$	13.58	14.89	1.31 ($\chi = 0.5$)	
$\rightarrow CH_3^+ + C_2H_4 + H + 2e$	15.18	16.65	1.47	
$\rightarrow CH_3^+ + C_2H_3 + H_2 + 2e$	15.42	17.00	1.58	
$\rightarrow CH_3^+ + C_2H + H_2 + H + 2e$	19.59	21.70	2.11	
$\rightarrow CH_2^+ + C_2H_6 + 2e$	16.76	18.04	1.28	
$\rightarrow CH_2^+ + C_2H_5 + H + 2e$	21.14	23.95	2.81	
$\rightarrow CH_2^+ + C_2H_4 + H_2 + 2e$	18.19	19.97	1.78	
$(a_1)^\dagger \rightarrow CH^+ + C_2H_6 + H + 2e$	19.29	22.15	2.86	
$(a_2)^\dagger \rightarrow CH^+ + C_2H_5 + H_2 + 2e$	19.13	22.48	3.35	
$(a_3)^\dagger \rightarrow CH^+ + C_2H_4 + H_2 + H + 2e$	18.44	21.61	3.17	

[†]Channels a_i , share equally the respective ion production cross sections.

9 Tables

Table 12: Main electron-impact dissociative excitation channels of C_3H_y ($0 \leq y \leq 8$), their threshold energies (E_{th}) (Refs. [8, 9]), mean total kinetic energy of fragments $\overline{E_K}$, and cross section branching ratios at $E \simeq 80$ eV (R'_{DE}).

Reaction channel	$E_{th} = \overline{E_{el}^{(-)}} \text{ (eV)}$	$\overline{E_K} \text{ (eV)}$	R'_{DE}
$e + C_3 \rightarrow C_2 + C + e$	9.27	2.66	0.94
$\rightarrow 3C + e$	16.67	2.78	0.06 *
$e + C_3H \rightarrow C_3 + H + e$	8.61	2.23	0.67
$\rightarrow C_2 + CH + e$	12.64	2.20	0.11
$\rightarrow C + C_2H + e$	10.31	2.34	0.22
$e + C_3H_2 \rightarrow C_3H + H + e$	3.21	1.93 ($\chi = 1.5$)	0.78
$\rightarrow C_3 + H_2 + e$	5.30	2.18 ($\chi = 0.7$)	0.15
$\rightarrow C_2H + CH + e$	7.21	1.51	0.04
$\rightarrow C + C_2H_2 + e$	8.68	1.40	0.03
$e + C_3H_3 \rightarrow C_3H_2 + H + e$	5.68	1.72	0.30
$\rightarrow C_3H + H_2 + e$	3.74	2.04 ($\chi = 1.2$)	0.56
$\rightarrow C_3H + 2H + e$	7.89	1.65	0.05
$\rightarrow C_2H_2 + CH + e$	7.50	1.71	0.05
$\rightarrow C_2H + CH_2 + e$	7.87	1.65	0.04
$e + C_3H_4 \rightarrow C_3H_3 + H + e$	4.16	1.08	0.44
$\rightarrow C_3H_2 + H_2 + e$	4.72	1.22	0.23
$\rightarrow C_3H + H_2 + H + e$	6.45	1.67	0.07
$\rightarrow C_3 + 2H_2 + e$	8.92	2.31	0.02
$\rightarrow C_2H_3 + CH + e$	9.54	2.20	0.02
$\rightarrow C_2H_2 + CH_2 + e$	5.98	1.55	0.08
$\rightarrow C_2H + CH_3 + e$	6.01	1.56	0.08
$\rightarrow C_2 + CH_4 + e$	8.07	2.09	0.03
$\rightarrow C + C_2H_4 + e$	8.17	2.12	0.03

* Calculated as $\frac{1}{3}$ of $\sigma(C_3^{**})$ for formation of autoionizing C_3^{**} dissociative state.

Table 12: (continued)

Reaction channel	$E_{th} = \overline{E_{el}^{(-)}} \text{ (eV)}$	$\overline{E_K} \text{ (eV)}$	R'_{DE}
$e + C_3H_5 \rightarrow C_3H_4 + H + e$	4.37	1.94 ($\chi = 0.8$)	0.25
$\rightarrow C_3H_3 + H_2 + e$	2.43	1.46 ($\chi = 1.5$)	0.54
$\rightarrow C_3H + 2H_2 + e$	4.79	2.13 ($\chi = 0.8$)	0.06
$\rightarrow C_2H_2 + CH_3 + e$	4.02	2.01 ($\chi = 1.0$)	0.09
$\rightarrow C_2H + CH_4 + e$	4.78	2.39 ($\chi = 1.0$)	0.06
$e + C_3H_6 \rightarrow C_3H_5 + H + e$	5.35	1.53 ($\chi = 0.4$)	0.25
$\rightarrow C_3H_4 + H_2 + e$	3.76	2.05 ($\chi = 1.2$)	0.30
$\rightarrow C_3H_3 + H_2 + H + e$	6.49	1.68	0.05
$\rightarrow C_3H_2 + 2H_2 + e$	7.02	1.82	0.04
$\rightarrow C_2H_4 + CH_2 + e$	5.82	1.51	0.06
$\rightarrow C_2H_3 + CH_3 + e$	5.81	1.51	0.06
$\rightarrow C_2H_2 + CH_4 + e$	3.35	2.01 ($\chi = 1.5$)	0.22
$e + C_3H_7 \rightarrow C_3H_6 + H + e$	3.16	1.58 ($\chi = 1.0$)	0.32
$\rightarrow C_3H_5 + H_2 + e$	2.40	1.55 ($\chi = 1.8$)	0.36
$\rightarrow C_3H_4 + H_2 + H + e$	5.59	2.30 ($\chi = 0.7$)	0.03
$\rightarrow C_3H_3 + 2H_2 + e$	3.64	1.82 ($\chi = 1.0$)	0.09
$\rightarrow C_2H_4 + CH_3 + e$	3.12	2.08 ($\chi = 2.0$)	0.13
$\rightarrow C_2H_3 + CH_4 + e$	3.89	2.50 ($\chi = 1.8$)	0.07
$e + C_3H_8 \rightarrow C_3H_7 + H + e$	5.82	1.51	0.22
$\rightarrow C_3H_6 + H_2 + e$	2.66	1.33 ($\chi = 1.0$)	0.34
$\rightarrow C_3H_4 + 2H_2 + e$	4.26	1.22 ($\chi = 0.4$)	0.07
$\rightarrow C_2H_6 + CH_2 + e$	5.70	1.48	0.03
$\rightarrow C_2H_5 + CH_3 + e$	5.05	1.31	0.04
$\rightarrow C_2H_4 + CH_4 + e$	2.10	1.26 ($\chi = 1.5$)	0.30

9 Tables

Table 13: Main electron-impact dissociative excitation channels of $C_3H_y^+$ ($0 \leq y \leq 8$), their threshold energies (E_{th}), mean total kinetic energies of products ($\overline{E_K}$) and cross section branching ratios at $E \simeq 30 - 40$ eV (R'_{DE^+}).

Reaction channel	$E_{th} = \overline{E_{el}^{(-)}} \text{ (eV)}$	$\overline{E_K} \text{ (eV)}$	R'_{DE^+}
$e + C_3^+ \rightarrow C_2^+ + C + e$	8.67	2.25	0.44
$\rightarrow C^+ + C_2 + e$	8.48	2.20	0.47
$\rightarrow C^+ + 2C + e$	16.82	4.36	0.09
$e + C_3H^+ \rightarrow C_3^+ + H + e$	8.48	2.20	0.28
$\rightarrow C_3 + H^+ + e$	9.81	2.54	0.31
$\rightarrow C_2^+ + CH + e$	11.35	3.20	0.08
$\rightarrow C_2 + CH^+ + e$	11.31	2.93	0.08
$\rightarrow C^+ + C_2H + e$	8.83	2.29	0.14
$\rightarrow C + C_2H^+ + e$	9.29	2.41	0.11
$e + C_3H_2^+ \rightarrow C_3H^+ + H + e$	5.79	1.24	0.23
$\rightarrow C_3H + H^+ + e$	5.99	1.55	0.30
$\rightarrow C_3^+ + H_2 + e$	7.14	1.85	0.12
$\rightarrow C_3 + H_2^+ + e$	10.95	2.84	0.04
$\rightarrow C_2H^+ + CH + e$	9.29	2.41	0.04
$\rightarrow C_2H + CH^+ + e$	7.98	2.07	0.06
$\rightarrow C_2^+ + CH_2 + e$	11.15	2.89	0.02
$\rightarrow C_2 + CH_2^+ + e$	9.79	2.54	0.03
$\rightarrow C^+ + C_2H_2 + e$	7.05	1.83	0.09
$\rightarrow C + C_2H_2^+ + e$	7.22	1.87	0.07

Table 13: (continued)

Reaction channel	$E_{th} = \overline{E_{el}^{(-)}} \text{ (eV)}$	$\overline{E_K} \text{ (eV)}$	R'_{DE+}
$e + C_3H_3^+ \rightarrow C_3H_2^+ + H + e$	9.52	2.47	0.18
$\rightarrow C_3H_2 + H^+ + e$	13.80	3.58	0.10
$\rightarrow C_3H^+ + H_2 + e$	8.18	2.12	0.12
$\rightarrow C_3H + H_2^+ + e$	11.85	3.07	0.05
$\rightarrow C_2H_3^+ + C + e$	10.42	2.70	0.06
$\rightarrow C_2H_3 + C^+ + e$	14.50	3.76	0.03
$\rightarrow C_2H_2^+ + CH + e$	11.95	3.10	0.04
$\rightarrow C_2H_2 + CH^+ + e$	10.92	2.83	0.06
$\rightarrow C_2H^+ + CH_2 + e$	12.81	3.32	0.03
$\rightarrow C_2H + CH_2^+ + e$	11.18	2.90	0.05
$\rightarrow C_2^+ + CH_3 + e$	14.12	3.66	0.03
$\rightarrow C_2 + CH_3^+ + e$	12.00	3.11	0.04
$\rightarrow C^+ + C_2H_3 + e$	13.31	3.45	0.04
$\rightarrow C + C_2H_3^+ + e$	10.85	2.81	0.06
$e + C_3H_4^+ \rightarrow C_3H_3^+ + H + e$	2.65	1.59 ($\chi = 1.5$)	0.60
$\rightarrow C_3H_3 + H^+ + e$	8.25	2.21	0.09
$\rightarrow C_3H_2^+ + H_2 + e$	4.81	1.25	0.09
$\rightarrow C_2H_3^+ + CH + e$	7.06	1.83	0.04
$\rightarrow C_2H_2^+ + CH_2 + e$	7.38	1.91	0.03
$\rightarrow C_2H_2 + CH_2^+ + e$	6.03	1.56	0.05
$\rightarrow C_2H^+ + CH_3 + e$	7.70	2.00	0.03
$\rightarrow C_2H + CH_3^+ + e$	5.31	1.38	0.07
$e + C_3H_5^+ \rightarrow C_3H_4^+ + H + e$	6.29	1.63	0.12
$\rightarrow C_3H_4 + H^+ + e$	10.66	2.76	0.08
$\rightarrow C_3H_3^+ + H_2 + e$	2.95	1.77 ($\chi = 1.5$)	0.61
$\rightarrow C_2H_3^+ + CH_2 + e$	7.36	1.91	0.04
$\rightarrow C_2H_2^+ + CH_3 + e$	7.13	1.85	0.03
$\rightarrow C_2H^+ + CH_4 + e$	7.92	2.05	0.04
$\rightarrow CH_3^+ + C_2H_2 + e$	5.02	1.30	0.08

Table 13: (continued)

Reaction channel	$E_{th} = \overline{E_{el}^{(-)}} \text{ (eV)}$	$\overline{E_K} \text{ (eV)}$	R'_{DE+}
$e + C_3H_6^+ \rightarrow C_3H_5^+ + H + e$	3.34	1.11 ($\chi = 0.5$)	0.28
$\rightarrow C_3H_5 + H^+ + e$	10.38	2.69	0.09
$\rightarrow C_3H_4^+ + H_2 + e$	3.52	1.17 ($\chi = 0.5$)	0.20
$\rightarrow C_3H_3^+ + H_2 + H + e$	4.60	1.19	0.09
$\rightarrow C_3H_2^+ + 2H_2 + e$	7.97	2.07	0.03
$\rightarrow C_2H_5^+ + CH + e$	7.51	1.95	0.02
$\rightarrow C_2H_4^+ + CH_2 + e$	6.88	1.78	0.03
$\rightarrow C_2H_3^+ + CH_3 + e$	4.24	1.41 ($\chi = 0.5$)	0.08
$\rightarrow C_2H_2^+ + CH_4 + e$	4.53	1.51 ($\chi = 0.5$)	0.07
$\rightarrow CH_4^+ + C_2H_2 + e$	5.84	1.52	0.04
$\rightarrow CH_3^+ + C_2H_3 + e$	5.97	1.55	0.04
$\rightarrow CH_2^+ + C_2H_4 + e$	6.74	1.75	0.03
$e + C_3H_7^+ \rightarrow C_3H_6^+ + H + e$	3.85	1.10 ($\chi = 0.4$)	0.22
$\rightarrow C_3H_6 + H^+ + e$	10.29	2.76	0.08
$\rightarrow C_3H_5^+ + H_2 + e$	2.43	1.00 ($\chi = 0.7$)	0.40
$\rightarrow C_3H_3^+ + 2H_2 + e$	3.90	1.30 ($\chi = 0.5$)	0.08
$\rightarrow C_2H_5^+ + CH_2 + e$	6.57	1.70	0.03
$\rightarrow C_2H_4^+ + CH_3 + e$	5.40	1.40	0.04
$\rightarrow C_2H_3^+ + CH_4 + e$	3.33	1.25 ($\chi = 0.6$)	0.09
$\rightarrow CH_3^+ + C_2H_4 + e$	4.99	1.66 ($\chi = 0.5$)	0.06
$e + C_3H_8^+ \rightarrow C_3H_7^+ + H + e$	2.20	1.32 ($\chi = 1.5$)	0.03
$\rightarrow C_3H_6^+ + H_2 + e$	0.27	0.18 ($\chi = 2$)	0.93
$\rightarrow C_2H_5^+ + CH_3 + e$	1.80	0.90 ($\chi = 1$)	0.01
$\rightarrow C_2H_4^+ + CH_4 + e$	0.97	0.58 ($\chi = 1.5$)	0.03

9 Tables

Table 14: Main electron-impact dissociative ionization channels of $C_3H_y^+$ ($0 \leq y \leq 8$), their threshold energies (E_{th}) and cross section branching ratios (R'_{DI^+})*.

Reaction channel	$E_{th} = \overline{E_{el}^{(-)}} \text{ (eV)}$	R'_{DI^+}
$e + C_3^+ \rightarrow C_2^+ + C^+ + 2e$	28.57	0.65
$\rightarrow C^+ + C^+ + C + 2e$	27.17	0.35
$e + C_3H^+ \rightarrow C_3^+ + H^+ + 2e$	31.68	0.58
$\rightarrow C_2^+ + CH^+ + 2e$	31.59	0.19
$\rightarrow C^+ + C_2H^+ + 2e$	29.94	0.23
$e + C_3H_2^+ \rightarrow C_3H^+ + H^+ + 2e$	28.25	0.46
$\rightarrow C_3^+ + H_2^+ + 2e$	32.52	0.16
$\rightarrow C_2H^+ + CH^+ + 2e$	29.32	0.08
$\rightarrow C_2^+ + CH_2^+ + 2e$	30.46	0.09
$\rightarrow C^+ + C_2H_2^+ + 2e$	18.42	0.21
$e + C_3H_3^+ \rightarrow C_3H_2^+ + H^+ + 2e$	32.45	0.40
$\rightarrow C_3H^+ + H_2^+ + 2e$	33.29	0.16
$\rightarrow C_2H_3^+ + C^+ + 2e$	30.78	0.12
$\rightarrow C_2H_2^+ + CH^+ + 2e$	31.29	0.12
$\rightarrow C_2H^+ + CH_2^+ + 2e$	31.69	0.10
$\rightarrow C_2^+ + CH_3^+ + 2e$	32.10	0.10
$e + C_3H_4^+ \rightarrow C_3H_3^+ + H^+ + 2e$	26.46	0.38
$\rightarrow C_3H_2^+ + H_2^+ + 2e$	30.79	0.15
$\rightarrow C_3H^+ + H^+ + H_2 + 2e$	30.52	0.09
$\rightarrow C_2H_4^+ + C^+ + 2e$	29.26	0.08
$\rightarrow C_2H_3^+ + CH^+ + 2e$	27.67	0.08
$\rightarrow C_2H_2^+ + CH_2^+ + 2e$	27.66	0.08
$\rightarrow C_2H^+ + CH_3^+ + 2e$	27.34	0.08
$\rightarrow C_2^+ + CH_4^+ + 2e$	30.53	0.06

* $\overline{E_k^{tot}} = 11.8 \text{ eV}$ for charged heavy products in all reactions. For the neutral products $\overline{E_K} \simeq 0 \text{ eV}$.

Table 14: (continued)

Reaction channel	$E_{th} = \overline{E_{el}^{(-)}} \text{ (eV)}$	R'_{DI^+}
$e + C_3H_5^+ \rightarrow C_3H_4^+ + H^+ + 2e$	30.5	0.36
$\rightarrow C_3H_3^+ + H_2^+ + 2e$	28.4	0.14
$\rightarrow C_3H_2^+ + H^+ + H_2 + 2e$	33.6	0.06
$\rightarrow C_3H_2^+ + H + H_2^+ + 2e$	35.5	0.05
$\rightarrow C_3H^+ + H_2 + H_2^+ + 2e$	34.5	0.05
$\rightarrow C_2H_5^+ + C^+ + 2e$	29.5	0.06
$\rightarrow C_2H_4^+ + CH^+ + 2e$	29.7	0.06
$\rightarrow C_2H_3^+ + CH_2^+ + 2e$	27.6	0.07
$\rightarrow C_2H_2^+ + CH_3^+ + 2e$	26.9	0.07
$\rightarrow C_2H^+ + CH_4^+ + 2e$	29.2	0.06
$\rightarrow C_2^+ + CH_4^+ + H + 2e$	36.2	0.02
$e + C_3H_6^+ \rightarrow C_3H_5^+ + H^+ + 2e$	27.6	0.34
$\rightarrow C_3H_4^+ + H_2^+ + 2e$	29.6	0.13
$\rightarrow C_3H_3^+ + H^+ + H_2 + 2e$	28.8	0.06
$\rightarrow C_3H_3^+ + H + H_2^+ + 2e$	30.6	0.05
$\rightarrow C_3H_2^+ + H_2^+ + H_2 + 2e$	33.1	0.05
$\rightarrow C_2H_6^+ + C^+ + 2e$	31.2	0.05
$\rightarrow C_2H_5^+ + CH^+ + 2e$	28.0	0.06
$\rightarrow C_2H_4^+ + CH_2^+ + 2e$	27.3	0.06
$\rightarrow C_2H_3^+ + CH_3^+ + 2e$	24.5	0.07
$\rightarrow C_2H_2^+ + CH_4^+ + 2e$	27.5	0.06
$\rightarrow C_2H^+ + CH_4^+ + H + 2e$	32.6	0.03
$\rightarrow C_2H^+ + CH_4 + H^+ + 2e$	33.5	0.02
$\rightarrow C_2^+ + CH_4^+ + H_2$	33.9	0.02

Table 14: (continued)

Reaction channel	$E_{th} = \overline{E_{el}^{(-)}} \text{ (eV)}$	R'_{DI^+}
$e + C_3H_7^+ \rightarrow C_3H_6^+ + H^+ + 2e$	28.1	0.33
$\rightarrow C_3H_5^+ + H_2^+ + 2e$	28.7	0.14
$\rightarrow C_3H_4^+ + H_2^+ + H + 2e$	31.5	0.06
$\rightarrow C_3H_4^+ + H_2 + H^+ + 2e$	33.3	0.06
$\rightarrow C_3H_3^+ + H_2^+ + H_2 + 2e$	29.8	0.06
$\rightarrow C_2H_6^+ + CH^+ + 2e$	30.8	0.05
$\rightarrow C_2H_5^+ + CH_2^+ + 2e$	27.1	0.06
$\rightarrow C_2H_4^+ + CH_3^+ + 2e$	25.6	0.07
$\rightarrow C_2H_3^+ + CH_4^+ + 2e$	26.6	0.06
$\rightarrow C_2H_2^+ + CH_4^+ + H + 2e$	31.3	0.03
$\rightarrow C_2H_2^+ + CH_4 + H^+ + 2e$	32.2	0.03
$\rightarrow C_2H^+ + CH_4^+ + H_2 + 2e$	31.8	0.03
$\rightarrow C_2H^+ + CH_4 + H_2^+ + 2e$	34.5	0.02
$e + C_3H_8^+ \rightarrow C_3H_7^+ + H^+ + 2e$	26.3	0.31
$\rightarrow C_3H_6^+ + H_2^+ + 2e$	27.3	0.12
$\rightarrow C_3H_5^+ + H_2^+ + H + 2e$	29.5	0.05
$\rightarrow C_3H_5^+ + H_2 + H^+ + 2e$	27.7	0.05
$\rightarrow C_3H_4^+ + H_2^+ + H_2 + 2e$	29.7	0.05
$\rightarrow C_3H_3^+ + H^+ + 2H_2 + 2e$	28.9	0.05
$\rightarrow C_3H_3^+ + H_2^+ + H_2 + H + 2e$	30.7	0.03
$\rightarrow C_3H_2 + H_2^+ + 2H_2 + 2e$	33.2	0.03
$\rightarrow C_2H_6^+ + CH_2^+ + 2e$	27.0	0.04
$\rightarrow C_2H_5^+ + CH_3^+ + 2e$	22.5	0.05
$\rightarrow C_2H_4^+ + CH_4^+ + 2e$	24.9	0.05
$\rightarrow C_2H_3^+ + CH_4^+ + H + 2e$	27.5	0.03
$\rightarrow C_2H_3^+ + CH_4 + H^+ + 2e$	28.4	0.03
$\rightarrow C_2H_3^+ + CH_3^+ + H_2 + 2e$	24.5	0.04
$\rightarrow C_2H_3^+ + CH_3 + H_2^+ + 2e$	30.1	0.02
$\rightarrow C_2H_2^+ + CH_4^+ + H_2 + 2e$	27.6	0.03
$\rightarrow C_2H_2^+ + CH_4 + H_2^+ + 2e$	30.3	0.02

9 Tables

Table 15: Main dissociative recombination channels of $C_3H_y^+$, their cross section branching ratios (R_{DR}), total kinetic energy of dissociation products ($E_k^{(0)}$) in their ground state and for zero electron impact energy, and possible excited products for $E \lesssim 1$ eV.

Reaction channel	R_{DR}	$E_k^{(0)}$ (eV)	Excited products for $E \lesssim 1$ eV
$e + C_3^+ \rightarrow C_2 + C$	1.00	4.99	$C(^1D; ^1S; ^5S_2^0)$, $C_2(a; b; A; c; d; C; e)$
$e + C_3H^+ \rightarrow C_3 + H$	0.75	6.32	$C_3(a; b; A; B; ^1S_u^+)$
$\rightarrow C_2H + C$	0.15	4.73	$C(^1D; ^1S; ^5S_2^0)$, $C_2H(A, B^1, B)$
$\rightarrow C_2 + CH$	0.10	2.26	$C_2(a; b; A; c; d)$, $CH(a, A)$
$e + C_3H_2^+ \rightarrow C_3H + H$	0.52	9.15	$H(n=2)$
$\rightarrow C_3 + H + H$	0.31	2.77	$C_3(a; b)$
$\rightarrow C_3 + H_2$	0.08	7.31	$C_3(a; b; A; B; ^1S_u^+)$
$\rightarrow C_2H_2 + C$	0.03	6.05	$C(^1D; ^1S; ^5S_2^0)$
$\rightarrow C_2H + CH$	0.04	4.73	$CH(a; A; B; C)$, $C_2H(A; B^1; B)$
$\rightarrow C_2 + CH_2$	0.02	3.15	$C_2(a; b; A; c; d)$, $CH_2(a; b; c)$
$e + C_3H_3^+ \rightarrow C_3H_2 + H$	0.33	3.38	$C_3H_2(A; B)$
$\rightarrow C_3H + H + H$	0.50	2.10	
$\rightarrow C_3H + H_2$	0.06	6.64	
$\rightarrow C_3H_2 + H$	0.03	0.27	$C_3H_2(A)$
$\rightarrow C_2H_2 + CH$	0.03	2.55	$CH(a; A)$
$\rightarrow C_2 + CH_3$	0.02	0.95	$C_2(a; b; A)$
$\rightarrow C_2H + CH_2$	0.03	2.12	$CH_2(a; b)$
$e + C_3H_4^+ \rightarrow C_3H_3 + H$	0.30	7.28	
$\rightarrow C_3H_2 + H + H$	0.55	2.32	$C_3H_2(A; B)$
$\rightarrow C_3H_2 + H_2$	0.06	6.86	$C_3H_2(A; B; C)$
$\rightarrow C_3H + H_2 + H$	0.04	5.58	
$\rightarrow C_2 + CH_4$	0.03	4.38	$C_2(a; b; A; c; d; C)$
$\rightarrow C + C_2H_4$	0.02	4.31	$C(^1D; ^1S)$

Table 15: (continued)

Reaction channel	R_{DR}	$E_k^{(0)}$ (eV)	Excited products for $E \lesssim 1$ eV
$e + C_3H_5^+ \rightarrow C_3H_4 + H$	0.27	5.70	
$\rightarrow C_3H_3 + H + H$	0.56	2.62	
$\rightarrow C_3H_3 + H_2$	0.04	7.16	†
$\rightarrow C_3H_2 + H_2 + H$	0.03	2.20	$C_3H_2(A; B)$
$\rightarrow C_2H + CH_4$	0.03	6.95	$C_2H(A; B^1; B; C)$
$\rightarrow C_2H_4 + CH$	0.02	3.20	$CH(a; A; B)$
$\rightarrow C_2H_3 + CH_2$	0.02	3.01	$C_2H_3(A), CH_2(a; b; c)$
$\rightarrow C_2H_2 + CH_3$	0.03	6.33	$CH_3(3s)$
$e + C_3H_6^+ \rightarrow C_3H_5 + H$	0.26	5.90	$C_3H_5(A; B; C; 3d)$
$\rightarrow C_3H_4 + H + H$	0.58	3.47	
$\rightarrow C_3H_4 + H_2$	0.04	8.01	†
$\rightarrow C_3H_3 + H_2 + H$	0.04	4.93	
$\rightarrow C_2H_5 + CH$	0.02	2.51	$CH(a; A)$
$\rightarrow C_2H_4 + CH_2$	0.03	5.41	$CH_2(a; b; c);$
$\rightarrow C_2H_3 + CH_3$	0.03	5.42	$C_2H_3(A; B), CH_3(3s)$
$e + C_3H_7^+ \rightarrow C_3H_6 + H$	0.27	5.97	
$\rightarrow C_3H_5 + H + H$	0.55	2.15	$C_3H_5(A)$
$\rightarrow C_3H_5 + H_2$	0.05	6.69	$C_3H_5(A; B; C; 3d; 4s)$
$\rightarrow C_3H_4 + H_2 + H$	0.02	2.26	
$\rightarrow C_2H_6 + CH$	0.03	3.19	$CH(a; A; B)$
$\rightarrow C_2H_5 + CH_2$	0.02	3.25	$CH_2(a; b; c)$
$\rightarrow C_2H_4 + CH_3$	0.03	6.51	$CH_3(3s; 3p)$
$\rightarrow C_2H_3 + CH_4$	0.03	6.16	$C_2H_3(A; B)$

†This channel is only open for $E \gtrsim 1$ eV.

Table 15: (continued)

Reaction channel	R_{DR}	$E_k^{(0)}$ (eV)	Excited products for $E \lesssim 1$ eV
$e + \text{C}_3\text{H}_8^+ \rightarrow \text{C}_3\text{H}_7 + \text{H}$	0.28	6.67	$\text{C}_3\text{H}_7(3s; 3p; 3d)$
$\rightarrow \text{C}_3\text{H}_6 + \text{H} + \text{H}$	0.56	5.09	
$\rightarrow \text{C}_3\text{H}_6 + \text{H}_2$	0.06	9.63	$\text{H}_2(\text{B})$
$\rightarrow \text{C}_3\text{H}_5 + \text{H}_2 + \text{H}$	0.04	5.81	$\text{C}_3\text{H}_5(\text{A}; \text{B}; \text{C}; 3d)$
$\rightarrow \text{C}_2\text{H}_6 + \text{CH}_2$	0.03	6.74	$\text{CH}_2(\text{a}; \text{b}; \text{c})$
$\rightarrow \text{C}_2\text{H}_5 + \text{CH}_3$	0.03	7.22	$\text{CH}_3(3s; 3p), \text{C}_2\text{H}_5(3s; 3p)$

9 Tables

Table 16: Charge exchange reaction channels in $H^+ + C_3H_y$ thermal collisions: Total rate coefficients (K_{CX}^{tot}), channel branching ratios (R_{CX}), reaction exothermicities (ΔE), and values of parameters a and β in Eq. 73b.

Reaction channel	K_{CX}^{tot} (10^{-9} cm ³ /s)	R_{CX}	ΔE (eV)	a	β
$H^+ + C_3 \rightarrow H + C_3^+$	4.0	0.70	1.00	—	—
$\rightarrow HC_2 + C^+$		0.18	0.62	30.0	2.5
$\rightarrow HC_2^+ + C$		0.12	0.40	30.0	2.5
$H^+ + C_3H \rightarrow H + C_3H^+$	3.8	0.65	0.90	—	—
$\rightarrow H_2 + C_3^+$		0.35	0.75	30.0	2.5
$H^+ + C_3H_2 \rightarrow H + C_3H_2^+$	4.0	0.65	3.17	—	—
$\rightarrow H_2 + C_3H^+$		0.35	4.15	30.0	2.5
$H^+ + C_3H_3 \rightarrow H + C_3H_3^+$	4.2	0.65	5.26	—	—
$\rightarrow H_2 + C_3H_2^+$		0.35	2.74	35.0	2.5
$H^+ + C_3H_4 \rightarrow H + C_3H_4^+$	4.4	0.70	3.24	—	—
$\rightarrow H_2 + C_3H_3^+$		0.30	6.71	40.0	2.5
$H^+ + C_3H_5 \rightarrow H + C_3H_5^+$	4.6	0.70	5.47	—	—
$\rightarrow H_2 + C_3H_4^+$		0.15	5.34	335.0	2.5
$\rightarrow H + H_2 + C_3H_3^+$		0.10	3.28	335.0	3.0
$\rightarrow 2H_2 + C_3H_2^+$		0.05	1.78	335.0	3.0
$H^+ + C_3H_6 \rightarrow H + C_3H_6^+$	4.8	0.65	3.98	—	—
$\rightarrow H_2 + C_3H_5^+$		0.15	6.18	185.0	2.5
$\rightarrow H + H_2 + C_3H_4^+$		0.05	1.52	185.0	3.0
$\rightarrow 2H_2 + C_3H_3^+$		0.15	5.01	185.0	3.0
$H^+ + C_3H_7 \rightarrow H + C_3H_7^+$	5.0	0.65	6.05	—	—
$\rightarrow H_2 + C_3H_6^+$		0.15	6.73	650.0	2.5
$\rightarrow H + H_2 + C_3H_5^+$		0.10	4.51	650.0	3.0
$\rightarrow 2H_2 + C_3H_4^+$		0.10	4.40	650.0	3.0
$H^+ + C_3H_8 \rightarrow H + C_3H_8^+$	5.2	0.65	2.64	—	—
$\rightarrow H_2 + C_3H_7^+$		0.15	6.29	150.0	2.5
$\rightarrow H + H_2 + C_3H_6^+$		0.10	2.25	150.0	3.0
$\rightarrow 2H_2 + C_3H_5^+$		0.10	4.86	150.0	3.0

9 Tables

Table 17: Values of coefficients c_i in Eq. 77 for total charge exchange cross sections in $H^+ + C_3H_y$ collisions. ($a(-x)$ denotes $a \times 10^{-x}$)

c_i	C_3	C_3H^*	C_3H_2	C_3H_3	C_3H_4	C_3H_5	C_3H_6	C_3H_7	C_3H_8
c_1	2.80	1.81	2.90	3.05	3.08	2.63	2.79	2.92	3.04
c_2	0.65	0.85	0.61	0.052	1.57	335.0	185.0	650.0	150.0
c_3	1.08	1.15	1.06	1.68	1.25	1.75	1.75	1.75	1.75
c_4	4.40	6.68	5.26	6.58	2.33	8.47	9.46	13.13	9.68
c_5	3.95	8.30	3.95	4.07	0.0	0.0	0.0	0.0	0.0
c_6	0.15	0.17	0.15	0.14	0.0	0.0	0.0	0.0	0.0
c_7	0.0	0.0	0.0	0.0	0.015	0.14	0.14	0.14	0.14
c_8	8.92(-6)	2.10(-8)	8.95(-6)	5.75(-6)	1.10(-6)	4.58(-6)	6.20(-6)	1.25(-5)	1.17(-4)
c_9	1.26	1.85	1.25	1.23	1.31	1.18	1.16	1.10	0.90
c_{10}	9.84(-20)	4.45(-20)	9.82(-20)	6.60(-23)	1.93(-21)	6.03(-20)	9.76(-20)	1.95(-20)	3.78(-19)
c_{11}	4.10	4.20	4.10	4.60	4.32	4.12	4.08	4.20	3.97

*The cross section for $H^+ + C_3H$ system refers only to the electron capture process (i.e. particle exchange contribution is excluded)

A.1 Values of fitting parameters I_c and A_i in Eq.(47) for total and partial ionization cross sections of C_2H_y ($y = 1 - 6$).

A Appendix

A.1 Values of fitting parameters I_c and A_i in Eq.(47) for total and partial ionization cross sections of C_2H_y ($y = 1 - 6$).

e + C₂H
(a) Total cross section

process	I_p	$A_i, i=1-3$ $A_i, i=4-6$		
$e + C_2H \rightarrow \text{total ionization}$	1.1220E+01	3.2202E+00	-2.8152E+00	-5.8088E+00
		2.9504E+01	-5.8412E+01	3.9669E+01

(b) Partial cross sections

process	I_p	$A_i, i=1-3$ $A_i, i=4-6$		
$e + C_2H \rightarrow C_2H^+ + 2e$	1.1000E+01	2.8838E+00	-2.5628E+00	-5.4320E+00
		2.8889E+01	-5.7295E+01	3.7708E+01
$e + C_2H \rightarrow C_2^+ + H + 2e$	1.6600E+01	1.8190E-01	-1.3742E-01	1.9606E-01
		1.5691E+00	-3.4910E+00	2.8130E+00
$e + C_2H \rightarrow CH^+ + C + 2e$	2.0000E+01	1.0185E-01	-9.2971E-02	2.0310E-02
		1.8823E-01	9.2660E-01	-5.2016E-01
$e + C_2H \rightarrow C^+ + CH + 2e$	2.1500E+01	6.8836E-02	-7.7999E-02	2.6112E-01
		-4.3316E-01	1.0820E+00	-5.5750E-01
$e + C_2H \rightarrow C_2 + H^+ + 2e$	1.8100E+01	-5.1850E-03	4.5961E-02	-7.0162E-01
		3.8420E+00	-5.5680E+00	3.2844E+00

A.1 Values of fitting parameters I_c and A_i in Eq.(47) for total and partial ionization cross sections of C_2H_y ($y = 1 - 6$).

e + C₂H₂

(a) Total cross section

process	I_p	$A_i, i=1-3$		
		$A_i, i=4-6$		
$e + C_2H_2 \rightarrow \text{total ionization}$	1.5500E+01	4.4672E+00	-1.3171E+00	-1.9831E+01
		8.1048E+01	-1.3186E+02	7.8763E+01

(b) Partial cross sections

process	I_p	$A_i, i=1-3$		
		$A_i, i=4-6$		
$e + C_2H_2 \rightarrow C_2H_2^+ + 2e$	1.5400E+01	4.2151E+00	-1.4139E+00	-1.5703E+01
		6.1345E+01	-1.0070E+02	5.6335E+01
$e + C_2H_2 \rightarrow C_2H^+ + H + 2e$	1.7700E+01	6.1452E-01	-3.4326E-01	-1.9464E+00
		1.3746E+01	-2.4790E+01	1.4872E+01
$e + C_2H_2 \rightarrow C_2^+ + H_2 + 2e$	2.2600E+01	-1.2316E-01	1.7484E-01	7.3057E-01
		8.9691E-01	-2.7137E+00	2.4490E+00
$e + C_2H_2 \rightarrow CH^+ + CH + 2e$	2.3900E+01	-9.6563E-02	1.7049E-01	1.6868E+00
		-4.9120E+00	1.0656E+01	-5.5749E+00
$e + C_2H_2 \rightarrow C^+ + CH_2 + 2e$	2.8500E+01	2.9296E-02	1.0247E-01	1.5647E+00
		-6.8246E+00	1.4659E+01	-8.3645E+00
$e + C_2H_2 \rightarrow H^+ + C_2H + 2e$	2.4000E+01	2.6407E-03	2.0240E-01	7.3429E-03
		-9.3824E-01	7.7448E+00	-5.1682E+00
$e + C_2H_2 \rightarrow C_2H_2^{2+} + 3e^\dagger$	5.0000E+01	5.8712E-02	-9.1017E+00	5.5948E+01
		-1.2562E+02	1.2516E+02	-4.6304E+01
$e + C_2H_2 \rightarrow C_2H^{2+} + H + 3e^\dagger$	7.0000E+01	1.4407E-04	-6.8112E-04	5.1788E-02
		-1.2682E-01	1.2149E-01	-4.3423E-02

[†]These processes are not discussed in the present work, and are included here only for completeness.

A.1 Values of fitting parameters I_c and A_i in Eq.(47) for total and partial ionization cross sections of C_2H_y ($y = 1 - 6$).

e + C₂H₃

(a) Total cross section

process	I_p	$A_i, i=1-3$		
		$A_i, i=4-6$		
$e + C_2H_3 \rightarrow \text{total ionization}$	1.0230E+01	3.7814E+00	-3.1886E+00	-8.8629E+00
		3.6097E+01	-6.6447E+01	4.1577E+01

(b) Partial cross sections

process	I_p	$A_i, i=1-3$		
		$A_i, i=4-6$		
$e + C_2H_3 \rightarrow C_2H_3^+ + 2e$	1.0000E+01	2.1638E+00	-1.8885E+00	-3.9536E+00
		1.6627E+01	-3.1823E+01	1.9787E+01
$e + C_2H_3 \rightarrow C_2H_2^+ + H + 2e$	1.2300E+01	9.1180E-01	-8.4482E-01	-8.3155E-01
		4.7606E+00	-1.0715E+01	7.7800E+00
$e + C_2H_3 \rightarrow C_2H^+ + H_2 + 2e$ † $e + C_2H_3 \rightarrow C_2H^+ + 2H + 2e$ †	1.3100E+01	3.6351E-01	-3.1960E-01	-6.6137E-01
		4.2235E+00	-8.4395E+00	6.1642E+00
$e + C_2H_3 \rightarrow C_2H^+ + H_2 + 2e$	1.3100E+01	3.3047E-01	-2.9055E-01	-6.0125E-01
		3.8396E+00	-7.6723E+00	5.6039E+00
$e + C_2H_3 \rightarrow C_2H^+ + 2H + 2e$	1.3100E+01	3.3047E-02	-2.9055E-02	-6.0125E-02
		3.8396E-01	-7.6723E-01	5.6039E-01
$e + C_2H_3 \rightarrow C_2^+ + H_2 + H + 2e$	2.3400E+01	5.1232E-02	-3.4944E-02	3.3463E-01
		-7.4796E-01	1.3188E+00	-5.9278E-01
$e + C_2H_3 \rightarrow CH_2^+ + CH + 2e$	2.0000E+01	2.6169E-02	-1.8406E-02	3.0591E-02
		7.0391E-02	-1.3010E-01	1.6045E-01
$e + C_2H_3 \rightarrow CH^+ + CH_2 + 2e$	2.5000E+01	3.6483E-02	-6.5833E-02	1.6869E+00
		-4.2141E+00	6.0795E+00	-2.6635E+00
$e + C_2H_3 \rightarrow C^+ + CH_3 + 2e$	2.1100E+01	1.0349E-01	-1.1251E-01	5.2156E-01
		-1.6825E+00	2.8676E+00	-1.3848E+00
$e + C_2H_3 \rightarrow H^+ + C_2H_2 + 2e$	2.1100E+01	1.1828E-01	-1.2858E-01	5.9606E-01
		-1.9229E+00	3.2773E+00	-1.5826E+00

†The H₂ and 2H channels contribute to the C₂H⁺ ion production cross section by 70% and 30%, respectively.

A.1 Values of fitting parameters I_c and A_i in Eq.(47) for total and partial ionization cross sections of C_2H_y ($y = 1 - 6$).

e + C₂H₄

(a) Total cross section

process	I_p	$A_i, i=1-3$		
		$A_i, i=4-6$		
$e + C_2H_4 \rightarrow$ total ionization	1.0450E+01	4.3521E+00	-4.0953E+00	-5.4465E+00
		1.9260E+01	-3.9235E+01	2.7143E+01

(b) Partial cross sections

process	I_c	$A_i, i=1-3$		
		$A_i, i=4-6$		
$e + C_2H_4 \rightarrow C_2H_4^+ + 2e$	1.1000E+01	2.1339E+00	-2.1027E+00	-1.4991E+00
		7.6831E+00	-1.8586E+01	1.3248E+01
$e + C_2H_4 \rightarrow C_2H_3^+ + H + 2e$	1.2600E+01	1.0771E+00	-1.1006E+00	-7.1624E-01
		5.6861E+00	-1.3597E+01	1.0568E+01
$e + C_2H_4 \rightarrow C_2H_2^+ + H_2 + 2e$ †	1.4300E+01	6.3131E-01	-5.7812E-01	-6.2781E-01
		5.3546E+00	-1.1487E+01	9.5818E+00
$e + C_2H_4 \rightarrow C_2H^+ + H_2 + H + 2e$	2.3500E+01	3.0122E-01	-2.8740E-01	-1.9558E-01
		1.8746E+00	-1.8614E+00	7.4894E-01
$e + C_2H_4 \rightarrow C_2^+ + 2H_2 + 2e$	2.5600E+01	1.4016E-02	-3.3329E-02	4.8119E-01
		-1.2222E+00	2.0053E+00	-9.5120E-01
$e + C_2H_4 \rightarrow CH_3^+ + CH + 2e$	2.1500E+01	6.7093E-02	-3.2712E-02	-2.5428E-01
		1.5686E+00	-2.2885E+00	1.3626E+00
$e + C_2H_4 \rightarrow CH_2^+ + CH_2 + 2e$	2.1500E+01	6.1553E-02	-3.0011E-02	-2.3328E-01
		1.4391E+00	-2.0995E+00	1.2501E+00
$e + C_2H_4 \rightarrow CH^+ + CH_3 + 2e$	2.7400E+01	4.7646E-02	-3.0637E-02	2.2730E-01
		-4.6992E-01	7.4920E-01	-3.5489E-01
$e + C_2H_4 \rightarrow C^+ + CH_2 + H_2 + 2e$ ‡	2.8800E+01	2.0449E-02	-7.1556E-03	2.1225E-01
$e + C_2H_4 \rightarrow C^+ + CH_3 + H + 2e$ ‡		-6.3042E-01	9.6428E-01	-4.3114E-01
$e + C_2H_4 \rightarrow C^+ + CH_4 + 2e$ ‡				

†The cross section includes a 15 % contribution from the $C_2H_2^+ + 2H$ channel.

‡The weights of $CH_2 + H_2$, $CH_3 + H$ and CH_4 productions cross sections are 0.3, 0.3 and 0.4, respectively

A.1 Values of fitting parameters I_c and A_i in Eq.(47) for total and partial ionization cross sections of C_2H_y ($y = 1 - 6$).

e + C₂H₅

(a) Total cross section

process	I_p	$A_i, i=1-3$		
		$A_i, i=4-6$		
$e + C_2H_5 \rightarrow$ total ionization	1.0720E+01	3.2266E+00	-2.9214E+00	-4.6995E+00
		2.0847E+01	-4.3907E+01	3.2627E+01

(b) Partial cross sections

process	I_p	$A_i, i=1-3$		
		$A_i, i=4-6$		
$e + C_2H_5 \rightarrow C_2H_5^+ + 2e$	9.2900E+00	1.0396E+00	-1.0585E+00	-7.8373E-01
		4.4709E+00	-1.0590E+01	7.2951E+00
$e + C_2H_5 \rightarrow C_2H_4^+ + H + 2e$	1.1500E+01	7.3095E-01	-7.1416E-01	-5.0556E-01
		4.1229E+00	-9.9820E+00	7.4219E+00
$e + C_2H_5 \rightarrow C_2H_3^+ + H_2 + 2e$ †	1.2100E+01	8.1673E-01	-7.8552E-01	-1.1560E+00
		9.7883E+00	-2.1341E+01	1.5713E+01
$e + C_2H_5 \rightarrow C_2H_2^+ + H_2 + H + 2e$	1.6300E+01	3.8144E-01	-3.7062E-01	-1.8209E-01
		2.1859E+00	-2.5851E+00	2.3403E+00
$e + C_2H_5 \rightarrow C_2H^+ + 2H_2 + 2e$	1.8100E+01	2.6686E-01	-3.2896E-01	8.6054E-01
		-2.9524E+00	5.1638E+00	-2.4925E+00
$e + C_2H_5 \rightarrow CH_3^+ + CH_2 + 2e$	1.8100E+01	2.1412E-01	-2.8591E-01	1.0153E+00
		-3.9444E+00	6.5300E+00	-3.4506E+00
$e + C_2H_5 \rightarrow CH_2^+ + CH_3 + 2e$	1.8700E+01	8.0482E-02	-1.3470E-01	8.2172E-01
		-3.0297E+00	4.7510E+00	-2.1714E+00
$e + C_2H_5 \rightarrow CH^+ + CH_4 + 2e$	2.0000E+01	3.5922E-02	-7.9976E-02	5.6120E-01
		-1.6337E+00	2.1472E+00	-7.6633E-01
$e + C_2H_5 \rightarrow C^+ + CH_4 + H + 2e$ ‡	2.4600E+01	-3.4867E-03	1.6590E-02	9.1837E-02
$e + C_2H_5 \rightarrow C^+ + CH_3 + H_2 + 2e$ ‡		-3.1695E-02	6.7634E-03	1.7756E-01

† This cross section includes a 20% contribution from the $C_2H_3^+ + 2H$ channel.

‡ $CH_4 + H$ and $CH_3 + H_2$ channels share the C^+ production cross section equally.

A.1 Values of fitting parameters I_c and A_i in Eq.(47) for total and partial ionization cross sections of C_2H_y ($y = 1 - 6$).

e + C₂H₆

(a) Total cross section

process	I_p	$A_i, i=1-3$		
		$A_i, i=4-6$		
$e + C_2H_6 \rightarrow$ total ionization	1.1520E+01	5.2541E+00	-5.4485E+00	4.0002E-01
		-1.4406E+00	-8.0654E+00	1.1302E+01

(b) Partial cross sections

process	I_c	$A_i, i=1-3$		
		$A_i, i=4-6$		
$e + C_2H_6 \rightarrow C_2H_6^+ + 2e$	1.1600E+01	8.2615E-01	-8.2021E-01	-5.6633E-02
		-2.1538E-01	-3.3404E-01	-2.2170E-01
$e + C_2H_6 \rightarrow C_2H_5^+ + H + 2e$	1.2650E+01	5.5541E-01	-5.4868E-01	-6.5438E-01
		4.1294E+00	-8.2258E+00	4.8497E+00
$e + C_2H_6 \rightarrow C_2H_4^+ + H_2 + 2e$	1.1810E+01	3.2570E+00	-3.2295E+00	-2.3531E+00
		4.2286E+00	-4.0175E+00	
$e + C_2H_6 \rightarrow C_2H_3^+ + H_2 + H + 2e$	1.5000E+01	1.2029E+00	-1.0931E+00	-9.2486E-01
		2.5826E+00	-1.0069E+00	
$e + C_2H_6 \rightarrow C_2H_2^+ + 2H_2 + 2e$	1.6000E+01	2.2917E-01	-7.6755E-02	-5.1260E-01
		4.2754E-01	3.4436E+00	-1.5903E+00
$e + C_2H_6 \rightarrow C_2H^+ + 2H_2 + H + 2e$	2.7500E+01	-1.0284E-01	1.0591E-01	2.4415E+00
		-7.2489E+00	1.2360E+01	-6.6793E+00
$e + C_2H_6 \rightarrow CH_3^+ + CH_3 + 2e$	1.5500E+01	2.9446E-01	-3.4463E-01	4.1525E-01
		-7.9157E-01	7.6763E-01	-1.7526E-01
$e + C_2H_6 \rightarrow CH_2^+ + CH_4 + 2e$	2.6000E+01	-1.5131E-01	8.9757E-02	9.5436E-01
		4.9445E-01	-9.6513E-01	6.8539E-01

A.1 Values of fitting parameters I_c and A_i in Eq.(47) for total and partial ionization cross sections of C_2H_y ($y = 1 - 6$).

e + C_2H_6 , (b) Partial cross sections, continued

process	I_c	$A_i, i=1-3$		
		$A_i, i=4-6$		
$e + C_2H_6 \rightarrow CH^+ + CH_4 + H + 2e^\dagger$	2.4200E+01	-9.2310E-02	-1.2519E-02	1.1308E+00
$e + C_2H_6 \rightarrow CH^+ + CH_3 + H_2 + 2e^\dagger$		-2.9895E+00	5.0173E+00	-2.4317E+00
$e + C_2H_6 \rightarrow C_2^+ + 3H_2 + 2e$	3.0200E+01	-2.4726E-02	-1.2327E-01	1.6520E+00
		-5.5917E+00	8.8261E+00	-4.4963E+00
$e + C_2H_6 \rightarrow C^+ + CH_4 + H_2 + 2e$	3.0500E+01	-3.3797E-02	-2.7912E-02	7.5677E-01
		-2.3435E+00	4.1065E+00	-2.2066E+00
$e + C_2H_6 \rightarrow C_2H_5^{2+} + H + 3e^\ddagger$	3.5500E+01	-3.8235E-03	4.7880E-03	1.0142E-01
		-1.0201E-01	4.6253E-02	-2.4543E-03

[†]CH₄ + H and CH₃ + H₂ channels share the CH⁺ production cross section equally.

[‡]This process is not discussed in this work. It is included here only for completeness.

A.2 Values of fitting parameters I_c and A_i in Eq.(81) for total ionization cross sections of C_3H_y ($y = 1 - 8$) and partial ionization cross sections of C_3H_8 .

A.2 Values of fitting parameters I_c and A_i in Eq.(81) for total ionization cross sections of C_3H_y ($y = 1 - 8$) and partial ionization cross sections of C_3H_8 .

(a) Total cross sections

$e + C_3H$

process	I_p	$A_i, i=1-3$ $A_i, i=4-6$		
$e + C_3H \rightarrow$ total ionization	1.3400E+01	2.9764E+00	-2.3477E+00	-1.3216E+01
		7.3427E+01	-1.3479E+02	9.1416E+01

$e + C_3H_2$

process	I_p	$A_i, i=1-3$ $A_i, i=4-6$		
$e + C_3H_2 \rightarrow$ total ionization	1.2500E+01	3.4541E+00	-2.5401E+00	-1.5431E+01
		7.8784E+01	-1.4284E+02	9.3027E+01

$e + C_3H_3$

process	I_p	$A_i, i=1-3$ $A_i, i=4-6$		
$e + C_3H_3 \rightarrow$ total ionization	8.3400E+00	3.9516E+00	6.1981E+00	-8.5488E+01
		2.4758E+02	-3.1654E+02	1.4805E+02

$e + C_3H_4$

process	I_p	$A_i, i=1-3$ $A_i, i=4-6$		
$e + C_3H_4 \rightarrow$ total ionization	9.6900E+00	5.6635E+00	-3.4929E+00	-2.5611E+01
		8.4138E+01	-1.2944E+02	7.1372E+01

$e + C_3H_5$

process	I_p	$A_i, i=1-3$ $A_i, i=4-6$		
$e + C_3H_5 \rightarrow$ total ionization	9.9000E+00	6.1485E+00	-3.4551E+00	-3.2501E+01
		1.0869E+02	-1.6248E+02	8.5999E+01

A.2 Values of fitting parameters I_c and A_i in Eq.(81) for total ionization cross sections of C_3H_y ($y = 1 - 8$) and partial ionization cross sections of C_3H_8 .

e + C₃H₆

process	I_p	$A_i, i=1-3$ $A_i, i=4-6$		
$e + C_3H_6 \rightarrow$ total ionization	9.9000E+00	6.8619E+00 5.3625E+01	-5.7820E+00 -9.3645E+01	-1.5514E+01 5.5264E+01

e + C₃H₇

process	I_p	$A_i, i=1-3$ $A_i, i=4-6$		
$e + C_3H_7 \rightarrow$ total ionization	9.1000E+00	6.3672E+00 1.2121E+02	-2.3655E+00 -1.6787E+02	-4.0355E+01 8.3031E+01

e + C₃H₈

process	I_p	$A_i, i=1-3$ $A_i, i=4-6$		
$e + C_3H_8 \rightarrow$ total ionization	1.1080E+01	9.2375E+00 2.0096E+01	-8.9512E+00 -3.5203E+01	-8.1610E+00 2.0414E+01

A.2 Values of fitting parameters I_c and A_i in Eq.(81) for total ionization cross sections of C_3H_y ($y = 1 - 8$) and partial ionization cross sections of C_3H_8 .

(b) Partial cross sections for C_3H_8

process	I_p	$A_i, i=1-3$		
		$A_i, i=4-6$		
$e + C_3H_8 \rightarrow C_3H_8^+ + 2e$	1.4300E+01	1.1449E+00	-6.1376E-01	-2.7962E+00
		6.2843E+00	-7.7244E+00	2.8788E+00
$e + C_3H_8 \rightarrow C_3H_7^+ + H + 2e$	1.4320E+01	1.0161E+00	-1.0639E+00	1.1574E+00
		-4.4077E+00	5.0090E+00	-2.6962E+00
$e + C_3H_8 \rightarrow C_3H_6^+ + H_2 + 2e$ †	1.8110E+01	2.0241E-01	-1.0303E-01	-1.5354E-01
		6.5766E-01	-1.5173E+00	1.0456E+00
$e + C_3H_8 \rightarrow C_3H_5^+ + H_2 + H + 2e$	1.5400E+01	6.2959E-01	-5.7820E-01	-4.2275E-01
		1.0438E+00	-1.2310E+00	1.5894E-01
$e + C_3H_8 \rightarrow C_3H_4^+ + 2H_2 + 2e$	1.6250E+01	9.2480E-02	-7.0635E-02	-1.9218E-01
		6.0213E-01	-6.7201E-01	2.2408E-01
$e + C_3H_8 \rightarrow C_3H_3^+ + 2H_2 + H + 2e$	1.9000E+01	8.5033E-01	-5.9487E-01	-2.9271E+00
		1.4455E+01	-1.9396E+01	8.6935E+00
$e + C_3H_8 \rightarrow C_3H_2^+ + 3H_2 + 2e$	2.5030E+01	-2.6317E-01	3.3089E-01	1.6290E+00
		-3.4753E+00	7.9786E+00	-4.1578E+00
$e + C_3H_8 \rightarrow C_3H^+ + 3H_2 + H + 2e$	2.6000E+01	-1.8486E-01	1.9884E-01	1.0565E+00
		-3.8196E+00	9.3217E+00	-5.2271E+00
$e + C_3H_8 \rightarrow C_3^+ + 4H_2 + 2e$ ‡	3.7000E+01	-1.8126E-02	-1.2458E-02	7.8290E-01
		-2.2762E+00	4.4177E+00	-2.6932E+00
$e + C_3H_8 \rightarrow C_2H_5^+$ (total)	1.5500E+01	3.3493E+00	-1.4701E+00	-1.1776E+01
		3.7323E+01	-5.4124E+01	2.7061E+01
$e + C_3H_8 \rightarrow C_2H_5^+ + CH_3 + 2e$	1.3920E+01	1.8084E+00	-1.4952E+00	-2.6108E+00
		9.2923E+00	-1.5153E+01	7.6576E+00
$e + C_3H_8 \rightarrow C_2H_5^+ + CH_2 + H + 2e$	1.3520E+01	9.6666E-01	-8.2170E-01	-1.4347E+00
		5.0765E+00	-8.1327E+00	4.0249E+00
$e + C_3H_8 \rightarrow C_2H_5^+ + CH + H_2 + 2e$	1.5440E+01	4.9612E-01	-2.0251E-01	-1.9007E+00
		6.0396E+00	-8.6886E+00	4.3218E+00

† This cross section includes a 20 % contribution from the $C_3H_6^+ + 2H$ channel.

‡ This process was not discussed in the text (see Table 11), but it is included here for completeness.

A.2 Values of fitting parameters I_c and A_i in Eq.(81) for total ionization cross sections of C_3H_y ($y = 1 - 8$) and partial ionization cross sections of C_3H_8 .

(b) Partial cross sections, continued

process	I_p	$A_i, i=1-2$ $A_i, i=3-4$ $A_i, i=5-6$
$e + C_3H_8 \rightarrow C_2H_4^+$ (total)	1.4190E+01	2.0981E+00 -2.3192E+00 2.6151E+00 -9.6433E+00 1.1904E+01 -6.4075E+00
$e + C_3H_8 \rightarrow C_2H_4^+ + CH_4 + 2e$	1.4190E+01	9.4413E-01 -1.0436E+00 1.1768E+00 -4.3395E+00 5.3567E+00 -2.8834E+00
$e + C_3H_8 \rightarrow C_2H_4^+ + CH_3 + H + 2e$	1.4190E+01	7.3433E-01 -8.1173E-01 9.1530E-01 -3.3752E+00 4.1664E+00 -2.2426E+00
$e + C_3H_8 \rightarrow C_2H_4^+ + CH_2 + H_2 + 2e$	1.4190E+01	3.1471E-01 -3.4788E-01 3.9227E-01 -1.4465E+00 1.7856E+00 -9.6113E-01
$e + C_3H_8 \rightarrow C_2H_4^+ + CH + H_2 + H + 2e$	1.4190E+01	1.0490E-01 -1.1596E-01 1.3076E-01 -4.8217E-01 5.9519E-01 -3.2038E-01
$e + C_3H_8 \rightarrow C_2H_3^+$ (total)	2.4600E+01	3.1460E+00 -2.2731E+00 1.6790E+01 -5.9326E+01 7.6575E+01 -3.3943E+01
$e + C_3H_8 \rightarrow C_2H_3^+ + CH_4 + H + 2e$	1.7500E+01	4.8967E-01 -1.6033E-01 -2.3282E-01 -8.4995E-01 2.3019E+00 -1.1694E+00
$e + C_3H_8 \rightarrow C_2H_3^+ + CH_3 + H_2 + 2e$	2.4600E+01	1.5074E+00 -1.6355E-01 -1.1436E+00 3.4966E-01 1.9949E+00 -9.9793E-01

A.2 Values of fitting parameters I_c and A_i in Eq.(81) for total ionization cross sections of C_3H_y ($y = 1 - 8$) and partial ionization cross sections of C_3H_8 .

(b) Partial cross sections, continued

process	I_p	$A_i, i=1-2$	
		$A_i, i=3-4$	$A_i, i=5-6$
$e + C_3H_8 \rightarrow C_2H_3^+ + CH_2 + H_2 + H + 2e^\dagger$	3.3000E+01	1.0379E-01 -2.7020E+00 -8.2132E+00	4.1519E-01 7.2257E+00 3.4544E+00
$e + C_3H_8 \rightarrow C_2H_3^+ + CH + 2H_2 + 2e^\dagger$	2.8700E+01	1.9840E-01 -9.1546E-01 -2.4088E+00	1.2298E-01 2.2331E+00 9.6347E-01
$e + C_3H_8 \rightarrow C_2H_2^+$ (total)	2.1380E+01	4.0247E-01 -1.4692E-01 2.9111E+00	-2.9371E-01 1.0883E+00 -2.7502E+00
$e + C_3H_8 \rightarrow C_2H_2^+ + CH_4 + H_2 + 2e$	2.1380E+01	2.4148E-01 -8.8151E-02 1.7467E+00	-1.7622E-01 6.5296E-01 -1.6501E+00
$e + C_3H_8 \rightarrow C_2H_2^+ + CH_3 + H_2 + H + 2e$	2.1380E+01	1.0062E-01 -3.6730E-02 7.2778E-01	-7.3427E-02 2.7207E-01 -6.8754E-01
$e + C_3H_8 \rightarrow C_2H_2^+ + CH_2 + 2H_2 + 2e$	2.1380E+01	6.0371E-02 -2.2038E-02 4.3667E-01	-4.4056E-02 1.6324E-01 -4.1252E-01
$e + C_3H_8 \rightarrow C_2H^+$ (total)	2.3060E+01	2.0075E-01 4.4626E-01 3.2211E+00	-2.4075E-01 -2.0128E+00 -1.6941E+00
$e + C_3H_8 \rightarrow C_2H^+ + CH_4 + H_2 + H + 2e$	2.3060E+01	1.0037E-01 2.2313E-01 1.6105E+00	-1.2037E-01 -1.0064E+00 -8.4706E-01

[†]These channels are not discussed in the text (Table 11), but are included here for completeness.

A.2 Values of fitting parameters I_c and A_i in Eq.(81) for total ionization cross sections of C_3H_y ($y = 1 - 8$) and partial ionization cross sections of C_3H_8 .

(b) Partial cross sections, continued

process	I_p	$A_i, i=1-2$	
		$A_i, i=3-4$	$A_i, i=5-6$
$e + C_3H_8 \rightarrow C_2H^+ + CH_3 + 2H_2 + 2e$	2.3060E+01	6.0225E-02 1.3388E-01 9.6632E-01	-7.2224E-02 -6.0384E-01 -5.0824E-01
$e + C_3H_8 \rightarrow C_2H^+ + CH_2 + 2H_2 + H + 2e^\dagger$	2.3060E+01	4.0150E-02 8.9252E-02 6.4421E-01	-4.8150E-02 -4.0256E-01 -3.3882E-01
$e + C_3H_8 \rightarrow C_2^+$ (total)	3.9000E+01	-6.7956E-02 4.8662E-01 4.0249E+00	4.9925E-02 -2.0569E+00 -2.2366E+00
$e + C_3H_8 \rightarrow C_2^+ + CH_2 + 3H_2 + 2e^\dagger$	3.9000E+01	-3.0580E-02 2.1898E-01 1.8112E+00	2.2466E-02 -9.2560E-01 -1.0065E+00
$e + C_3H_8 \rightarrow C_2^+ + CH_4 + 2H_2 + 2e^\dagger$	3.9000E+01	-3.7376E-02 2.6764E-01 2.2137E+00	2.7459E-02 -1.1313E+00 -1.2301E+00
$e + C_3H_8 \rightarrow CH_3^+$ (total)	2.4200E+01	-2.9172E-02 -2.2765E+00 -7.6602E+00	3.9988E-01 9.4140E+00 2.2697E+00
$e + C_3H_8 \rightarrow CH_3^+ + C_2H_5 + 2e$	2.3000E+01	4.9544E-02 3.5653E+00 1.4136E+01	-3.9462E-01 -1.0382E+01 -6.4721E+00
$e + C_3H_8 \rightarrow CH_3^+ + C_2H_4 + H + 2e$	2.3000E+01	1.6084E-02 2.8600E+00 1.1321E+01	-3.1169E-01 -8.1452E+00 -5.2918E+00

[†]These channels are not discussed in the text (Table 11), but are included here for completeness.

A.2 Values of fitting parameters I_c and A_i in Eq.(81) for total ionization cross sections of C_3H_y ($y = 1 - 8$) and partial ionization cross sections of C_3H_8 .

(b) Partial cross sections, continued

process	I_p	A_i , i=1-2	
		A_i , i=3-4	A_i , i=5-6
$e + C_3H_8 \rightarrow CH_3^+ + C_2H_3 + H_2 + 2e$	2.0000E+01	-3.0758E-02 -1.1295E-01 -5.3867E-01	5.5540E-02 7.2093E-01 3.4627E-01
$e + C_3H_8 \rightarrow CH_3^+ + C_2H_2 + H_2 + H + 2e$	3.2900E+01	4.9495E-02 9.3415E-01 3.2824E+00	-7.9001E-02 -2.5830E+00 -1.4886E+00
$e + C_3H_8 \rightarrow CH_2^+$ (total)	2.1000E+01	1.2721E-02 1.1754E+00 9.1847E+00	-1.0856E-01 -4.9652E+00 -4.7603E+00
$e + C_3H_8 \rightarrow CH_2^+ + C_2H_6 + 2e$	2.1000E+01	5.7257E-03 5.2894E-01 4.1331E+00	-4.8853E-02 -2.2344E+00 -2.1422E+00
$e + C_3H_8 \rightarrow CH_2^+ + C_2H_5 + H + 2e$	2.1000E+01	2.5446E-03 2.3508E-01 1.8369E+00	-2.1712E-02 -9.9305E-01 -9.5207E-01
$e + C_3H_8 \rightarrow CH_2^+ + C_2H_4 + H_2 + 2e$	2.1000E+01	4.4531E-03 4.1140E-01 3.2147E+00	-3.7996E-02 -1.7378E+00 -1.6661E+00
$e + C_3H_8 \rightarrow CH^+$ (total) [†]	3.0770E+01	-3.9297E-02 5.0500E-01 6.3715E+00	5.5189E-02 -2.7586E+00 -3.8831E+00
$e + C_3H_8 \rightarrow C_3H_4^{2+} + 2H_2 + 3e$ [‡]	4.7550E+01	-7.4397E-02 -5.0397E-02	2.5027E-01 1.0253E-01

[†]The total CH^+ production cross section is shared equally among the $C_2H_6 + H$, $C_2H_5 + H_2$ and $C_2H_4 + H_2 + H$ channels.

[‡]These channels were not listed in Table 11, but are included here for completeness.

A.2 Values of fitting parameters I_c and A_i in Eq.(81) for total ionization cross sections of C_3H_y ($y = 1 - 8$) and partial ionization cross sections of C_3H_8 .

(b) Partial cross sections, continued

process	I_p	$A_i, i=1-2$	
		$A_i, i=3-4$	$A_i, i=5-6$
$e + C_3H_8 \rightarrow C_3H_3^{2+} + 2H_2 + H + 3e^\ddagger$	4.0040E+01	-5.5762E-02 2.2088E-01 -1.0952E+00	4.0342E-02 4.4344E-01 6.9354E-01
$e + C_3H_8 \rightarrow C_3H_2^{2+} + 3H_2 + 3e^\ddagger$	4.0880E+01	-5.7684E-02 -3.7592E-01 -4.0827E+00	1.0316E-01 2.8206E+00 1.9574E+00
$e + C_3H_8 \rightarrow C_3H_5^{2+} + H_2 + H + 3e^\ddagger$	3.4390E+01	1.3656E-03 -2.7414E-03 -6.6982E-03	-4.7994E-05 1.4041E-02 -5.3844E-03
$e + C_3H_8 \rightarrow C^+$ (total)	3.9040E+01	-1.9446E-01 2.0994E-02 1.6798E+00	2.5057E-01 -9.4116E-02 -1.1035E+00
$e + C_3H_8 \rightarrow C^+ + C_2H_6 + H_2 + 2e^\ddagger$	3.7040E+01	-1.3571E-02 4.8370E-01 3.7257E+00	-9.1608E-03 -2.0265E+00 -2.1042E+00
$e + C_3H_8 \rightarrow C^+ + C_2H_4 + 2H_2 + 2e^\ddagger$	3.7040E+01	-1.4702E-02 5.2401E-01 4.0362E+00	-9.9242E-03 -2.1954E+00 -2.2795E+00

[‡]These channels were not listed in Table 11, but are included here for completeness.